AD-A099 695 MICHIGAN STATE UNIV EAST LANSING DEPT OF METALLURGY -ETC F/G 11/6
AN EXPERIMENTAL STUDY OF THE INTERACTION OF STRAIN FIELDS BETWE--ETC(U)
MAR 81 G CLOUD, M TIPTON F33615-78-C-5123
UNCLASSIFIED AFWAL-TR-80-4205 NL

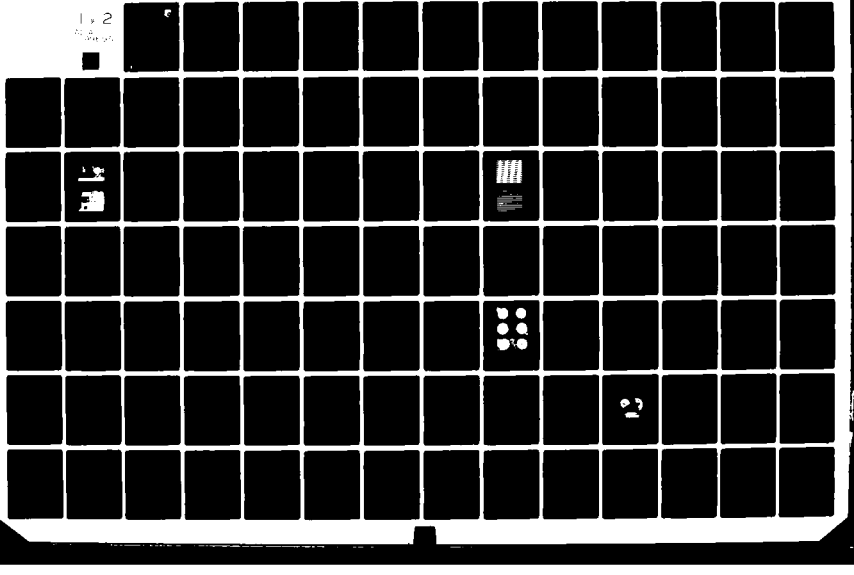

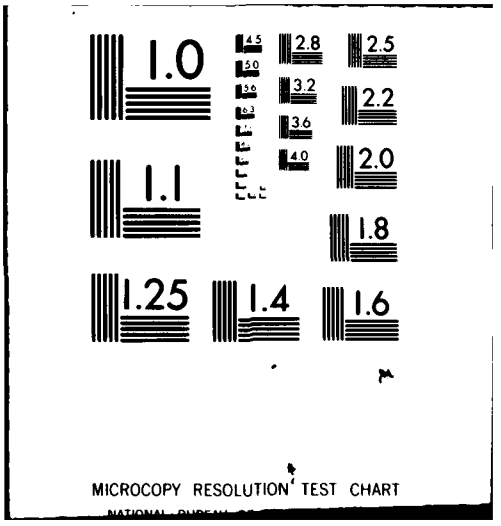
1.0
1.1
1.25
1.4
1.6
1.8
2.0
2.2
2.5
2.8
3.2
3.6
4.0
4.5
5.0
5.6
6.3
MICROCOPY RESOLUTION TEST CHART

AFWAL-TR-80-4205

AD A099695

AN EXPERIMENTAL STUDY OF THE INTERACTION OF STRAIN FIELDS BETWEEN COLDWORKED FASTENER HOLES

GARY CLOUD
MARK TIPTON
MICHIGAN STATE UNIVERSITY
EAST LANSING, MICHIGAN 48824

MARCH 1981

TECHNICAL REPORT AFWAL-TR-80-4205
Final Report for Period July 1978 to February 1980

Approved for public release; distribution unlimited.

MATERIALS LABORATORY
AIR FORCE WRIGHT AERONAUTICAL LABORATORIES
AIR FORCE SYSTEMS COMMAND
WRIGHT-PATTERSON AIR FORCE BASE, OHIO 45433

179

NOTICE

When Government drawings, specifications, or other data are used for any purpose other than in connection with a definitely related Government procurement operation, the United States Government thereby incurs no responsibility nor any obligation whatsoever; and the fact that the government may have formulated, furnished, or in any way supplied the said drawings, specifications, or other data, is not to be regarded by implication or otherwise as in any manner licensing the holder or any other person or corporation, or conveying any rights or permission to manufacture use, or sell any patented invention that may in any way be related thereto.

This report has been reviewed by the Office of Public Affairs (ASD/PA) and is releasable to the National Technical Information Service (NTIS). At NTIS, it will be available to the general public, including foreign nations.

This technical report has been reviewed and is approved for publication.

Robert C. Donath

ROBERT C. DONATH
Project Engineer
Metals Behavior Branch
Metals and Ceramics Division

WALTER H. REIMANN, Acting Chief
Metals Behavior Branch
Metals and Ceramics Division

"If your address has changed, if you wish to be removed from our mailing list, or if the addressee is no longer employed by your organization please notify AFWAL/MLLN, W-P AFB, OH 45433 to help maintain a current mailing list".

Copies of this report should not be returned unless return is required by security considerations, contractual obligations, or notice on a specific document.

AIR FORCE/56780/27 May 1981 — 300

SECURITY CLASSIFICATION OF THIS PAGE (When Data Entered)

REPORT DOCUMENTATION PAGE

READ INSTRUCTIONS BEFORE COMPLETING FORM

1. REPORT NUMBER: AFWAL-TR-80-4205	2. GOVT ACCESSION NO.: AD-A099695
3. RECIPIENT'S CATALOG NUMBER	
4. TITLE (and Subtitle): AN EXPERIMENTAL STUDY OF THE INTERACTION OF STRAIN FIELDS BETWEEN COLDWORKED FASTENER HOLES.	5. TYPE OF REPORT & PERIOD COVERED: FINAL rept. 1 Jul 78 - 15 FEB 80
	6. PERFORMING ORG. REPORT NUMBER
7. AUTHOR(s): Gary Cloud, Mark Tipton	8. CONTRACT OR GRANT NUMBER(s): F33615-78-C-5123 new
9. PERFORMING ORGANIZATION NAME AND ADDRESS: DEPT. OF METALLURGY, MECHANICS AND MATERIALS SCI. MICHIGAN STATE UNIVERSITY EAST LANSING, MICHIGAN 48824	10. PROGRAM ELEMENT, PROJECT, TASK AREA & WORK UNIT NUMBERS: Project 2418 Task 24180305
11. CONTROLLING OFFICE NAME AND ADDRESS: 2418 03	12. REPORT DATE: March 1981
	13. NUMBER OF PAGES: 123
14. MONITORING AGENCY NAME & ADDRESS (if different from Controlling Office): MATERIALS LABORATORY (AFWAL/MLLN) AIR FORCE WRIGHT AERONAUTICAL LABORATORIES AIR FORCE SYSTEMS COMMAND WRIGHT-PATTERSON AIR FORCE BASE, OHIO 45433	15. SECURITY CLASS. (of this report): UNCLASSIFIED
	15a. DECLASSIFICATION/DOWNGRADING SCHEDULE

16. DISTRIBUTION STATEMENT (of this Report)

Approved for public release; distribution unlimited

17. DISTRIBUTION STATEMENT (of the abstract entered in Block 20, if different from Report)

18. SUPPLEMENTARY NOTES

19. KEY WORDS (Continue on reverse side if necessary and identify by block number)

COLDWORKING	FATIGUE	STRAIN ANALYSIS
FASTENERS	MOIRE	
RESIDUAL STRAIN	MANDRELIZATION	
RESIDUAL STRESS	FRINGE PATTERNS	
SURFACE STRAINS	OPTICAL DIFFRACTION	

20. ABSTRACT (Continue on reverse side if necessary and identify by block number)

This report describes the experimental study investigatin the interaction of the residual surface strain fields caused by the coldworking of fastener holes in the near vicinity of one another. Testing was confined to 7075-T6 aluminum alloy, 1/4 inch (6.4 mm) in thickness. Fastener holes were .261 inch (6.6 mm) in diameter and the center-to-center separation between adjacent fasteners was 1.75 and 2.0 diameters.

Single-row in-line and double-row fastener patterns were the focus of this →

DD FORM 1 JAN 73 1473 EDITION OF 1 NOV 65 IS OBSOLETE

UNCLASSIFIED
SECURITY CLASSIFICATION OF THIS PAGE (When Data Entered)

study. Consecutive and non-consecutive sequences of pattern coldwork were chosen to model possible field situations. Experimental results indicate a direct relation exists between the degree of interaction between strain fields ahd the center-to-center separation between adjacent fastener holes. As noted from the measurement of residual diametral expansions, unsymmetric hole edge motions result in unsymmetric strain distributions. Sleeve failure and the coldworking of adjacent fastener holes can lead to unwanted residual tensile strains at a hole edge boundary.

FOREWORD

This report was prepared by the Department of Metallurgy, Mechanics and Materials Science, Michigan State University, East Lansing, Michigan 48824, under Contract No. F33615-78-C-5123, "Coldworked Hole Stress Analysis". The contract, which was initiated under Project No. 2418, Task 24180305, was administered under the direction of the Air Force Materials Laboratory, Metals Behavior Branch (AFWAL/MLLN), by Dr. Robert C. Donath, Project Engineer.

The research reported herein was submitted by Dr. Gary Cloud who was the Principal Investigator, and covers work conducted during the period 1 July 1978 to 15 February 1980.

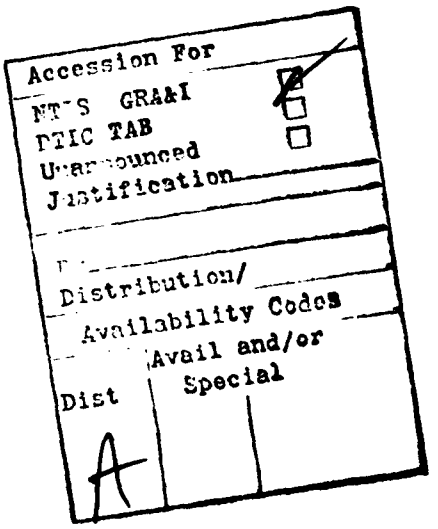

TABLE OF CONTENTS

LIST OF TABLES

LIST OF FIGURES

CHAPTER 1

INTRODUCTION

Flaw induced fatigue fracture has been responsible for limitations in the operational lives of both commercial and military aircraft. The fastener holes in aircraft structures can provide the origin for fatigue cracks. The fastener hole acts as a stress concentration area in the near vicinity of which the local stress can be much greater than the nominal stress in the bulk material. Surface flaws caused by standard hole generation techniques can amplify the stress concentration near a fastener hole leading to local yielding and crack initiation. Coldworking is a metalworking technique that has been shown to enhance the fatigue lives of some structures by inhibiting the growth of flaws in the vicinity of the fastener hole. Cesarz (2), points out that coldworking affects the material in two ways. "First it introduces a tangle of dislocations which restricts further dislocation glide, and second it causes residual elastic compressive strains to form near the coldworked area." There are several acceptable methods for coldworking a fastener hole. One way is to draw a tapered mandrel through a predrilled fastener hole.

1.1 Purpose

The purpose of this research was to study the strain distributions that exist between coldworked fastener holes that are in the near vicinity of one another. Included in the study were the residual strain

distributions in single- and double-row fastener patterns. Important parameters included variation in the order in which the holes in the pattern are coldworked and alterations of the separation between adjacent fastener holes.

Residual surface strain distributions were obtained by use of the moiré technique. The moiré effect is an optical phenomenon that involves mechanical interference between two superimposed arrays of lines. The moiré effect has been used successfully in prior studies of similar problems (2), (3), (4), and its adaptation to the problem under study posed no difficulty.

The experimental results of this investigation cannot be directly compared with any existing study because there has been no research in this area. Comparisons were made between the similar fastener geometries and levels of coldwork used in the study, and these served as the primary means of experimental evaluation. When applicable, comparisons were made with the work of Cloud (4). The results of the study are presented in graphical form and the comparisons are easily noted.

1.2 Organization of Thesis

A description of the materials used in the study and their preparation are given in Chapter 2. Included in this chapter is a brief description of the coldworking technique, and reference is given to the origin of the test patterns.

Chapter 3 is a comprehensive discussion of the experimental procedures used. Included are laboratory techniques and an explanation of the data reduction process. Discussed within the context of the Chapter are optical phenomena fundamental to the moiré technique.

Chapter 4 prepares the reader for the methodology used in presenting the results of the investigation.

The thesis is concluded by Chapter 5, in which the results of the investigation are presented.

CHAPTER 2

MATERIAL DESCRIPTION

2.1 Material Specification and Test Pattern Development

2.1.1 Material Specification

The specimens used in the study were cut from plates of 7075-T6 aluminum alloy, 1/4 inch (6.4 mm) in thickness. This type of aluminum has excellent abrasion resistance and is of high strength. The alloy finds extensive use in the aircraft industry because of its high strength-to-weight ratio. In the study, specimens #1, #2, #3, and #4 are from the same stock as that used by Cloud (4), Sharpe (11), and Adler and Dupree (1). It was not believed necessary to check their measurements of material properties. Specimens #5, #6, and #7 were cut from similar stock obtained from the Aluminum Company of America (ALCOA).

2.1.2 Test Pattern Development

Information concerning fastener locations was supplied to AFWAL/MI (Air Force Materials Laboratory, Wright Patterson Air Force Base), by Fairchild Republic Company of Farmingdale L.I., New York 11735. Supplied to AFWAL/MI was a draft of the company's "Fuel Tank Repair/Wing Panel Life Extension Improvement Program" prepared by H. W. Schmidt. The draft is a portion of a workbook that describes detailed instructions to achieve fuel tank leak repair and sealing improvement in conjunction with TCTO drawing instructions for wing center panel life extension improvement.

"Wing Center Panel Life Extension Improvement" is Fairchild Republic's terminology for a process which incorporates the coldworking of fastener holes.

The workbook focuses on the repair of identified leaks originating at fasteners. Subsequent leak repair and life extension improvement are described in detail. The workbook designates the coldwork areas, the sequence, and the coldworking procedure by which repair is to be accomplished. The technical drawings and coldwork instructions in the workbook were the basis for the test patterns chosen for the study. Attention was focused on a wing underside center spar where two wing skins are joined. At the center spar, each skin is attached by two parallel rows of fasteners. The fasteners are aligned and are not staggered. Figure 2.1 is an illustration of the layout of the fasteners in the area of interest. The section of the workbook applicable to the above area of interest is as follows:

"2.8.1 The maximum number of fasteners to be removed in each bay at any one time is as follows:

a. Six (6) fasteners in each forward spar, auxiliary aft spar, and rib. Since the center spar involved two (2) wing skins, six (6) fasteners in each skin may be removed at any one time. The fastener removal shall be accomplished one row at a time per spar span and shall be in the direction specified (if any). For example, the center spar accessible through door W-10 would be reworked as follows:

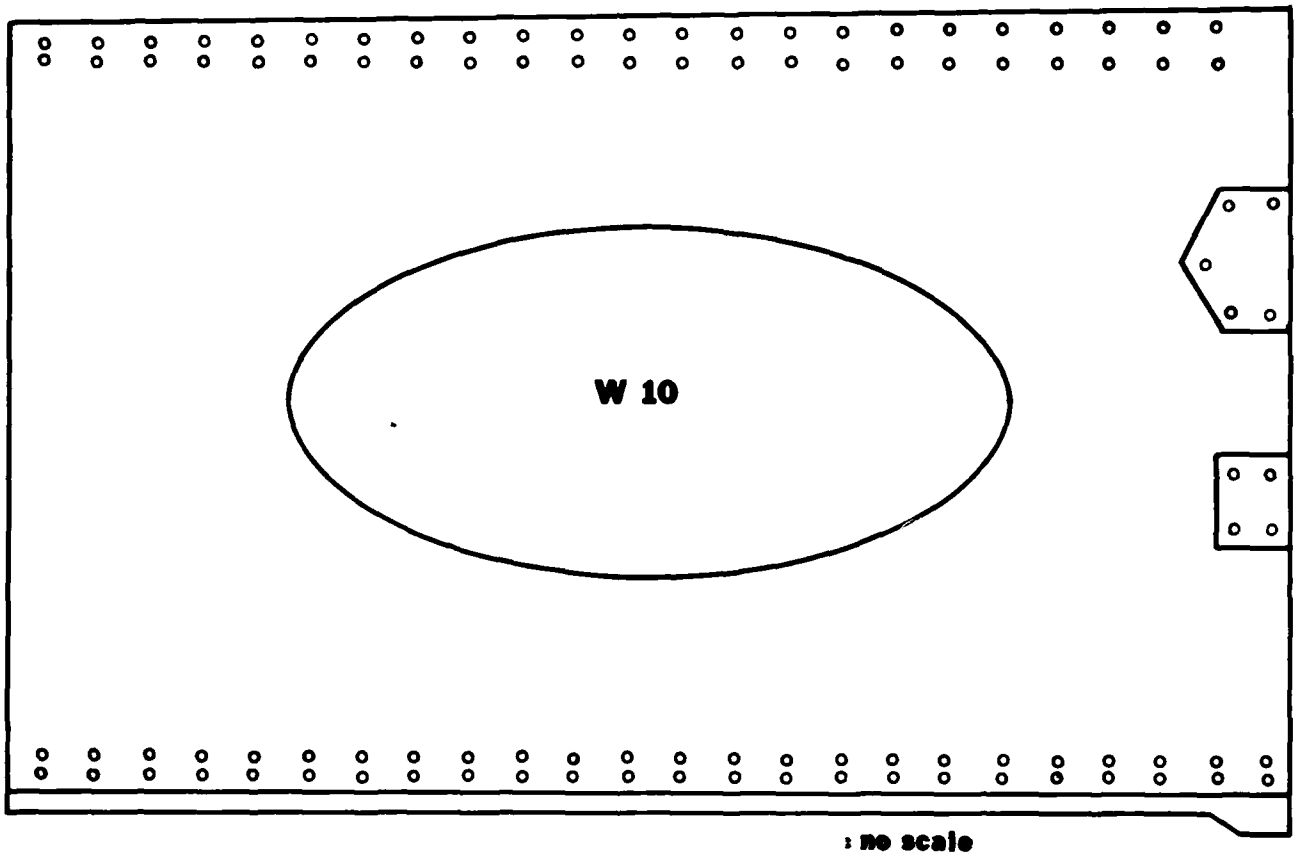

Figure 2.1 Geometric Orientation of Fasteners on a Wing Underside Center Spar.

(1) Direction of fastener removal is from rib station 66 to rib station 90. Since this is not a coldworked area, consecutive fasteners would not necessarily be removed.

(2) One row in each skin could be reworked at a time.

b. Instructions for RH wing tank also apply to LH wing tank."

Section 2.8.1 (a) of the Fairchild Manual led to the development of two-hole and five-hole single line fastener patterns. For these patterns, coldworking is to be accomplished one hole at a time and in a specified order. Specimens #2, #3, and #7 incorporated these hole test patterns; they are illustrated in Figure 2.2a and Figure 2.3b. The order of coldwork for all specimens is listed in Table 2.1. Section 2.8.1 (a-1) of the Fairchild Manual suggested also a three-hole single line pattern which had an odd sequence of coldwork. The simulation of the coldworking of nonconsecutive fastener holes is intended. The applicable test pattern is illustrated in Figure 2.b; it was used on specimen #4. Specimens #5 and #6 illustrated in Figure 2.3a model a double-row fastener pattern and were used to determine the inter-row influences that could result from the coldworking process.

2.2 Material Preparation

2.2.1 Coldworking Process

A common method of coldworking is a process in which a tapered mandrel is drawn through a predrilled fastener hole. The process is not new and much work has been devoted to its study. In particular, papers

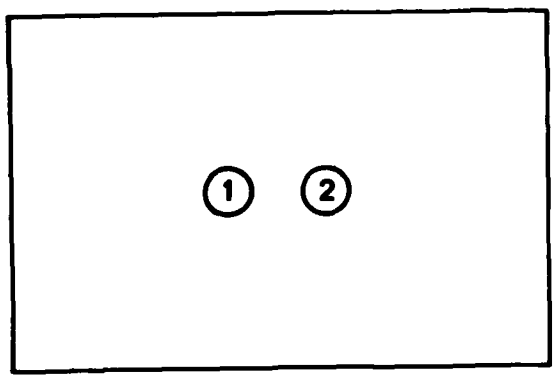

(A)

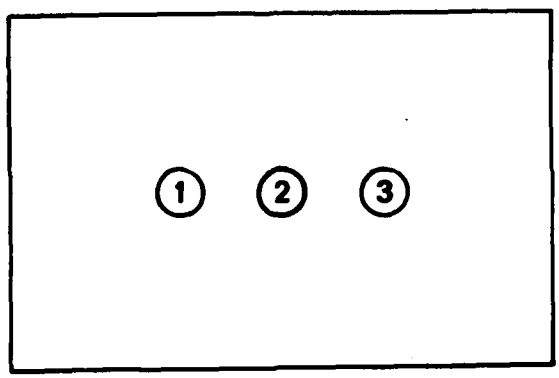

(B)

Figure 2.2 Two-Hole and Three-Hole In-Line Fastener Patterns.

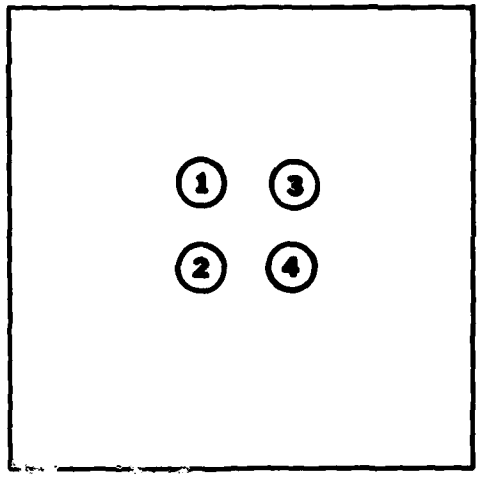

(A)

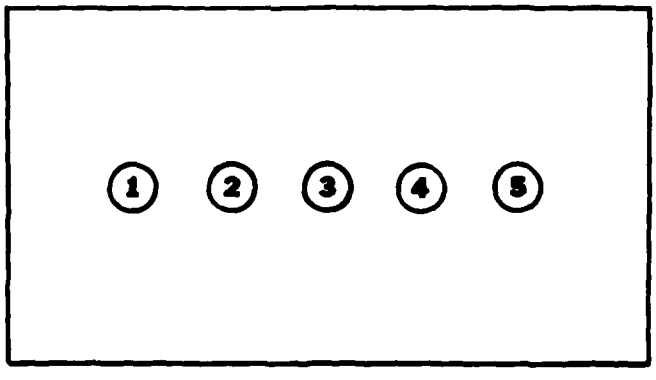

(B)

Figure 2.3 Four-Hole Double-Row and Five-Hole In-Line Fastener Patterns.

TABLE 2.1 ORDER OF COLDWORK

SPECIMEN	PATTERN	HOLE NO.	ORDER OF COLDWORK
2	in-line	1	1
		2	2
3	in-line	1	1
		2	2
		3	3
		4	4
		5	5
4	in-line	1	1
		2	3
		3	2
5	double-row	1	1
		2	2
		3	3
		4	4
6	double-row	1	1
		2	3
		3	2
		4	4
7	in-line	1	1
		2	2

and reports by Cloud (4), Sharpe (11), Cesarz (2), and Chandawanich (3) have proved to be of interest. The coldworking tools and supplies used in this investigation are marketed by

J. O. King Inc.
711 Trabert Ave. N.W.
Atlanta, Georgia 30318

The actual coldworking procedure is often termed mandrelization. In the King mandrelization procedure, a tapered mandrel is inserted into a lubricated stainless steel sleeve; both are then inserted into a fastener hole, and the mandrel is then pulled through as illustrated in Figure 2.4. The stainless steel sleeve is used to line the hole and to prevent damage during the coldworking process. An attached anvil functions to support the sleeve as the mandrel is pulled through. After coldworking, this anvil detaches from the sleeve and is discarded. The mandrel, sleeve, and the detached anvil are shown in Figure 2.5.

The magnitude or the degree of coldwork achieved for a particular fastener hole is often measured in terms of radial interference. The radial interference of a particular hole is determined as follows:

$$\text{Radial Interference} = \frac{M + 2T - D}{2}$$

M = Mandrel diameter

T = Sleeve thickness

D = Diameter of Fastener hole

From the above definition of radial interference, it can be seen that the degree of coldwork is based upon several measurements. Uncertainty in any of the measurements generates error in the computed radial interference. For this study, radial interference levels ranged from 6.3 to 7.55 mils. Industry has chosen 6 mils as an optimum level of coldwork, though there are no research data which entirely supports this choice.

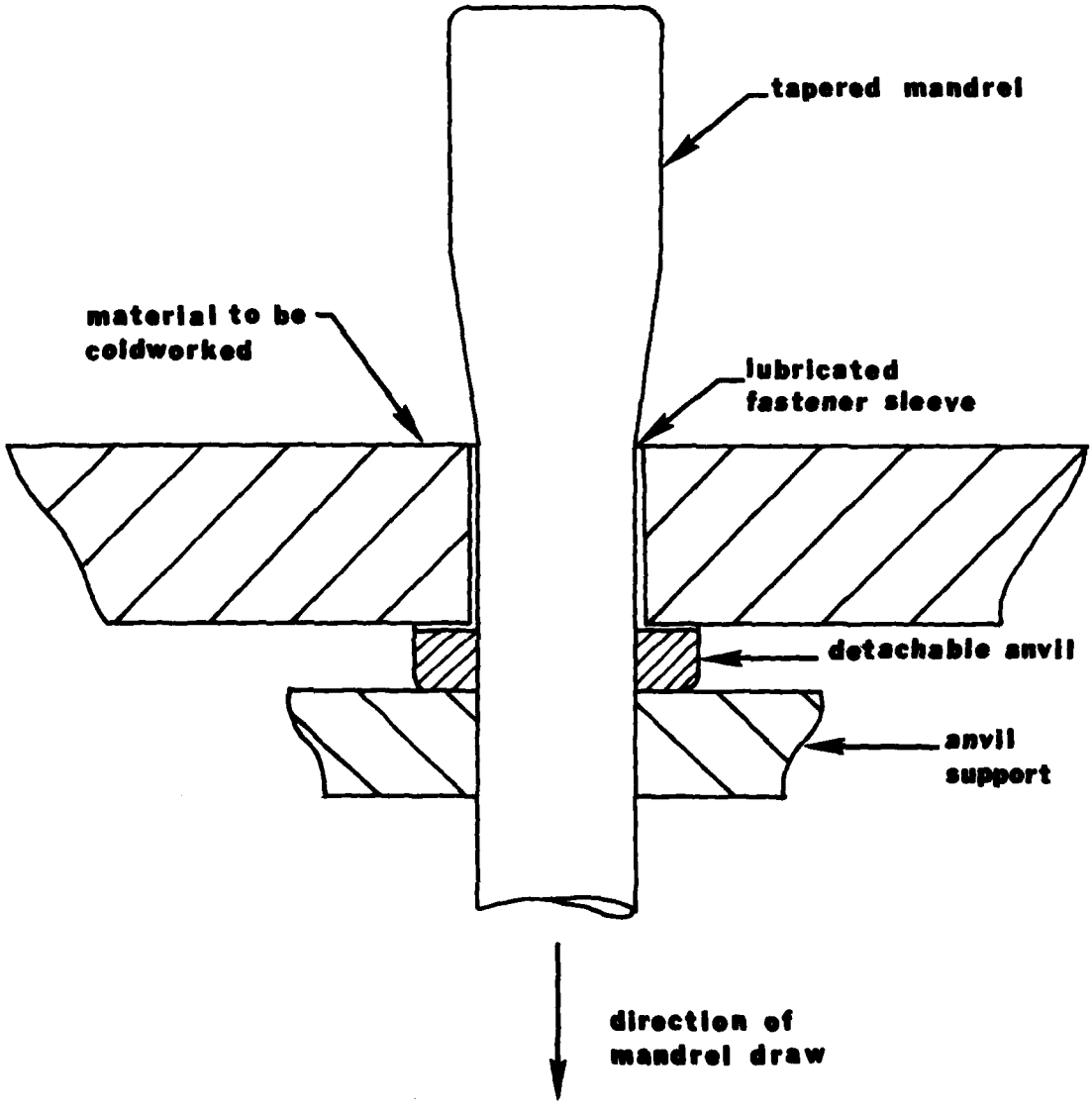

Figure 2.4 Schematic of the King Coldworking Process.

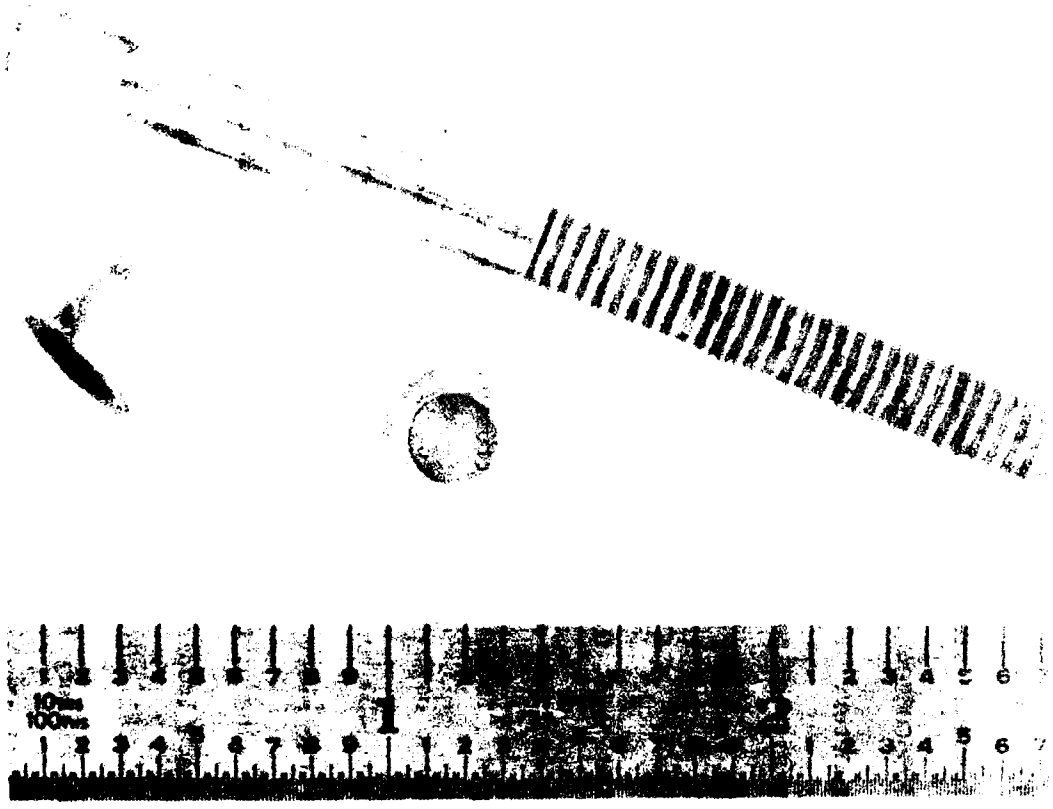

Figure 2.5 Photograph of Mandrel, Sleeve and a Detached Anvil.

Mandrels used in the study were J. O. King part numbers:

JK6540-08-257

JK6540-08-255

The mandrels varied in taper and profile. Mandrel diameters were measured at 45 degree intervals and the results are listed in Table 2.2.

The fastener sleeves used throughout the study are J. O. King part number JK5535C08Z04L. Sleeve thickness was obtained with a ball gage and a micrometer. Inner and outer sleeve diameters were measured and the thickness then computed. With the exception of those used in specimen #2, the fastener sleeves used had a measured thickness of .0096$\pm$ .0001 inches.

Protrusion of the fastener sleeves beyond the surface of the specimens severely interfered with specimen photography and postcoldwork measurement. To solve the protrusion problem, fastener sleeves were sanded down so as to lie flush to the surface of each specimen. Sanding was done with 400 grit silicon carbide metallography paper. Burrs around the lip of the sleeves were removed with a penknife.

Coldworking of the fastener holes was accomplished by mounting a specially made loading frame and a mandrel in an Instron testing machine. The experimental setup is shown in Figure 2.6 and Figure 2.7. To obtain a load-time history for each mandrelization, a load cell was constructed. This load cell also served to attach the frame to the Instron. The load cell was a simple cylindrical tension member with two foil strain gages attached longitudinally to its sides. The foil gages were Micro Measurements EA-13-125AD-120. The strain gages formed opposite arms of a 120 ohm Wheatstone bridge. The strain gages were mounted on opposite sides of the tension member so as to negate possible bending strains.

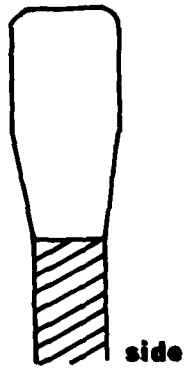

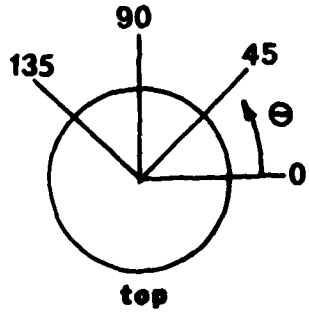

TABLE 2.2 MANDREL DIAMETERS ALONG RADIAL AXES

MANDREL	0°	45°	90°	135°
JK6540-08-257 (a)	0.2579	0.2571	0.2575	0.2581
Jk6540-08-257 (b)	0.2569	0.2569	0.2569	0.2569
JK6540-08-255	0.2550	0.2550	0.2550	0.2550

Figure 2.6 Photograph of Experimental Apparatus Used to Coldwork Test Specimens.

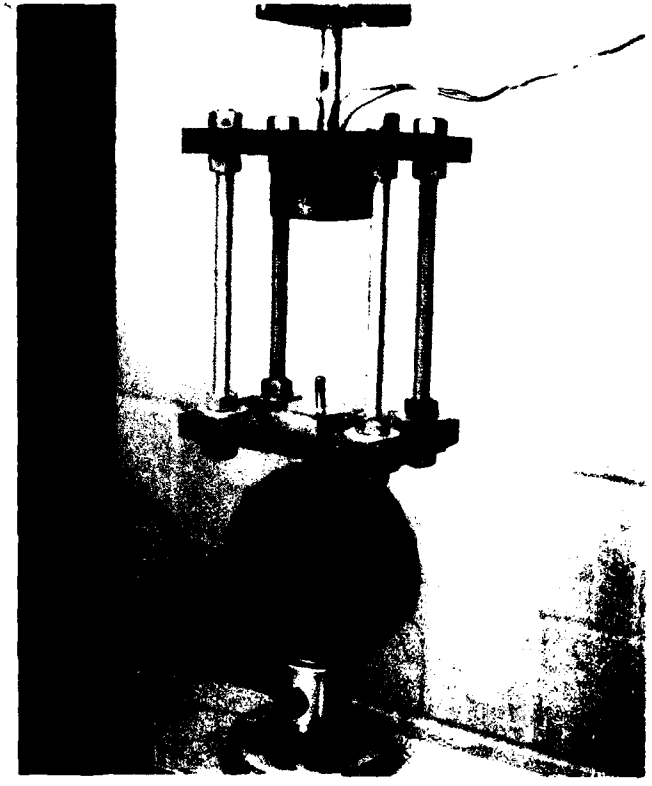

Figure 2.7 Photograph of Loading Frame and the Attached Load Cell.

Used to record the force for each mandrelization was a Sanborn Twin-Viso Cardiette strip chart recorder equipped with a strain gage amplifier. During coldworking, the draw rate of the Instron was .5 cm/min. and the chart speed was 1 mm/sec. A typical load-time record is illustrated in Figure 2.8 and the maximum loads incurred during coldworking for all specimens are given in the specimen data tables in Chapter 5. Noteworthy was the ability of the load cell to detect irregularities in the coldworking procedure. These discontinuities were signaled by jumps and serrations in the strip chart record and were indicative of sleeve slippage or of sleeve failure.

2.2.2 Specimen Preparation

The hole patterns used in this investigation were illustrated in Figures 2.2 and 2.3. Certain tolerances were maintained on the fastener holes in order to allow comparisons between the various fastener patterns and hole pairs.

The machining process for the fastener holes involved drilling an undersize hole 0.25 inches (6.4 mm) in diameter and then boring to 0.261 inches (6.66 mm) in diameter with a single point tool. This technique produced non-tapered holes having square edges at the surface interface.

Upon reception from the machine shop, each specimen was lapped prior to taking any precision measurements. Lapping is a surface preparation technique that produces a uniform surface with a fine matte structure. Lapping of the specimens was done on a Lapmaster #12 manufactured by Crane Packing Co. of Springfield, Illinois. Lapping times varied from fifteen to thirty minutes depending upon the initial condition of each specimen, the flow rate of the lapping medium to the specimen surface, and the desired surface finish. The lapping medium

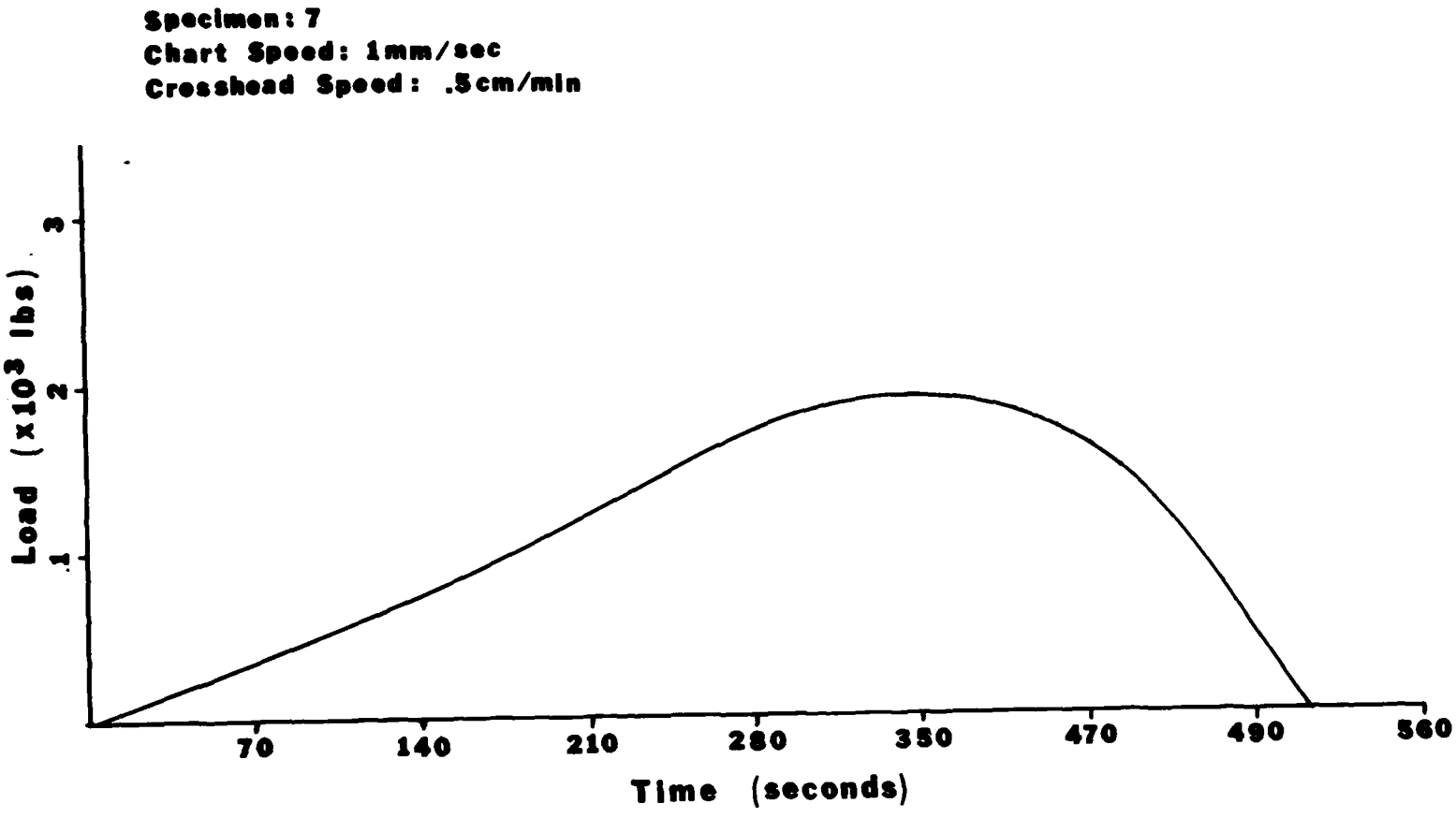

Figure 2.8 Typical Load-Time Record Obtained During Coldworking Procedure.

is a suspension made of 2.73 liters of oil and 142 grams of 1-micron lapping compound. Both the oil and the lapping compound are manufactured by the Crane Packing Co. The backsides of each specimen were lapped in order to provide a uniform flat base for seating the sleeves during the mandrelization process.

Once each specimen was lapped and cleaned, measurements of all critical dimensions were taken. These critical dimensions were the hole diameters, center to center hole separations, and the hole to edge distances. All measurements are surface measurements and were obtained by the use of a Leitz measuring microscope. The Leitz laboratory microscope is equipped with a measuring stage and two (X,Y) measuring spindles. The measuring stage has a range of 25 x 25 millimeters and the least reading on the spindles is 0.01 mm. Inspection of the critical dimensions led to the rejection of two specimens whose hole diameters differed from each other by almost 15%.

Fiducial marks were applied to the surface of specimens determined suitable for experimentation. The moiré technique requires several stages of photographic reproduction, so adequate fiducial marks are of great importance in maintaining correct specimen orientation and in determining magnification ratios. Fiducial marks were laid out in pencil and then lightly scribed into the specimen surface with a carbide-tipped scribe and straight edge. The scribe gave a burrless fiducial mark having excellent uniformity in width and depth.

After the application of the fiducial marks, the surface of each specimen was lightly polished with 0.5 micron alumina compound on a felt polishing wheel. Polishing times averaged only one to three minutes. The light surface polishing served no purpose other than to

aid in the photography of specimen gratings. Owing to the near-transparency of the photoresist coating and the dull matte finish of the lapped aluminum, gratings applied to a lapped surface are extremely difficult to see and photograph. The light polishing sufficiently alters the surface reflections of a specimen so as to allow efficient grating evaluation and photography, plus retention of the desirable surface characteristics associated with lapping.

Prior to the application of a specimen grating, a complete and precise map of each specimen surface was obtained. These maps included the aforementioned critical dimensions and all hole edge-to-fiducial mark distances. These specimen surface maps serve as a permanent record and as a computational aid.

CHAPTER 3

EXPERIMENTAL PROCEDURES

3.1 Moiré Method of Strain Analysis

3.1.1 Application of Moiré Analysis

The moiré effect is an optical phenomena that can be observed when two arrays of closely spaced lines are superimposed and viewed in either transmitted or reflected light. Alternating light and dark bands, called fringes, arise at definite intervals due to mechanical interference of light caused by the repetitive structure of the overlapping arrays. When used in strain analysis these fringes can be interpreted as being indicative of the displacements on the surface of the specimen.

The moiré method is a surface strain measurement technique which is whole field and noncontacting in nature. With appropriate techniques, the method of analysis can easily accomodate out-of-plane displacements and large plastic strains. Significant to moiré analysis is that the structural material under study is used for the actual testing. No assumptions of material linearity or similitude are required, and no material property calibrations are needed in the conversion of observed fringes to desired strains.

3.1.2 Moiré Technique

The moiré effect occurs when two similar, though not necessarily identical, arrays of equally spaced lines are superimposed upon one

another. This superposition of line arrays can be accomplished in many ways. For the case under study, the line arrays are termed gratings. Gratings applied to a specimen are termed specimen gratings and gratings used for analysis purposes are termed analyzer gratings.

An example of a moiré fringe pattern is shown in Figure 3.2. The fringe pattern was obtained by physically superimposing two line-space gratings, one of which is pictured in Figure 3.1. As defined, "a moiré fringe is a locus of points which have the same component of displacement in a direction perpendicular to the lines of the master grating" (4). In Figure 3.2, the dark bands are termed integral order moiré fringes and the light bands are called half order moiré fringes. Analysis of the displacement field can be accomplished utilizing either or both types of fringes. For this study, only the dark bands or integral order fringes were used.

In moiré analysis, the specimen grating is oriented so as to yield information about the normal strains in a preferred direction. This preferred direction is termed the principle direction of the grating and is perpendicular to the orientation of the grating lines. To determine the normal strain in the principal direction, it is necessary to establish the fringe order as a function of distance along an axis by plotting and/or numerical processing. These steps are illustrated in Figure 3.3. The relative displacement undergone between analyzer and specimen gratings at any point can easily be computed. From Durelli and Parks (9),

$$U = NP$$

U = Axial component of displacement

N = Fringe order number at point A

P = Pitch of the analyzer grating

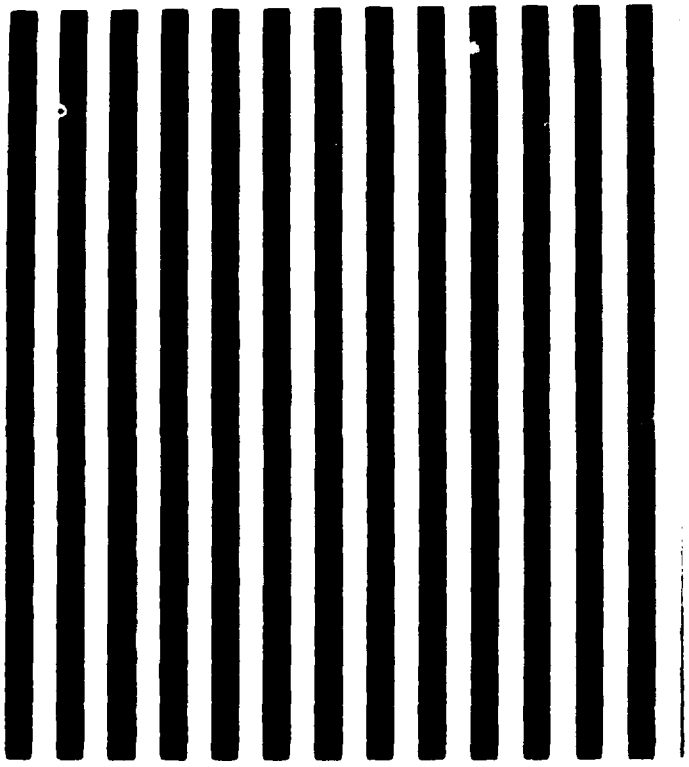

Figure 3.1 Line-Space Grating (8 Lines/Inch).

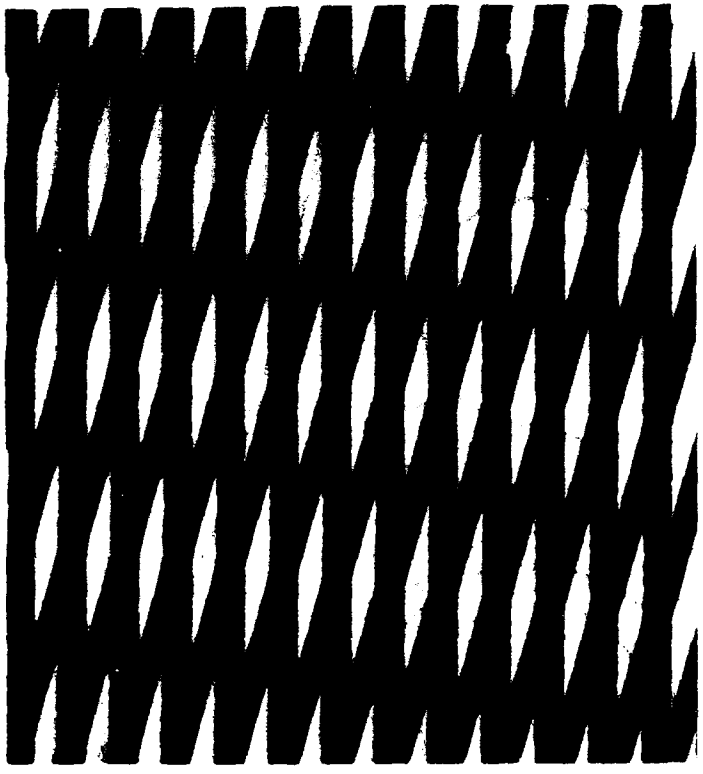

Figure 3.2 Moiré Interference Pattern Obtained by the Physical Superposition of Two 8 lpi Gratings.

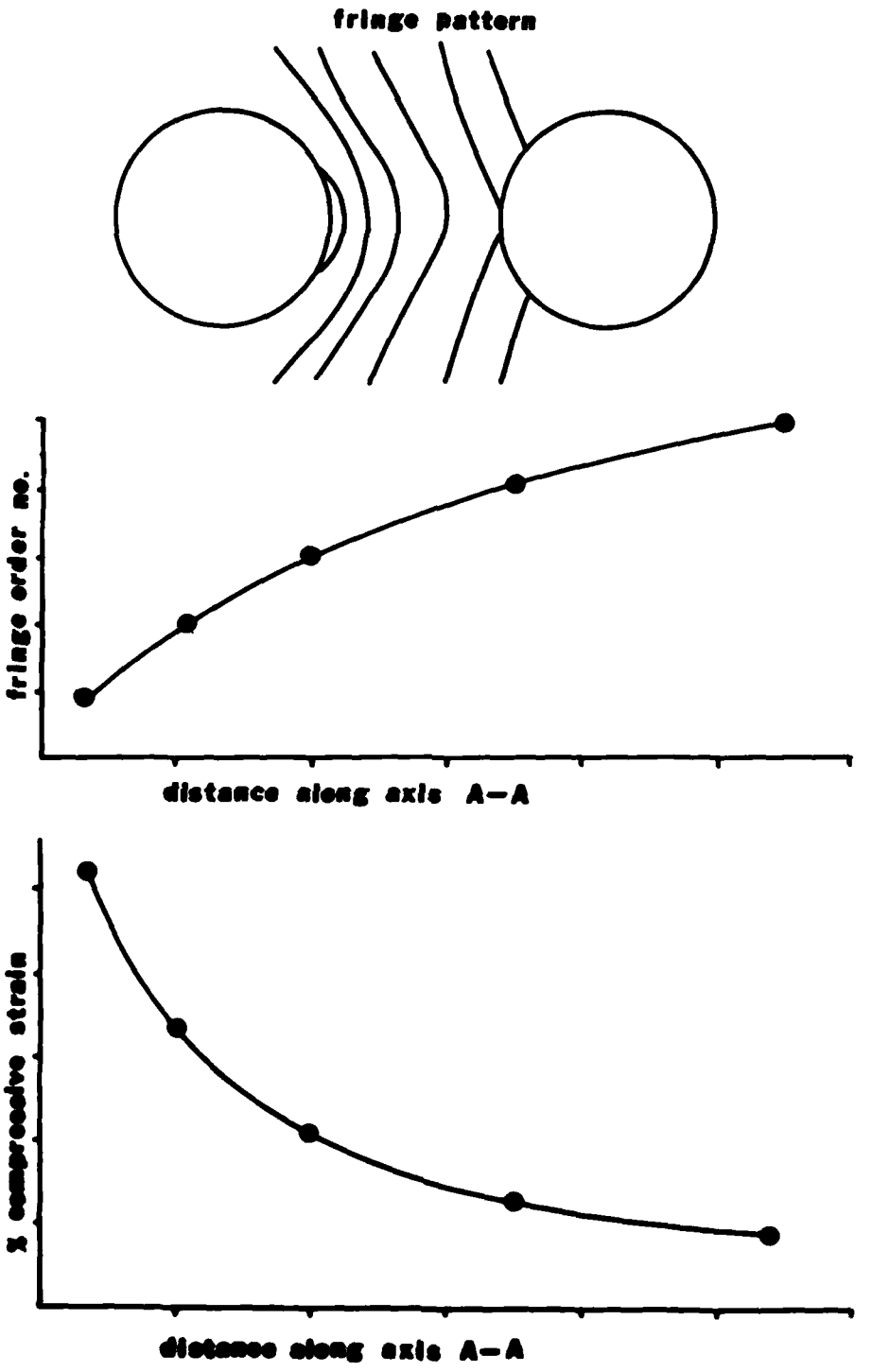

Figure 3.3 Stepwise Progression of the Data Reduction Procedure Required in Moiré Strain Analysis.

It is important to realize that the absolute fringe order is not of importance; but what is necessary is that, in the analysis, no fringes are repeated or skipped. From the Lagrangian definition of normal strains,

$$\varepsilon_A = \frac{\partial u}{\partial x}$$

$$\varepsilon_A = P \left(\frac{\partial N}{\partial x}\right)$$

ε_A = Axial component of strain

From the above, it can be seen that strain in a direction perpendicular to the orientation of the specimen grating is simply the pitch of the analyzer grating multiplied by the slope of the fringe order plot at the point in question. The strain distribution is illustrated in Figure 3.3c.

The precision of the moiré method is dependent upon the number of fringes or data points used in the definition of a given displacement fields. High density fringe patterns are possible in part through the use of high density gratings or through the use of pitch mismatch. An additional and equally viable technique for fringe multiplication is Coherent Optical Data Processing (4), (5). This method of fringe multiplication is discussed in section 3.2.2.

For any displacement field, as grating frequency is increased, so also is the number of moiré fringes. Increasing fringe density gives better definition to the displacement field. This results in increased efficiency in the differentiation of the experimental data from which the strains are determined. The use of high density moiré gratings is sometimes not wise in that there tends to be problems in handling and application.

The pitch mismatch method is a widely used technique by which fringe density can sometimes be increased. In the pitch mismatch method, an "unstrained" or "baseline" fringe pattern is formed prior to imposing any deformation. A baseline fringe pattern is formed by mismatching the pitch of the specimen and analyzer gratings. In doing so, the analyzer grating spatial frequency is usually some multiple (including one) of the specimen grating frequency plus some small additional amount. The "small additional mismatch" gives an additive increase in the number of fringes. It is used regardless of the use of multiplicative processing. If the frequency multiple is other than unity, there will be a fringe multiplication. Sensitivity multiplication results from the diffraction characteristics of the two gratings and such a process is included in the Optical Data Processing discussion of Section 3.2.2.

The baseline fringe pattern containing added fringes is interpreted as a fictitious displacement or strain. This fictitious displacement is constant over the region of interest and can be determined numerically in the following manner,

$$U_f = PN$$

U_f = Fictitious displacement

As previously described, the fictitious strain (Lagrangian), is easily derived from the displacement field. Hence,

$$\varepsilon_f = P \frac{\partial N}{\partial x}$$

Since the fictitious displacement is uniform across the region, $\frac{\partial N}{\partial x}$ is a constant. This results in the constant fictitious strain ε_f.

A second fringe pattern results after the region has undergone some deformation. It is this fringe pattern that will yield a measured displacement. This measured displacement is not the true displacement because it includes the fictitious displacement imposed by the initial pitch mismatch. In the pitch mismatch method, the quantity measured is the change in spacing that occurs between the baseline and the data fringe patterns. This change in spacing is indicative of the true displacement field. Computation of the true displacement and strain at any point follows directly from prior derivations.

$$U_t = U_m - U_f$$

$$U_t = P(N_M - N_f), \quad \text{where}$$

U_t = True displacement

U_m = Measured displacement

U_f = Fictitious displacement

The true strain is thus computed as follows,

$$\varepsilon_T = \varepsilon_m - \varepsilon_f$$

$$\varepsilon_T = P\,\partial\left(\frac{N_m - N_f}{\partial x}\right), \quad \text{where}$$

ε_T = True strain

ε_m = Measured strain

ε_f = Fictitious strain

3.1.3 Specimen Grating Production

The moiré method of strain analysis requires the presence of a moiré grating on the surface of each specimen. Line-space gratings of

1000 lines per inch (lpi) were used for the study. As noted in the literature, the success of the moiré method depends largely upon the quality of the applied specimen grating. Quality gratings can simplify and shorten the subsequent moiré analysis while yielding superior results (4).

Chosen for the study was the photoresist method of grating application. The photoresist method utilizes a light-sensitive polymeric coating applied to the specimen surface, its subsequent exposure to light, and the development of the coating. The photoresist method simply transfers the image of a master grating to the specimen surface by contact printing methods.

The light-sensitive coating used in the study was Shipley AZ1350-J manufactured by Shipley Company, Newton, Mass. The companion developer was obtained with the photoresist. This resist has a solids content of 30% and is formulated for the application of acid resist coatings to aluminum substrates.

Proper surface preparation is essential if the photoresist is to spread to a thin uniform coat. The cleaning procedure utilized throughout the study was simple but efficient. Each specimen was first cleaned by immersion in an acetone bath. Gauze sponges were used for surface cleaning and cotton tipped swabs were used to clean the insides of the fastener holes. Upon removal from the acetone bath, each specimen was spray washed with acetone and scrubbed with gauze sponges. Spray washing ceased when the sponges no longer showed signs of residue. Final degreasing was accomplished with Chlorothene-Nu, utilizing the previous spray-scrubbing procedure. The mild toxicity of the cleaning agents necessitated that the cleaning procedures be carried out under a laboratory fume hood.

The degree of success obtained with the moiré technique resides in the quality of the gratings applied to the surface of a specimen. In turn, quality gratings result from fine uniform coats of photoresist. As prior studies have indicated, resist application around fastener holes can prove to be extremely difficult (2), (4). The buildup and/or sagging of the resist film around physical discontinuities produces less-than-quality moiré gratings in these areas. In areas where there is a buildup of resist, the applied gratings can easily be seen to vary in density. Where sagging of the resist occurs, no moiré grating will be present. These application problems appear to be surface-tension phenomena rather than a result of improper cleaning.

Common methods of resist application include spinning, wiping, spraying, and rolling (4). Through the course of the study all application methods were tried and all were found deficient in some manner. Through trial and error, a resist application technique was developed that resulted in consistent and rapid reproduction of quality resist films. After the application of a resist coating, the specimens were baked for twenty minutes at 190°F (88°C).

Specimen gratings were printed into the photoresist coating by direct contact printing. The procedure and equipment used for printing was identical to that used by Cesarz (2), and Chandawanich (3). Figure 3.4 illustrates the optical system used for specimen grating production. The resist coated specimens were exposed through a grating submaster to unfiltered radiation from a 200 watt mercury arc lamp. Exposure times were forty seconds for a specimen-source distance of fifteen inches. Submasters used for grating production were made by Dr. Cloud while a

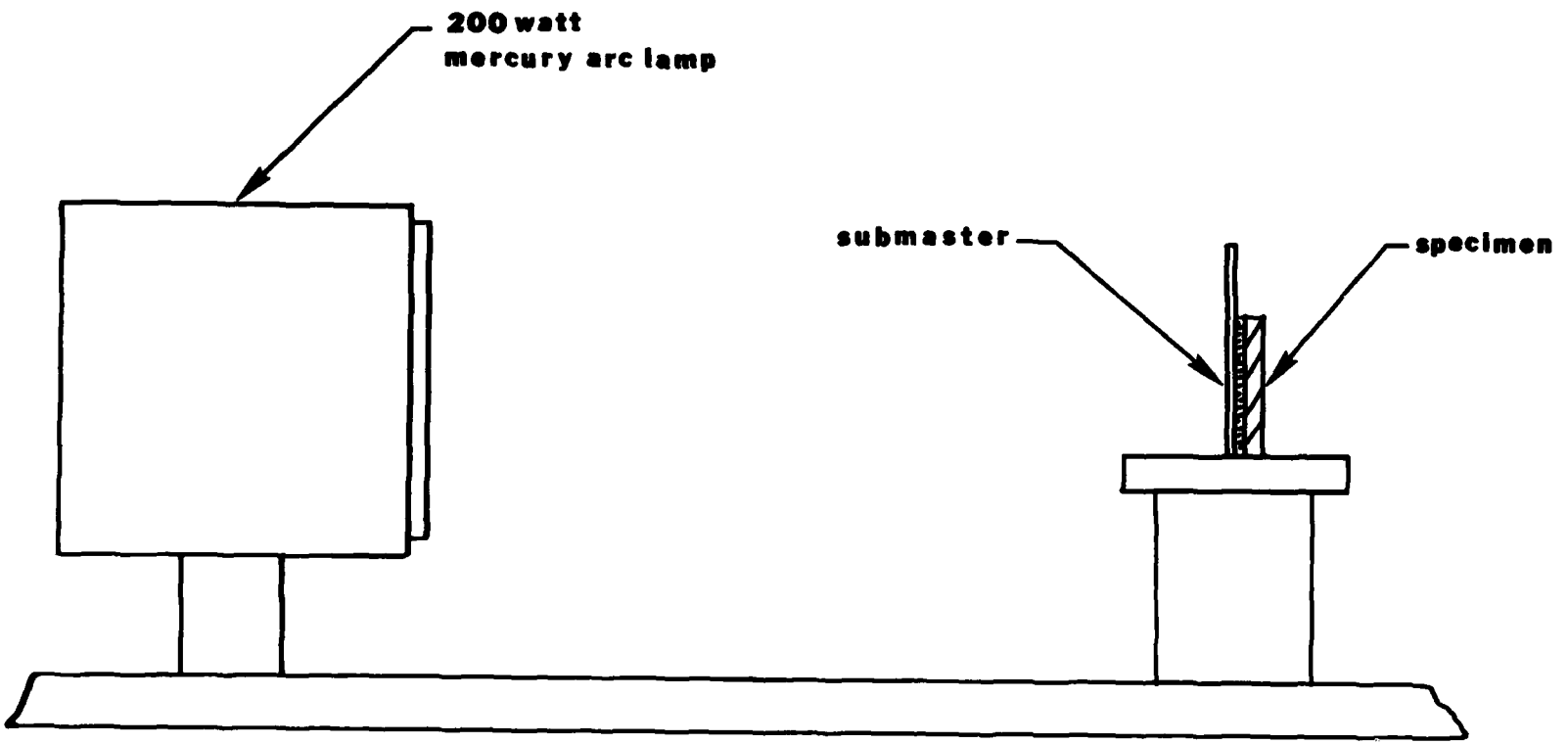

Figure 3.4 Optical System Used for Specimen Grating Production.

NCR Senior Resident Associate at AFML (4). Development of the resist was in a 1:1 dilution of Shipley AZ developer and water.

To enhance the visibility of the applied specimen gratings, a thin metal film was vacuum-deposited on top of the photoresist coating. Copper was used throughout the study. The copper film functions to obscure surface discontinuities which can cause difficulty in specimen photography (2), (4). The metal-coated gratings function partly as relief gratings in the photographic process. An excellent paper by Cloud, Radke and Peiffer (7) explores some of the possibilities for the vacuum deposition of metal film moiré gratings. The vacuum deposition unit used in the study was a Denton Vacuum model DV-502 manufactured by Denton Vacuum Inc., Cherry Hill, NJ, 08003.

3.1.4 Specimen Grating Photography

The formation of moiré fringes by the superposition of gratings was described in Section 3.1.2. The superposition of the gratings can be optical, physical, or a combination approach. Owing to out-of-plane displacements characteristic of the coldworking process, direct superposition of specimen and analyzer gratings is impossible. A combination approach termed Optical Data Processing was used as the method of moiré fringe formation. The technique as described by Cloud (4), (5), (6), is flexible and powerful. High-resolution photography is employed to store the image of the specimen grating on photographic plates. Specimen gratings are photographed in both their unstrained and strained states. The image of the grating on the photographic plate contains the information required in moiré analysis, and all data stored on the photographic plates are permanent and easily retrieved for future studies.

The optical system used for grating photography is illustrated in Figure 3.5. An 8 x 10 Linhof technical camera was used for the high-resolution photography of specimen gratings. The lens was a Schneider Optick Krueznach with an f4.5 lens of 11.8 inches (300 mm) focal length. The camera was mounted on a 3 x 6 foot cast iron lapping table resting on rubber air bags which served to insulate the table from building vibrations.

The camera was focused at a 2:1 magnification at an aperture setting of f11. For focusing, a blank photographic plate of the same thickness and type used in the specimen photography was developed, fixed, and mounted in a 4 x 5 plate holder which had the separator removed. The image of the specimen in the emulsion plane was examined with a microscope which had been adjusted to focus in the emulsion while its base rested on the opposite side of the film plate. The image of the specimen grating could then be checked over the entire area of interest for maximum sharpness and contrast. This focus procedure was rather tedious, but it did not need to be repeated as long as the photographic system was not disturbed.

Agfa-Gavert 10E56 Holotest film plates were used for the collection of specimen data throughout the study. The Agfa plates proved to be excellent in quality and performance. Development of the Afga plates was in Kodak HRP developer using a standard dilution of two parts water to one part HRP. Normal development times ranged from one to three minutes and was stopped when estimated light transmission of the plates approached fifty percent. Plates were fixed three to five minutes in Kodak Rapid Fixer.

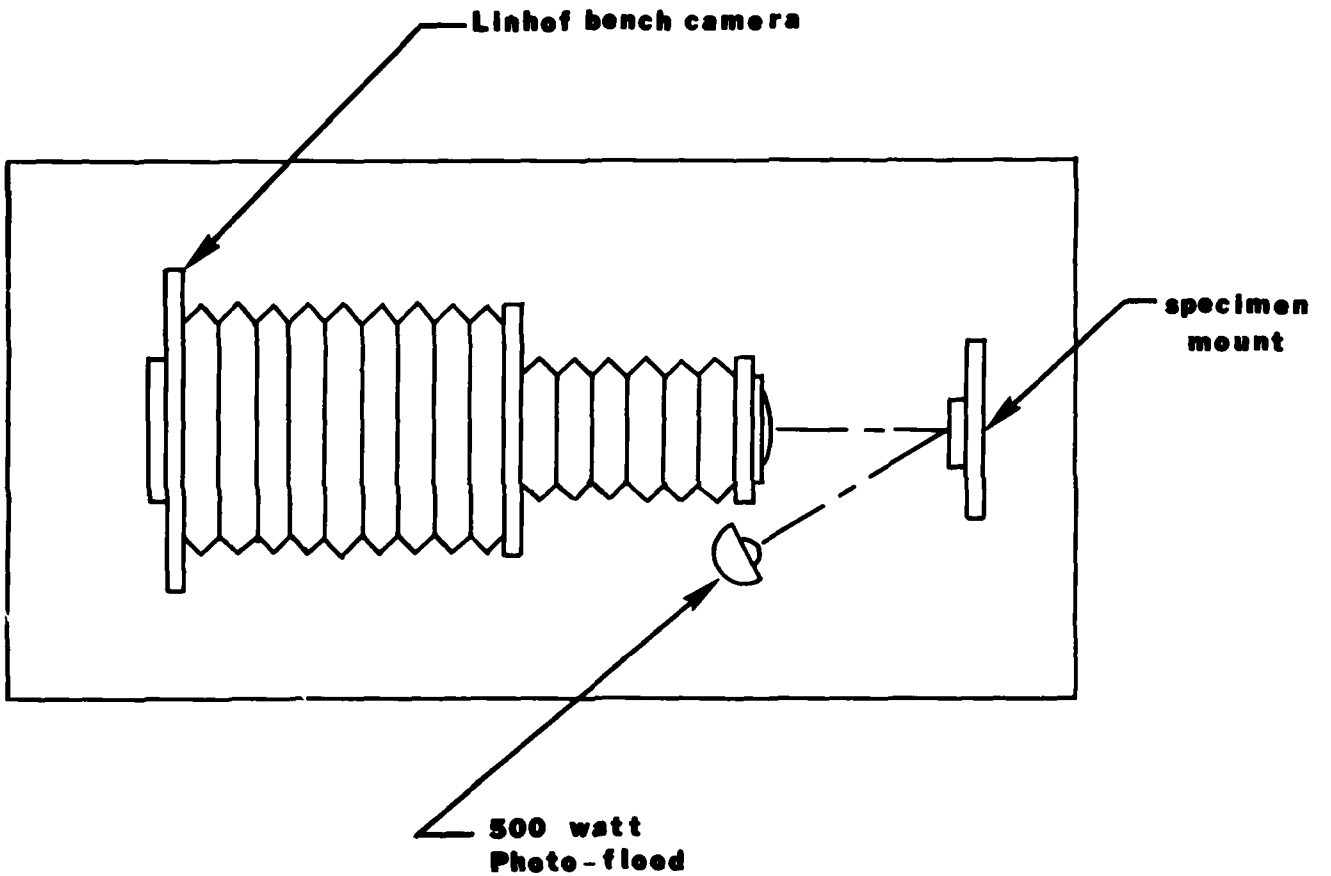

Figure 3.5 Optical System Used for Specimen Grating Photography.

3.2 Optical Data Processing System

3.2.1 Coherent Optical Data Processing

Coherent optical data processing is an optical spatial filtering process that enables the experimentalist to bypass some of the pitfalls of in real-time interferometry. The direct superposition of photoplates does not exploit the full potential of the information that is stored in the photoplates. Increased sensitivity and control of the measurement process is obtained by utilizing the basic procedures of optical data processing. The function and the theory behind optical data processing is outlined in papers and reports by Cloud (4), (6), and Duffy (8). The following discussion presents relevant aspects from Clouds work but does not offer a comprehensive treatment.

Physical phenomena used by Cloud to explain the optical filtering process are the diffraction of light by a grating and the Fourier transform properties of a lens. These two physical phenomena can both be used to explain moiré fringe formation and fringe multiplication. As noted, both treatments can be used as the single explanatory model; or the two approaches can be combined and pursued to a single consistent model (4). The diffraction model is presented here.

3.2.2 Diffraction by Superimposed Gratings

The diffraction model looks at the diversion of portions of an incident beam of light as it impinges on two superimposed gratings. Figure 3.6 illustrates the behavior of a single beam as it passes through a sinusoidal amplitude or phase grating. The beam is divided into three parts or diffraction orders. The zero diffraction order is the undisturbed portion of the beam that passes directly through the grating and

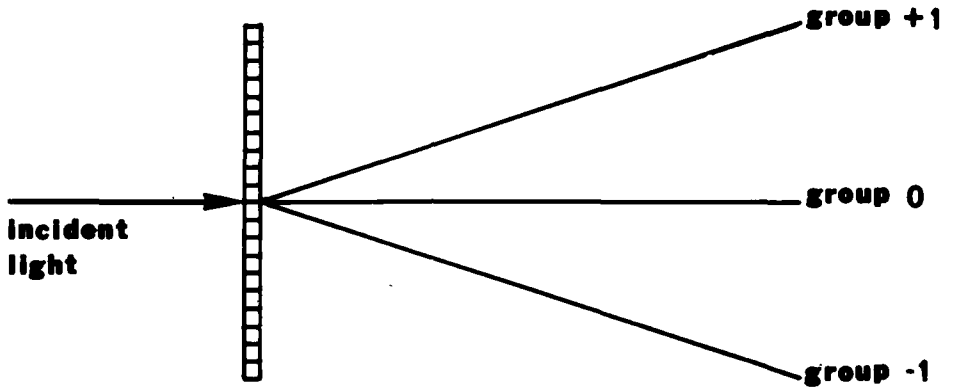

Figure 3.6 Diffraction of a Single Beam Passing Through a Sinusoidal Amplitude Grating.

undergoes no diffraction. The other diffraction orders are numbered consecutively, either positive or negative, as they increase in their angular separation from the path of the incident beam. The angle of diffraction, θ, is dependent upon the spatial frequency (lines/inch) of the gratings, the angle of incidence, and the wavelength of the light used for illumination.

When two sinusoidal amplitude gratings of nearly equal spatial frequency are superimposed, diffraction of the incident beam occurs at each of the gratings as illustrated in Figure 3.7. It can be seen that one beam passing through the two gratings gives rise to five diffraction orders. As illustrated, the second ray group contains beams diffracted only at the second grating and the first ray group is composed of beams diffracted from either of the two gratings. The two beams that comprise this first ray group diverge slightly from each other. The angular separation is due to the pitch and orientational differences that occurs between the two gratings.

A lens or imaging system (as in Figure 3.8) can be inserted into the paths of the beams, and this causes the rays of one group to converge and overlap. From the rays of group 1, the imaging system constructs two separate images that lie atop one another. Rays diffracted from the first grating will focus at a position slightly displaced from those rays diffracted at the second grating. The two superimposed images will interfere with one another provided that the component beams come from a source with sufficient coherence potential. The resulting interference pattern is a classic example of two beam interferometry. The degree of interference between the two images is dependent upon the spatial frequencies of the two gratings. A pattern of interference

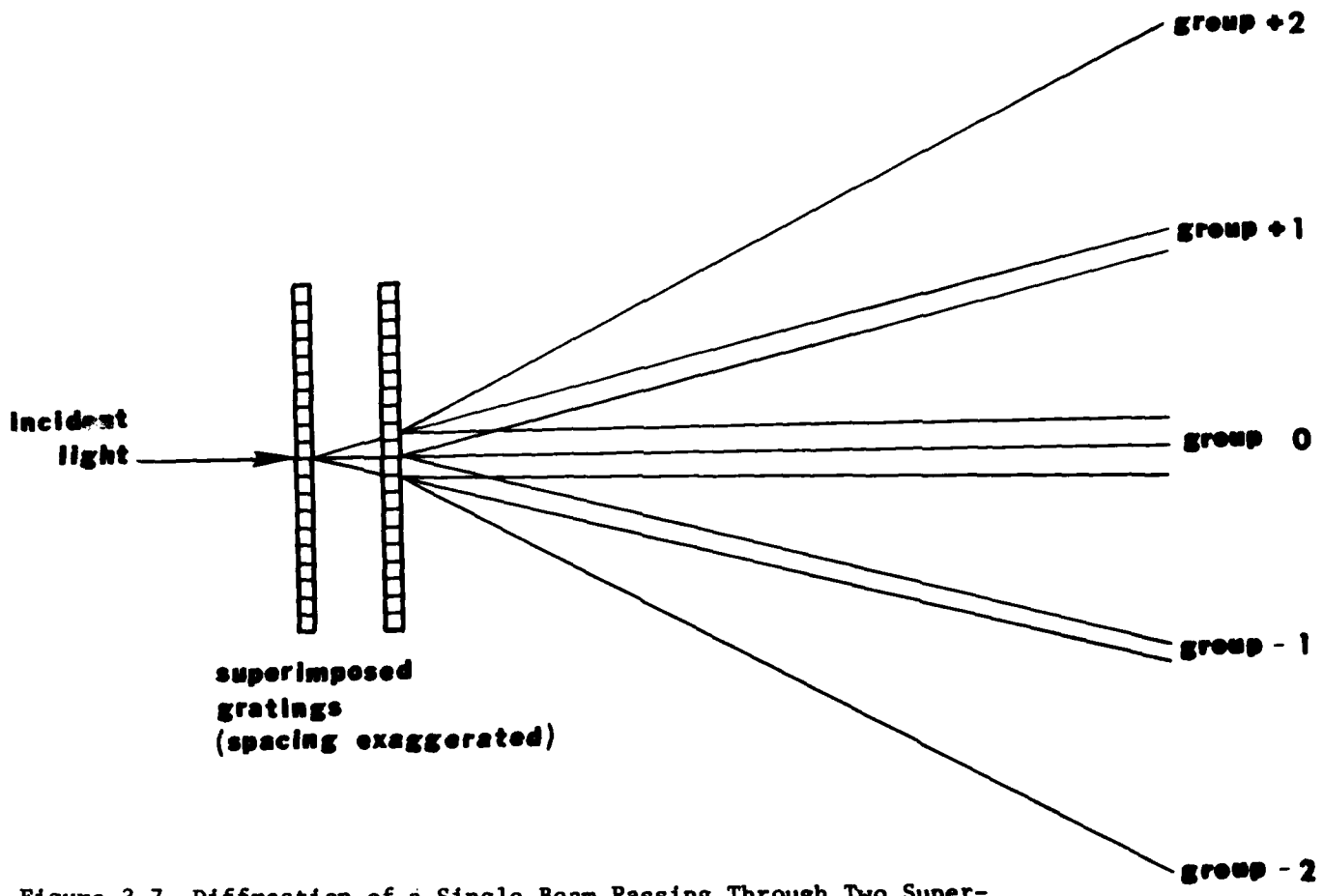

Figure 3.7 Diffraction of a Single Beam Passing Through Two Superimposed Sinusoidal Gratings of Nearly Equal Spatial Frequency.

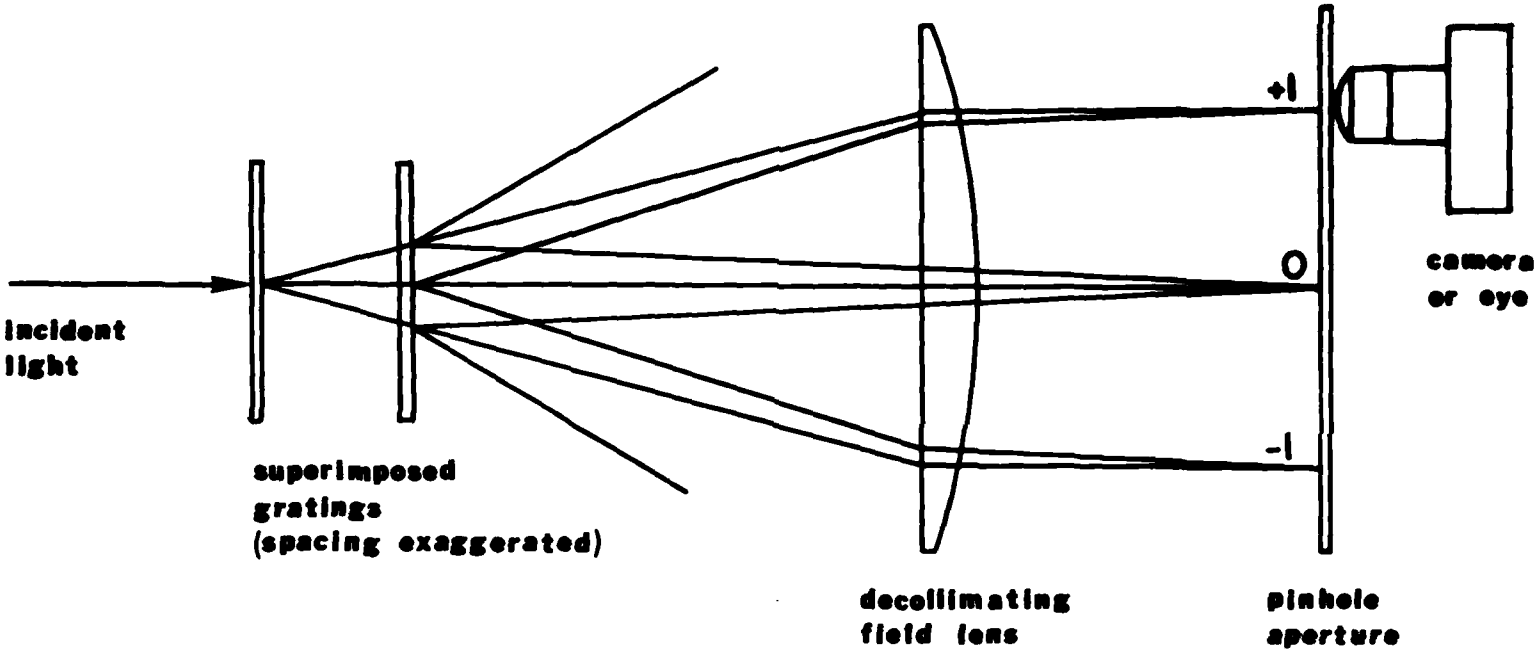

Figure 3.8 Imaging System Used in the Formation of Moiré Interference Patterns. From Cloud (4).

fringes becomes visible if the eye or a camera is placed at the focal plane of the imaging system and is used to view the image formed in a ray group.

The concept of the variability of moiré sensitivity arises when consideration is given to the higher order diffractions at the two superimposed gratings. Higher order diffractions lead to numerous ray groups or clusters of diffraction orders at the focal plane of the imaging system. Figure 3.8 illustrates that at the focal plane, these ray groups are oriented in a symmetrical distribution about the zero ray group. Each ray group corresponds to a grating frequency that is a multiple of the original base frequency of the two gratings. The image formed from any ray group contains an interference pattern that could have been obtained from two gratings having an effective grating frequency equal to the original base frequency multiplied by the ray group number. Such exploitation of higher order diffractions, leads to moiré sensitivity multiplication. There are some difficulties with this multiplication technique. For example, the fringe pattern formed in each of the ray groups are not identical in overall clarity or intensity. Background noise caused by other diffractions can sometimes obscure and render useless the interference pattern formed in the image.

Consideration must be given to a common experimental situation in which the two superimposed gratings are very different in spatial frequency. This occurs when one grating is a multiple of the other plus some small additional mismatch, as mentioned in Section 3.1.2. The diffractions occurring at the two gratings are now somewhat more complicated as is the composition of the various ray groups. Figure 3.9 illustrates the diffractions occurring at the gratings and the rays that

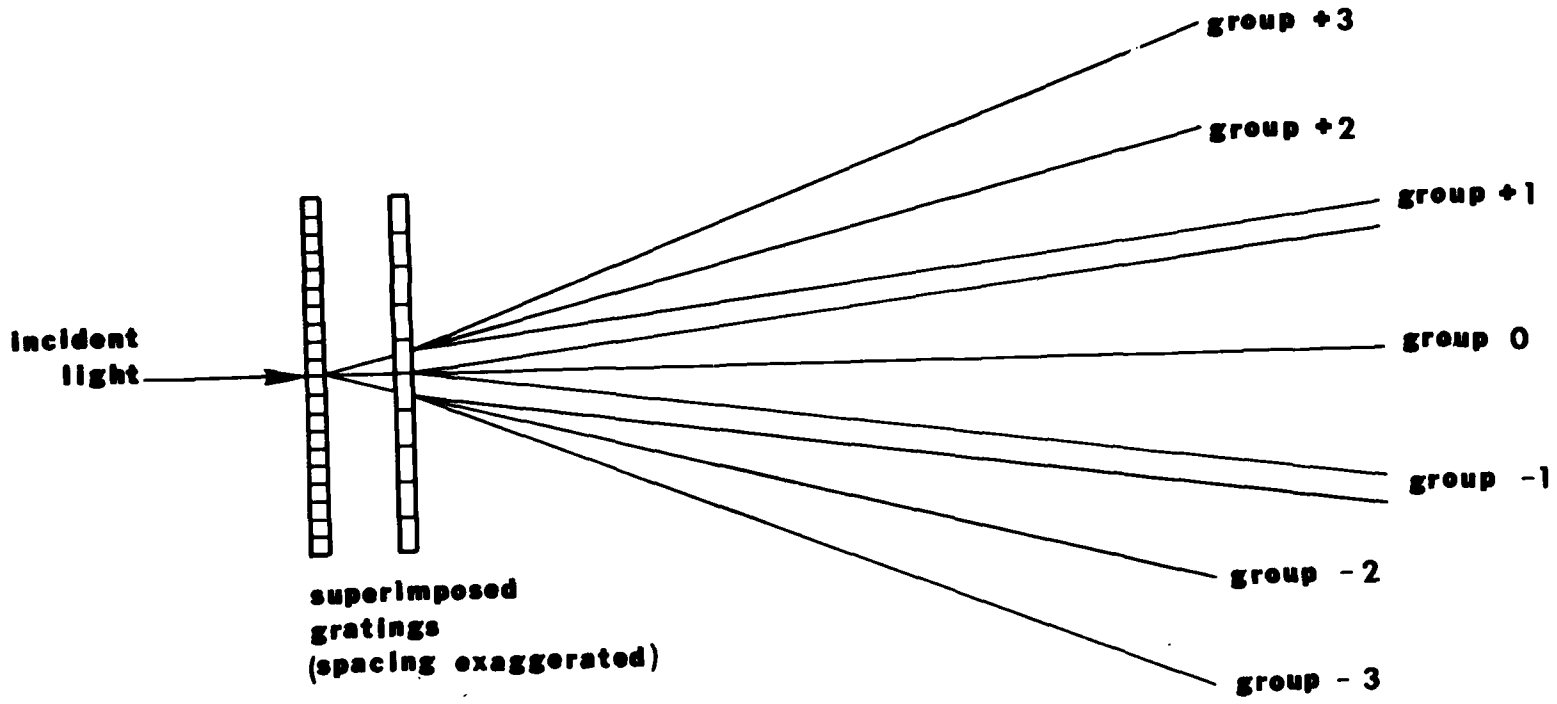

Figure 3.9 Diffraction of a Single Beam Passing Through Two Superimposed Gratings of Different Spatial Frequency.

comprise each of the associated ray groups, for the case when the fine grating was twice the frequency of the coarse grating. Given the natural attenuation of the higher order diffractions, only two of the component rays in any rays group will usually interact to form an interference pattern. The interference pattern so generated will correspond to an interference pattern constructed from two gratings of the higher spatial frequency. Again, general background noise that is present in some ray groups can serve to obscure the interference pattern. Since the interference pattern in all ray groups is identical, it is best to use the ray group that provides the best fringe visibility. Throughout the study, this method of mismatched gratings was utilized as the means of moiré fringe pattern multiplication.

Application of the diffraction models to moiré analysis requires only that the previous models be applied to a whole field. In whole field analysis, specimen gratings after deformation are not uniform but vary in pitch and orientation from point to point. Superposition of a uniform analyzer grating with the nonuniform specimen grating will result in fringes which will also vary in their orientation and spacing.

An important complication noted by Cloud (4), is that it is neither wise nor is it possible to work with sinusoidal gratings. As a result, there will exist higher order diffractions at each of the two gratings. The number or diffractions produced by a single ray passing through a nonsinusoidal grating is dependent upon the sharpness of the grating. Sharpness is the degree to which the grating approaches a rectangular wave periodic structure. As a result, the general interference observed in an image will involve more than two component images or beams, but

the higher order diffractions might be attenuated to a degree where only the basic two beams in any ray group are of any consequence.

3.2.3 Coherent Optical Fourier Data Processing

Coherent optical Fourier data processing arises from consideration of the Fourier transform properties of a lens and the optical filtering procedures that can be used at the transform plane of the lens. For the optical system illustrated in Figure 3.8, the two superimposed gratings act as an optical signal to the collimated light that passes through. The light is modulated by diffraction at the two gratings and is brought to a focus by the decollimating lens. The focal plane of the lens is termed the Fourier transform plane. It is at the transform plane that there appears a diffraction pattern that is related to the square of the amplitude or of the Fourier transform of the optical signal (superimposed gratings). As in the diffraction model, at the transform plane this diffraction pattern appears as a row of dots (ray groups); the position and brightness of these dots is indicative of the various harmonics of the grating. This occurs because a lens acts as a simple Fourier transforming device (4).

Coherent optical data processing, or spatial filtering, is the alteration of the light distribution at the transform plane. In moiré analysis, spatial filtering is accomplished by the elimination of all frequency components undesirable in the formation of the moiré interference pattern. In reference to the diffraction model, this filtering process is analogous to the elimination of all diffraction orders except the one of interest. Filtering at the transform plane is accomplished with an opaque mask with a single pinhole aperture. When the eye or

a camera is placed at this aperture, their lens systems serve to form the inverse Fourier transform and to recover the moiré interference pattern carried in the signal.

3.2.4 Moiré Fringe Pattern Photography

The optical Fourier data processing system is illustrated in Figure 3.10. The entire system rests upon a twenty foot steel optical bench that was designed and built at Michigan State University. Light emanating from a Jodon 12 MW helium-neon laser is passed through a Jodon pinhole spatial filter equipped with a 20X objective. Two thirteen inch diameter field lenses, each with a focal length of one meter, serve as collimating and transform lenses in the optical system. Light from the point source is collimated by the first lens, diffracted by the superimposed grating, and then brought to a focus by the decollimating lens. The imaging lens was placed at the focal plane of the decollimating lens. Fringe pattern photographs were obtained with a 35 mm Nikon F camera equipped with one extension ring and a 95 mm telephoto lens. An opaque filter with a 1/32 inch diameter pin hole positioned in its center was used to eliminate the undesired ray groups. It was found that slight modification of the geometry of the pinhole aperture could sometimes lead to better visibility of the fringe pattern in the ray group. Fringe pattern photographs were taken at exposures of 1/4 second at f4.5 using Kodak Plus-Xpan 135 black and white film. The film was processed according to instruction in Kodak D-76 developer, Kodak indicator stop bath, and Kodak fixer.

Enlargements were made on 8 x 10 sheets of F-4 Kodabromide paper. The lens used in the enlarging process was a Leitz Wetzlar Focotar

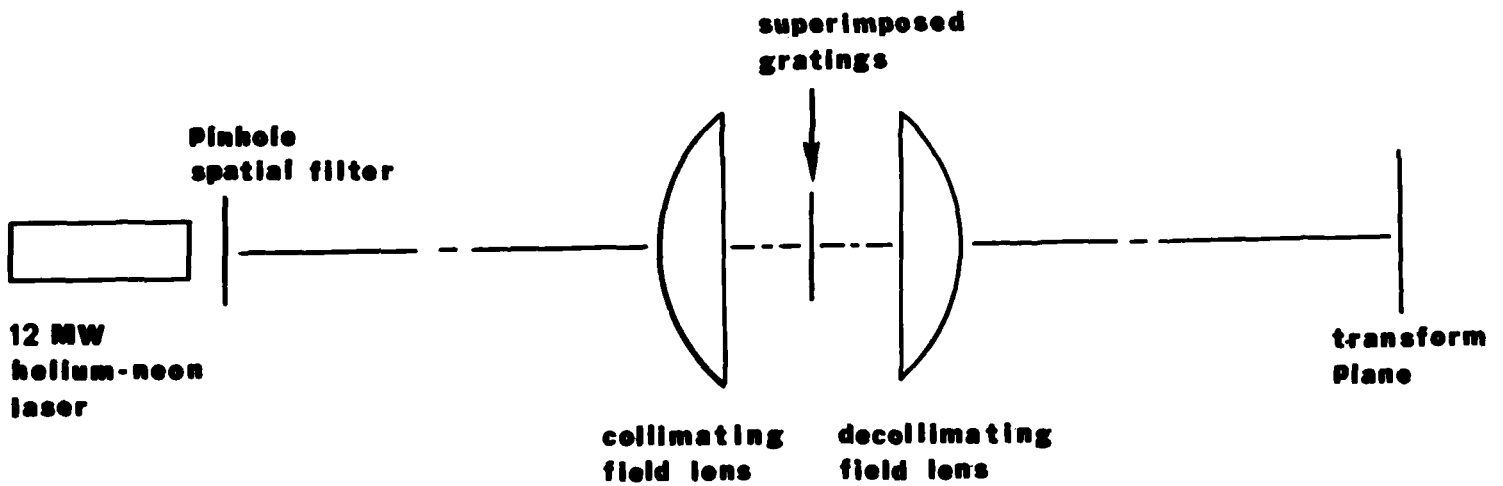

Figure 3.10 Schematic of the Coherent Optical Data Processing System.

1:4.5/50 at f4.5. The paper was processed in Kodak Dektol developer, Kodak indicator stop bath, and Kodak fixer.

CHAPTER 4

METHODS OF ANALYSIS AND PRESENTATION OF TYPICAL RESULTS

The various geometric configurations of the test patterns require a concise and systematic method of comparison in order to aid in subsequent analysis. It is the purpose of this section to outline the method used in the presentation of experimental results and to present generalities which are valid for all the test specimens.

4.1 Labeling System

The in-line fastener patterns had all fastener holes aligned on a common axis. This common axis has been termed the major axis and it connects the centers of adjacent fastener holes. Perpendicular to the major axis is the minor axis, Figure 4.1a illustrates the orientations of these axes. Measurements obtained along the major axis were the fastener hole diameters, center to center hole separations, edge to edge hole separations and distances to fiducial marks. Obtained along the minor axis were measurements of the fastener hole diameters and the distances to the fiducial marks. The major and minor fastener hole diameters are illustrated in Figure 4.1b. A complete and concise map of each specimen surface is constructed from these measurements.

Illustrated in Figure 4.2 is the labeling technique used to identify the fastener hole pair under study. In the illustration, two fastener

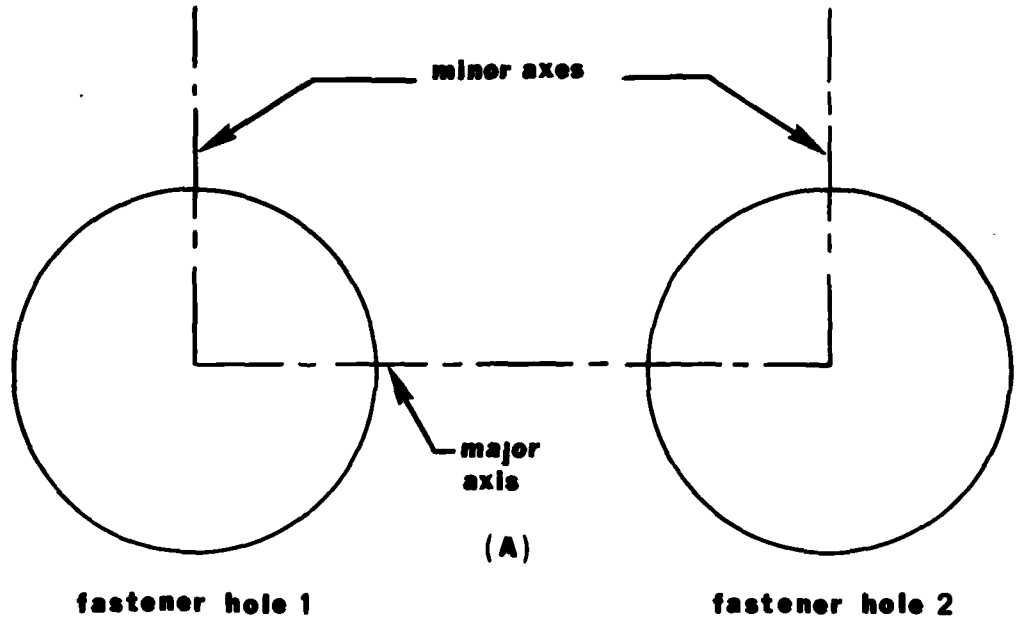

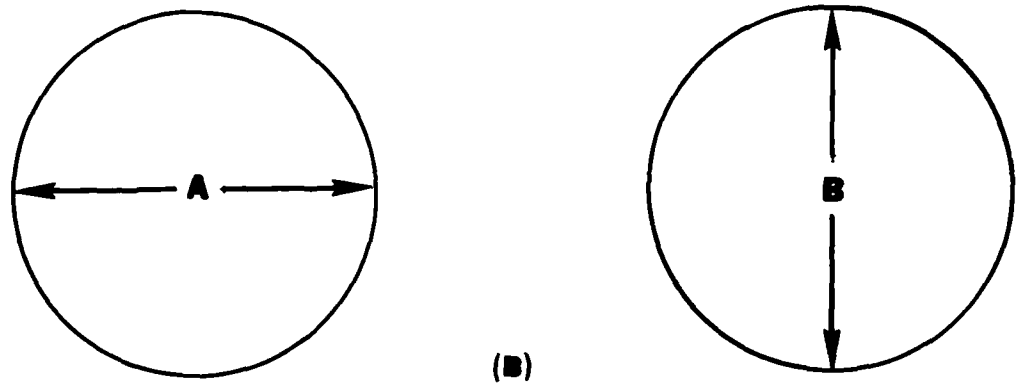

A: major diameter

B: minor diameter

Figure 4.1 Labeling Technique Used in the Identification of Inter-Hole Axes and Fastener Hole Diameters.

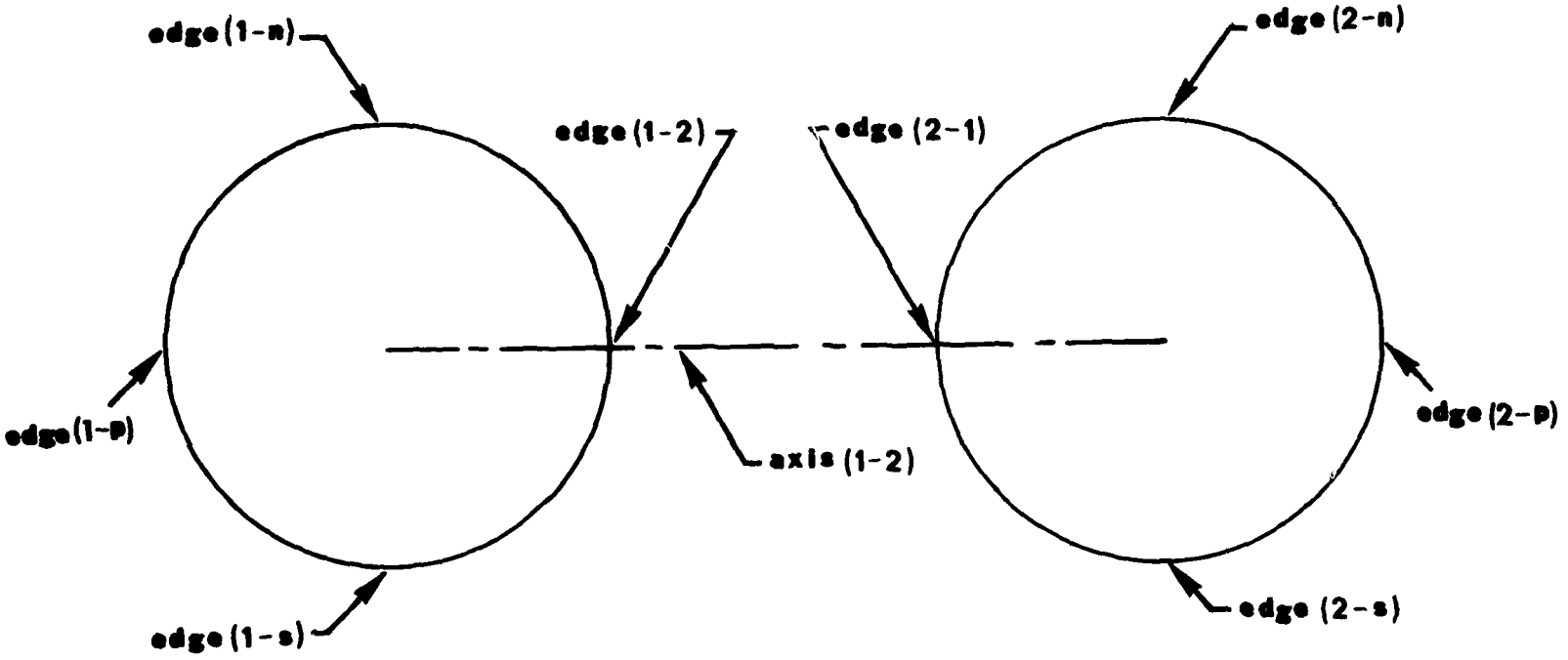

Figure 4.2 Labeling Technique Used in Identifying Areas of the Fastener Hole Pair Under Study.

holes are aligned on the major axis. The line segment separating the hole pair has been labeled axis (1-2). In this notation, axis (1-2) will refer to the axis line that connects the centers of fastener holes #1 and #2.

Each fastener hole edge is labeled as to its location on the major axis and the fastener hole of which it is a part. In the labeling process, the fastener hole number of which the edge is a part is given first and its followed by the number of the adjacent fastener hole. Edge (1-2) is the edge of fastener hole #1 adjacent to fastener hole #2. Likewise edge (2-1) is the edge of fastener hole #2 adjacent to fastener hole #1. Along the major axis referencing edge labels may contain a (P) indicating surrounding plate material. Along the minor axis, edge labels incorporate (N) for north and (S) for south.

The same labeling and orientation technique are also applied to the double-row fastener patterns. No alterations or special considerations are required for application to the two-row geometries.

4.2 Typical Fringe Patterns

The stepwise progression of the coldworking process is illustrated by the series of photographs in Figure 4.3. These photographs are typical of the fringe patterns obtained by the coldworking of adjacent fastener holes. The basic geometry of the fringe patterns for each stage in the coldworking process never changed to a noticable degree through the course of the study. The small and subtle changes in the fringe patterns for each specimen were revealed only when the individual fringe pattern photographs were digitized. It is these small changes in the fringe patterns that differentiate between the subsequent strain

distributions. The fringe pattern photographs are presented here so that there is no need to include them repeatedly in each of the subsequent sections. The analyzer grating used in the production of these and all data photographs had a spatial frequency of 980 lines per inch. No moiré sensitivity multiplication was utilized in the optical data processing stage.

Figure 4.3a is typical of a "baseline" or zero strain fringe pattern. The fringes result from mismatch between specimen and analyzer gratings, and are perpendicular to the major axis that connects the centers of fastener holes #1 and #2. In the photograph, fastener hole #1 is on the left and fastener hole #2 is on the right. Figure 4.3b is the fringe pattern along axis (1-2) after fastener hole #1 has been coldworked. The fringes emanate from the edge of fastener hole #1 and proceed in the direction of fastener hole #2. An important note is that, for the pitch mismatch used, fringes which are closer together than are the baseline fringes denote compressive strains; and fringes farther apart than the baseline fringes denote tensile strains. From the above, it can be determined that large compressive strains exist at edge (1-2) of fastener hole #1 and decrease as edge (2-1) of fastener hole #2 is approached. Figure 4.3c is the fringe pattern along axis (1-2) after fastener hole #2 has been coldworked. There are many more fringes in this pattern than there are in either the baseline or the initial coldwork fringe patterns. Closely spaced fringes near edge (2-1) of fastener hole #2 denote a region of high compressive strains.

It is important to recognize the definite nonsymmetry of this fringe pattern in that the fringe pattern is shifted toward fastener hole #2. Again, this is relevant to all data photographs in that the

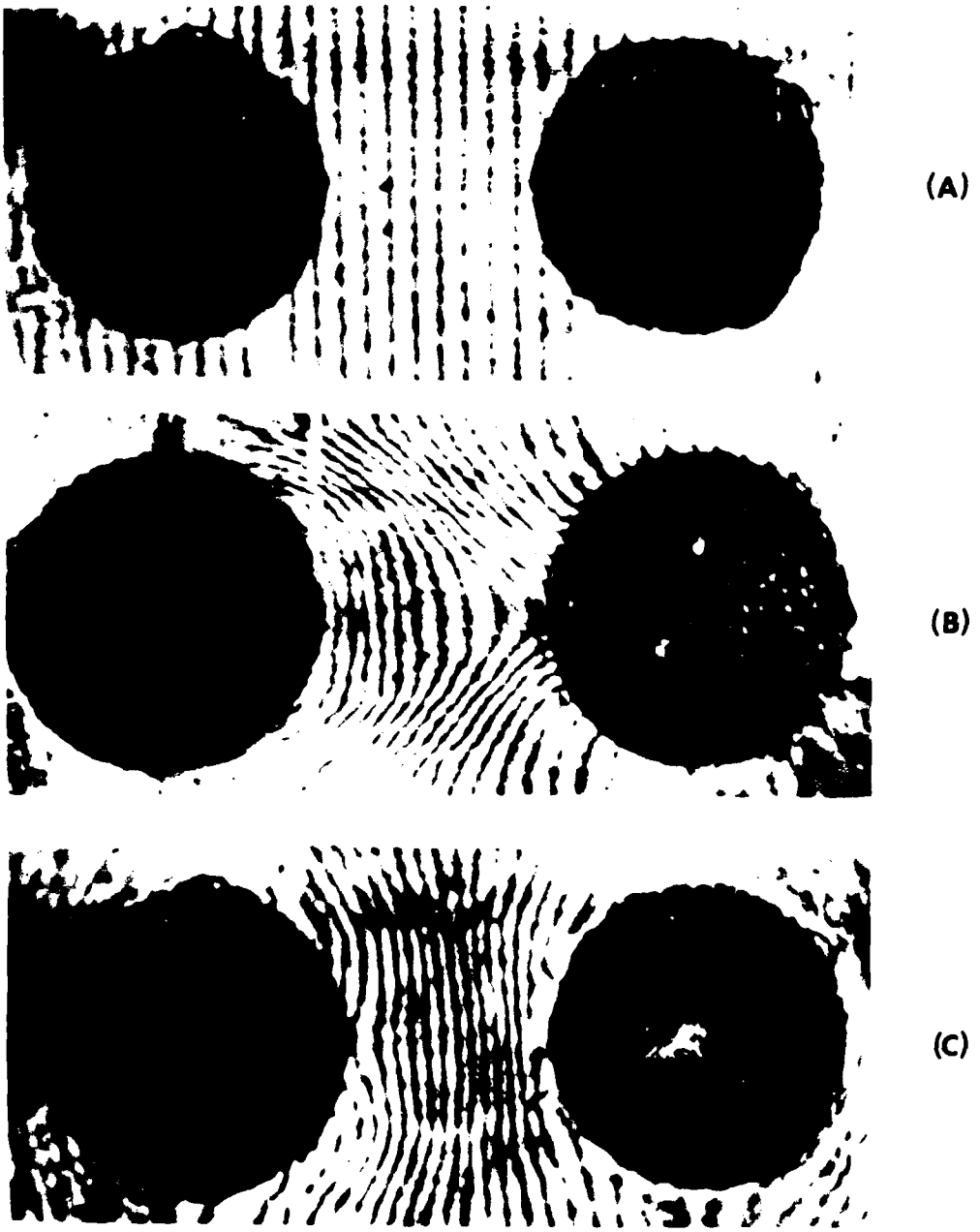

Figure 4.3 Typical Moiré Fringe Patterns Obtained when Two Adjacent Fastener Holes are Sequentially Coldworked; (A) Baseline, (B) Left Fastener Hole has been Coldworked, (C) Both Fastener Holes have been Coldworked.

fringe patterns are shifted toward the initially uncoldworked adjacent fastener hole. This means in general, that final strains near the initially uncoldworked hole are higher than those near the initial coldworked hole.

4.3 Data Reduction

Utilized for this study was a proven numerical data processing and plotting technique developed for moiré analysis by Cloud (4). Cloud supervised the development of the computer programs while an NCR Senior Research Associate at AFML. A listing of the programs along with further descriptions are contained in Technical Report AFML-TR-78-153 (4). The programs were adapted to the CDC 6500 computational facilities at Michigan State University and were tested to insure compatability.

Program "Moiré" is a detailed moiré analysis program. The purpose of this program is to allow for the detailed study of each data set and the results it produced. Graphical output from program "Moiré" is illustrated in Figures 4.4, 4.5, and 4.6. As noted in Figure 4.4, the program allows a pitch mismatch to be used. In this figure both the baseline and data fringe orders along a single radial generator are plotted. Errors in the input will immediately show up as serrations or some gross discontinuity in the plot. Radial displacements are illustrated in Figure 4.5 and the radial strains are shown in Figure 4.6.

Program "Cloud" is internally similar to program "Moiré" but allows for the input of a maximum of nine different data sets. Each data set is individually processed and the resulting strain distributions are plotted to common axes. Program "Cloud" was used primarily to test for repeatability and to establish the experimental error in the digitizing process. Graphical output from program "Cloud" is illustrated in Figure

4.7. This plot is representative of those obtained throughout the study and serves to illustrate the repeatability and scatter in the digitizing process. To construct these composite strain distributions, data and baseline photographs were digitized five to nine times and then randomly combined for analysis. Errant strain distributions signaled problems in either the coldworked or baseline information sets. The most common problem found in this way is missed fringes. Diagnosis of the faulty data was confirmed and corrected by use of program "Moiré" and its complete set of graphical output. In both programs, all graphical output is numerically generated.

4.4 Digitizing of Data Photographs

The analysis programs require that the locations of baseline and data fringes be input in numerical format and in specimen dimensions. This was accomplished by scaling and digitizing the 8" x 10" data and baseline fringe pattern photographs on a Micro-Dataizer manufactured by ATCO Corporation of Rockville, MD 20850. Standardization of the digitizing process was required so that direct comparisons could be made between the various fastener geometries. All photographs were digitized in a manner such that, in all stages of the coldworking process, digitizing progressed from the initial coldworked fastener hole toward the next adjacent fastener hole. By digitizing in this manner, all graphical plots of the strain distributions possess common axes and hole edges.

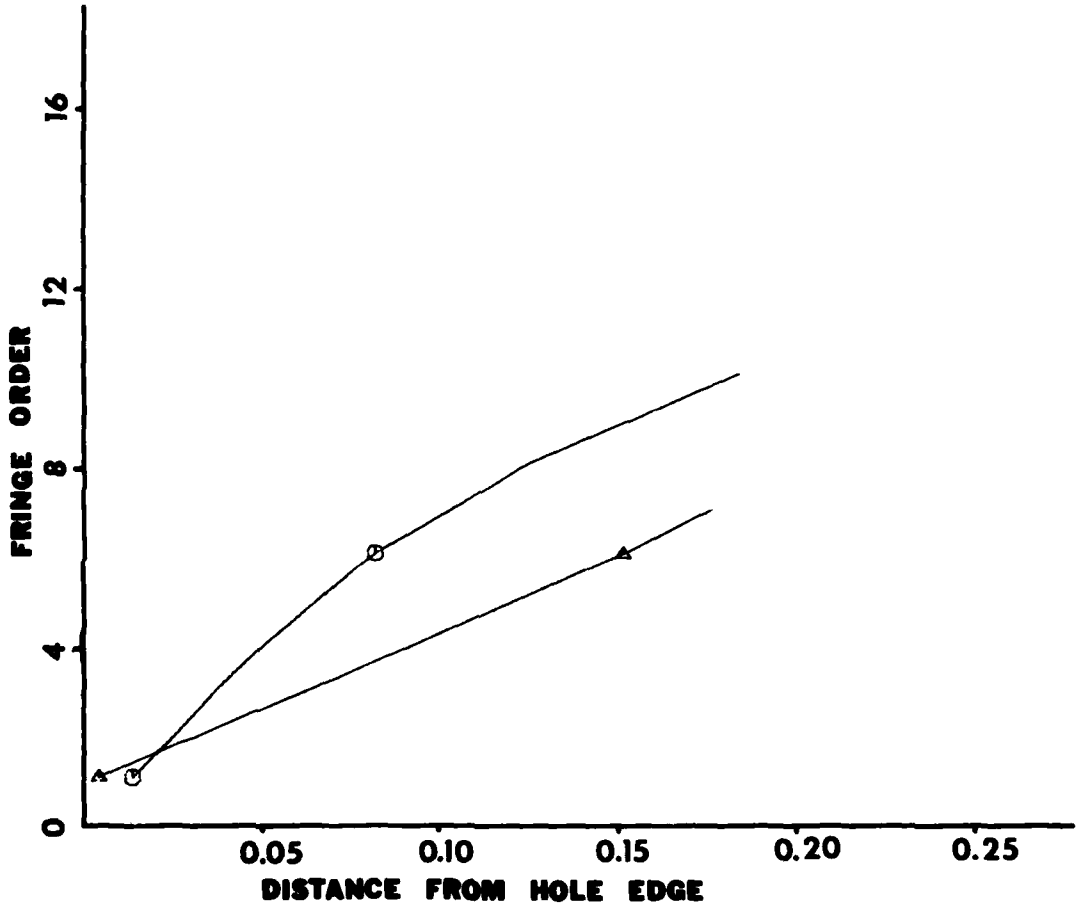

Figure 4.4 Typical Plot of Baseline and Coldwork Input Data (Program Moiré).

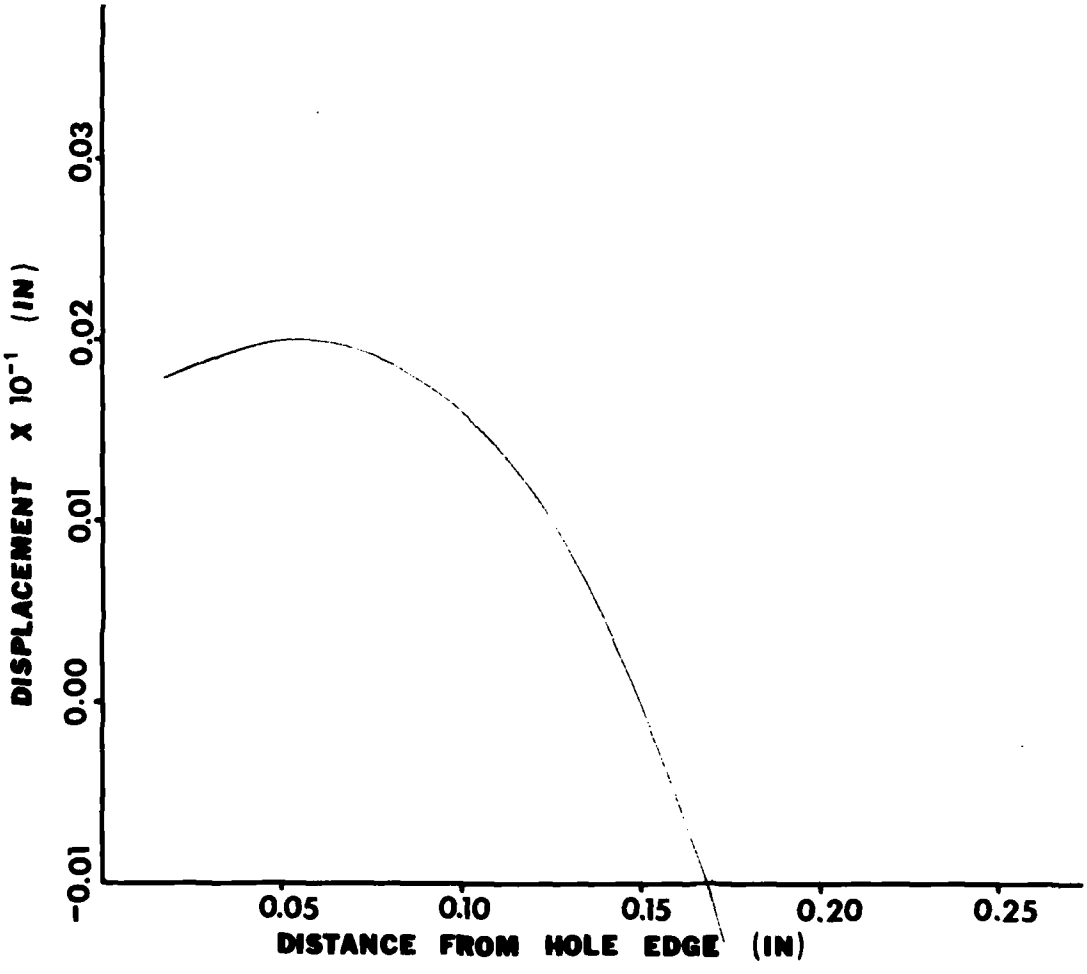

Figure 4.5 Typical Plot of Radial Displacement (Program Moiré).

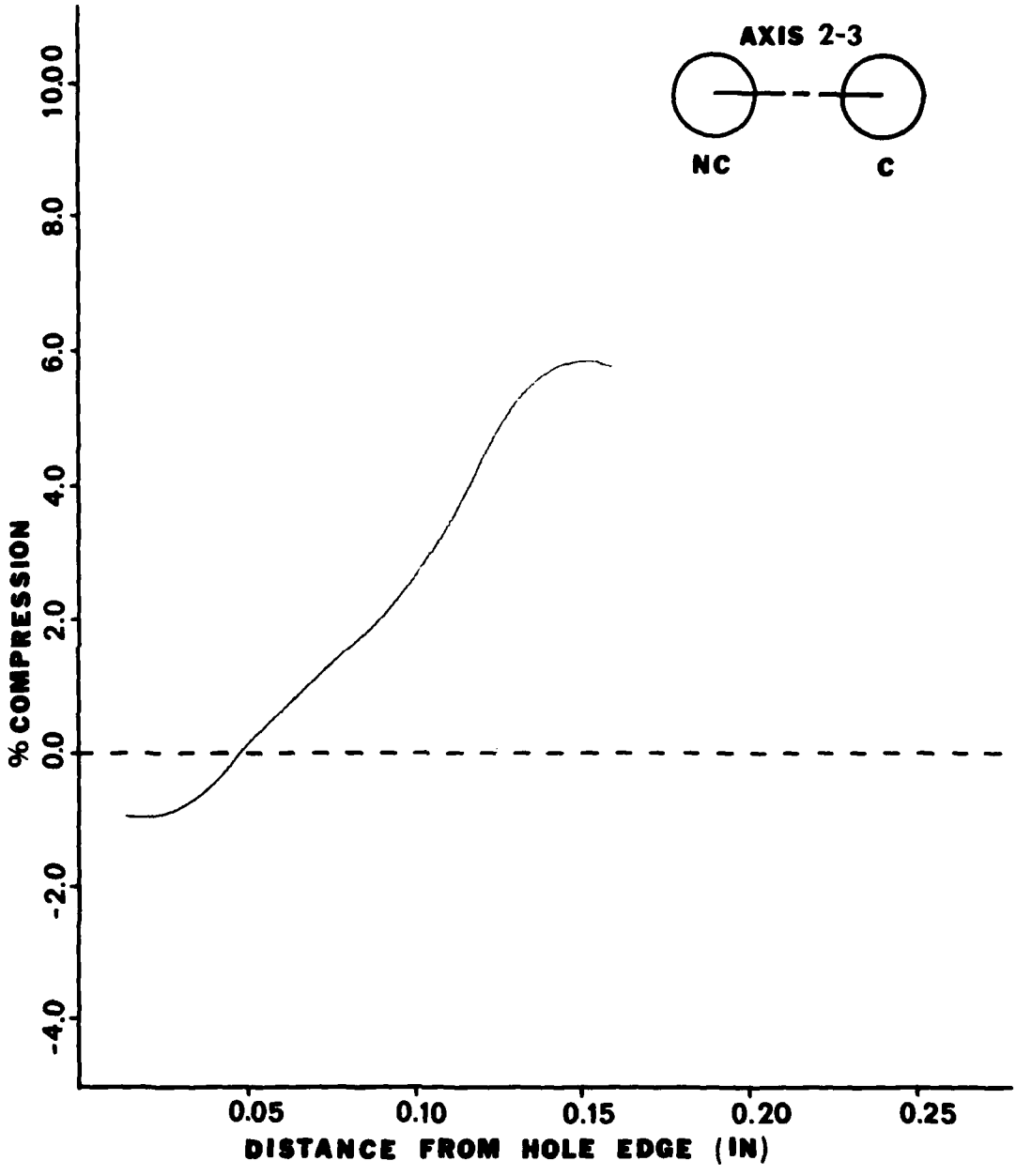

Figure 4.6 Typical Plot of Radial Strain (Program Moiré).

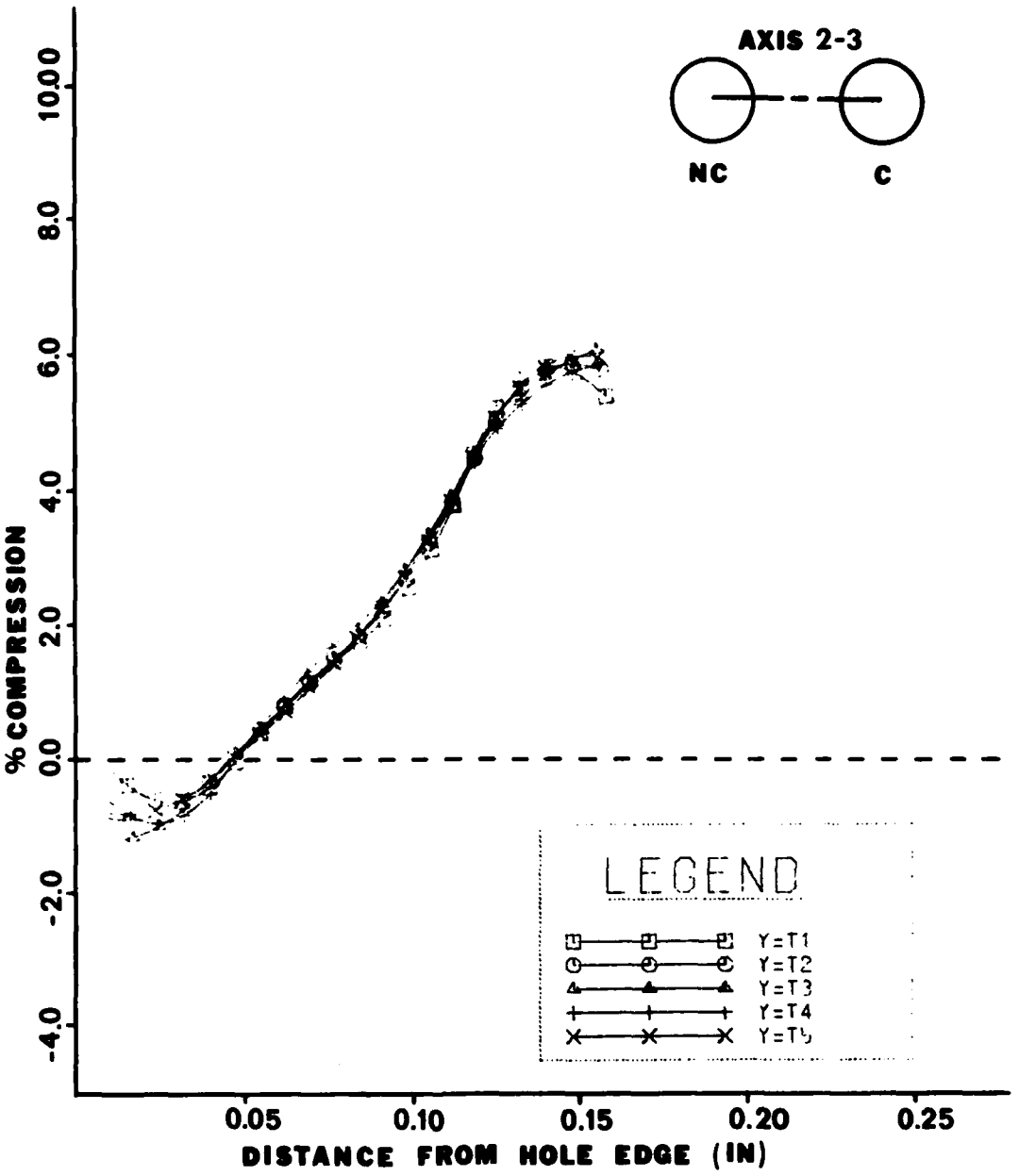

Figure 4.7 Typical Summary Plot of Radial Strains (Program Cloud).

CHAPTER 5

EXPERIMENTAL RESULTS AND CONCLUSIONS

Presented in this section are the experimental results and conclusions of the investigation. The results are presented in a manner such that logical progress is made through the various experimental test patterns.

The two-hole in-line fastener patterns are the subject of Section 5.1. These test specimens have the same level of coldwork but possess different hole separations. Evidence is given that the linear superposition of strain fields may be valid for certain fastener situations.

Section 5.2 is devoted to a three-hole in-line fastener pattern that has been coldworked in a nonconsecutive order. It is inferred that nonsymmetric strain distributions can result from a symmetric fastener pattern coldworked in nonconsecutive order.

A multiple hole in-line fastener pattern coldworked in consecutive order is the subject of Section 5.3. It is indicated that the coldworking process is dynamic in that significant hole edge motion occurs and this can significantly alter the inter-hole strain distributions.

Section 5.4 considers the double-row fastener patterns and the possible influence strains that occur between adjacent coldworked fasteners as caused by coldworking an adjacent row of fasteners.

Within each section, results are presented in a manner such that geometrically similar inter-hole axes are compared. Each inter-hole axis is given individual consideration as to the reason for its resulting strain distribution. Conclusions appear at the end of each section and can be applied to those sections that follow, and by doing so, the basic mechanics of the interaction process take form and can be generalized. General conclusions resulting from the entire investigation are summerized in Section 5.5. Section 5.6 gives consideration to several areas of future research that are an outgrowth of this investigation.

5.1 Coldworking Two Hole In-line Fasteners

5.1.1 Introduction

This section presents the residual surface strains and hole edge displacements that occur between two coldworked fastener holes in the near-vicinity of one another. Relevant to this section are specimens #2 and #7. Specimen geometry and other pertinent information are furnished in Figure 5.1 and Tables 5.1, 5.2, and 5.3. One level of coldwork and two different hole separations were used to gain information on the mechanics of the interaction process. Geometrical symmetry between the two fastener patterns was an important factor in evaluating and comparing experimental results.

5.1.2 Experimental Results

Residual surface strains were measured along the axial line that connects the centers of the two adjacent fastener holes in each pattern. Figure 5.2 illustrates the strain distribution that exists after hole #1 of specimen #7 has been coldworked. The strain plot exhibits small

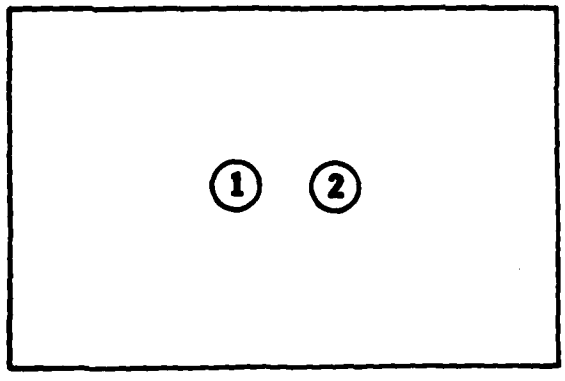

Figure 5.1 Two-Hole In-Line Fastener Pattern Used for Specimens #2 and #7.

TABLE 5.1 SPECIMEN DATA

SPECIMEN	HOLE NO.	INITIAL DIAMETER	RESIDUAL DIA. EXPANSION	RADIAL INTERFERENCE	MAX LOAD COLDWORK (LBS)
2	1*	0.2614	0.0032	0.0063	1047
	2	0.2614	0.0036	0.0061	848
7	1	0.2614	0.0036	0.0064	1414
	2	0.2614	0.0028	0.0064	1467

* Was coldworked three (3) times.

TABLE 5.2 HOLE EDGE MOTION - MAJOR AXIS

SPECIMEN	HOLE	EDGE	MOTION	EDGE	MOTION	SEPARATION
2	1	1-P	+0.0028	1-2	+0.0004	0.0024
	2	2-1	+0.0020	2-P	+0.0016	
7	1	1-P	+0.0004	1-2	+0.0031	0.0047
	2	2-1	+0.0016	2-P	+0.0012	

TABLE 5.3 HOLE EDGE MOTION - MINOR AXIS

SPECIMEN	HOLE	EDGE	MOTION	EDGE	MOTION
2	1	1-N	+0.0024	1-S	+0.0031
	2	2-N	+0.0024	2-S	+0.0024
7	1	1-N	+0.0008	1-S	+0.0043
	2	2-N	+0.0008	2-S	+0.0039

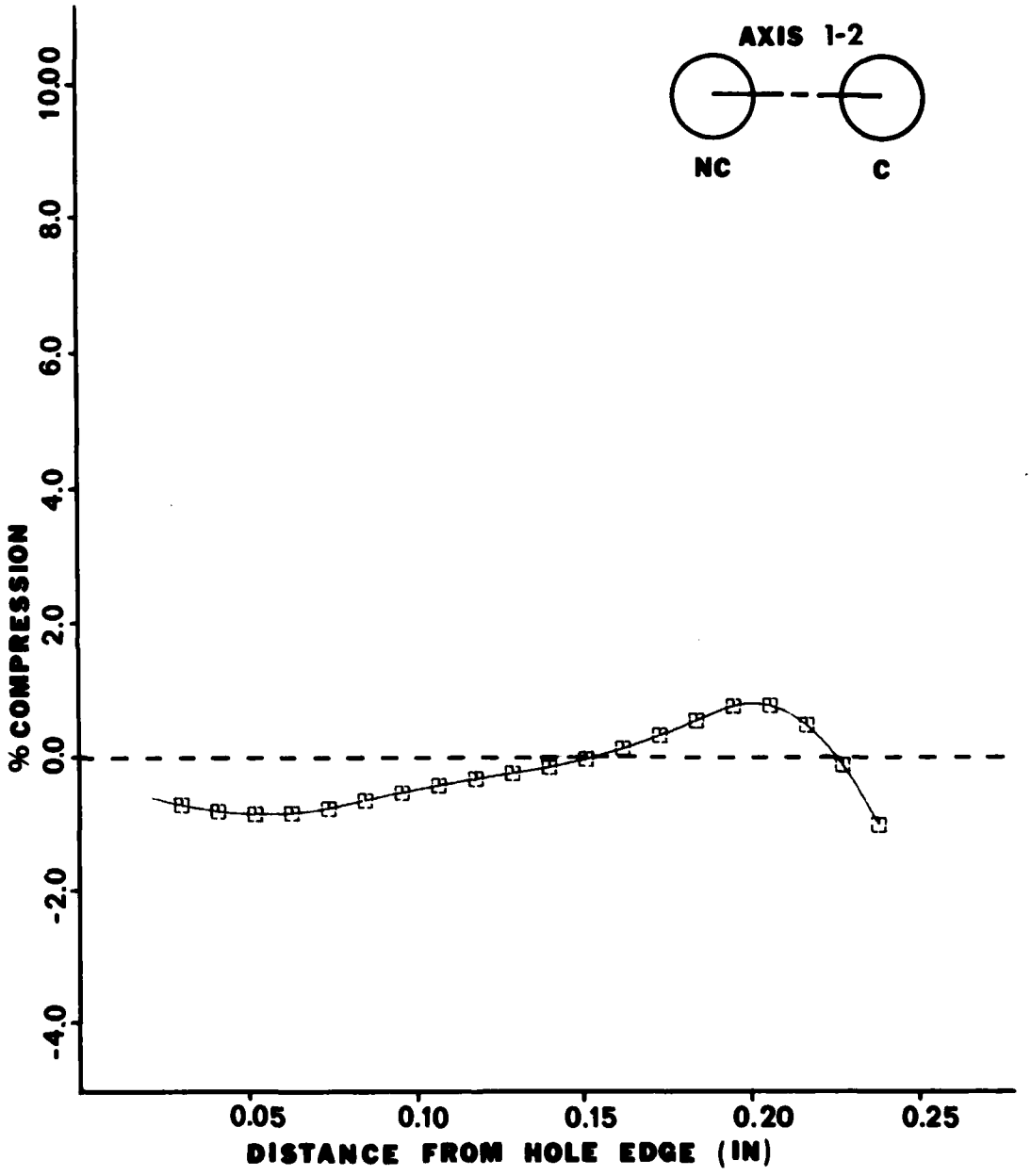

Figure 5.2 Strain Distribution Along Axis (1-2) After Fastener Hole #1 has been Coldworked (Specimen #7).

tensile strains at the edges of both the coldworked and the uncoldworked fastener holes. Small compressive strains exist for only a short distance near edge (1-2) of hole #1 before becoming tensile at the edge. This result seems contrary to results that would normally be expected from the coldworking process. A data check was made to ensure that there were no mistakes made in the digitizing process. No errors were found so the strain distribution is assumed to be representative and correct. Though small in magnitude, the existence of the tensile strains at the edge of a coldworked hole causes some unease. No strain plot is available for specimen #2 at this stage of testing because no intermediate data photograph of the specimen grating was obtained.

Figures 5.3 and 5.4 are the strain distributions for the two specimens after both fastener holes in the pattern have been coldworked. Comparison between the two distributions illustrates the influence of hole spacing on the resultant interaction of the strain fields caused by coldworking. Close examination of the strain plots indicates that the strain distributions for either hole spacing assume the same general shape. The strain distribution for specimen #7 is seen to be a stretched and attenuated version of that for specimen #2. This result is important in that it establishes part of the mechanism of the interaction process exhibited by the residual surface strain fields. The residual surface strain fields of coldworked fastener holes separated by 2.0 diameters exhibit less interaction than the strain fields between two coldworked fastener holes separated by 1.75 diameters.

For each specimen, zero residual radial strain exists at edge (1-2) of hole #1. The magnitude of the residual compressive strains gradually increase from zero and attain a neighborhood maximum about .04 inches

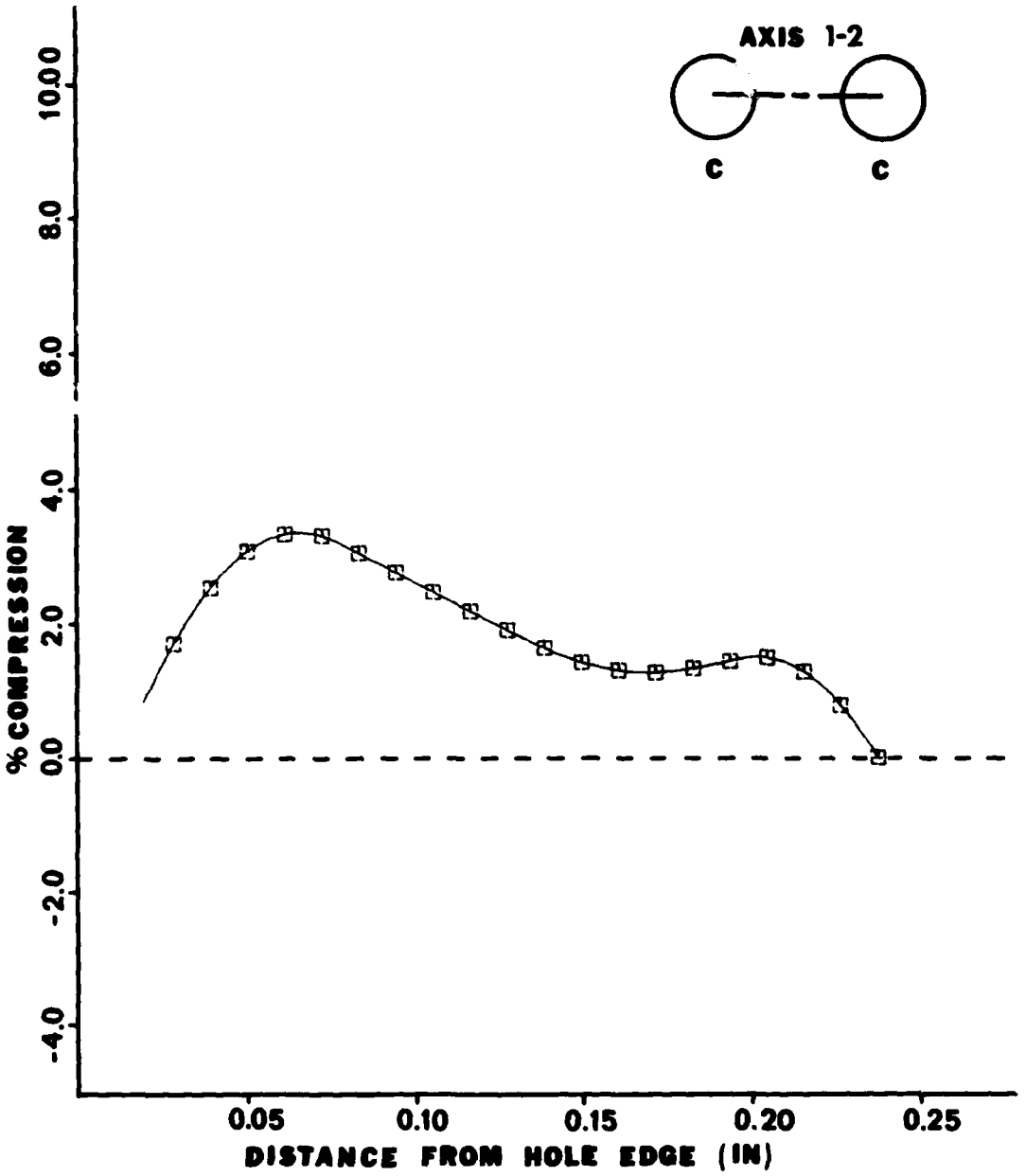

Figure 5.3 Strain Distribution Along Axis (1-2) After Fastener Holes #1 and #2 have been Coldworked (Specimen #7).

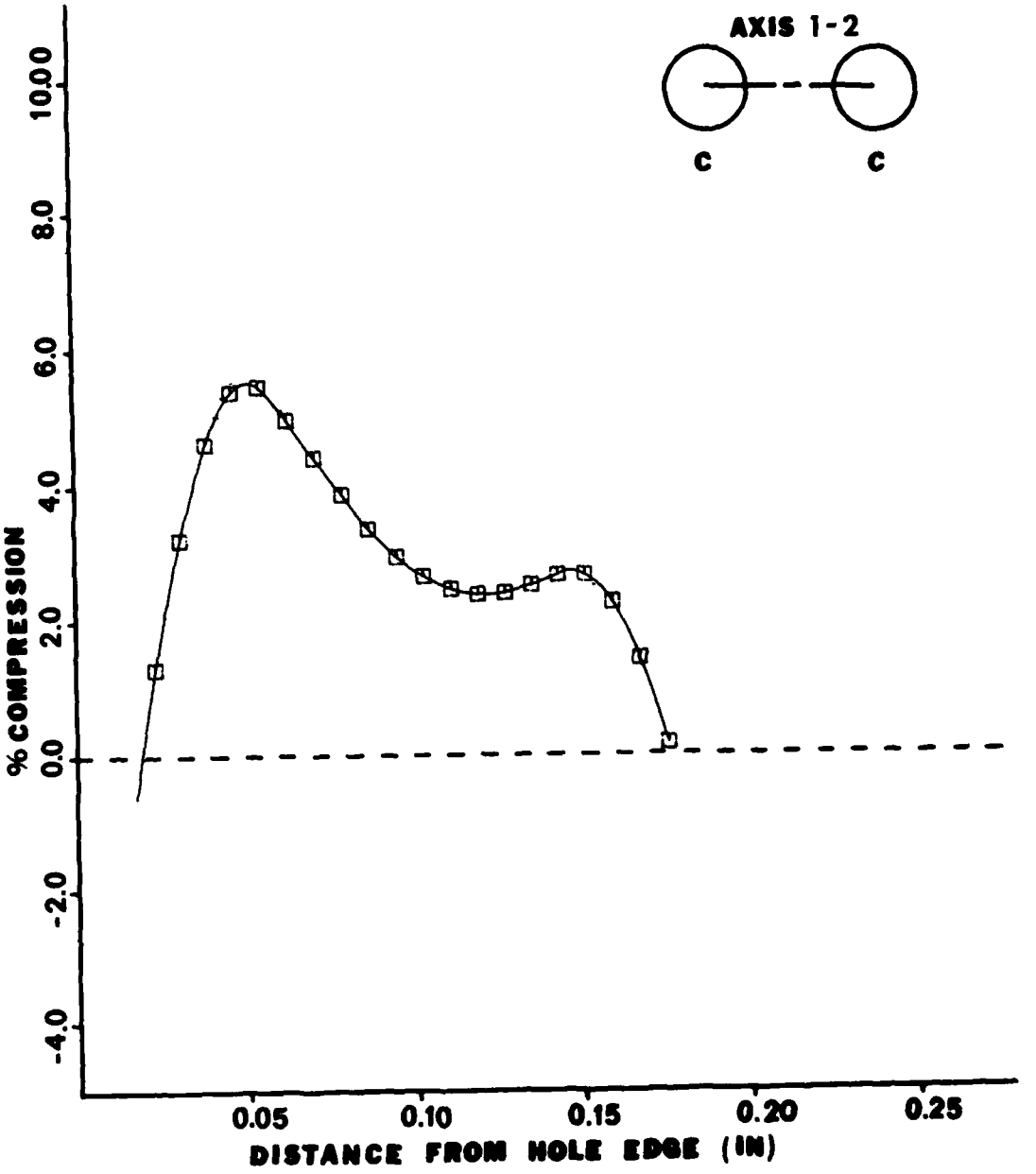

Figure 5.4 Strain Distribution Along Axis (1-2) After Fastener Holes #1 and #2 have been Coldworked (Specimen #2).

away from edge (1-2) of hole #1. From this point the strains decrease slightly and then gradually increase in magnitude until they attain their maximum value about .06 inches away from edge (2-1) of hole #2. After attaining this maxima, the strain plots curve downward and go to zero as edge (2-1) of hole #2 is approached.

The appearence of zero residual strain at the edge of each cold-worked fastener hole is troubling. Residual compressive strains of significant magnitude are present between the coldworked holes, but the results indicate that no effective coldworking has been accomplished at the hole boundary. Again, data checks were made and no errors were found. Close examination of each specimen revealed that within each fastener hole, the fastener sleeve was recessed from the surface by .02 inches. Recession of the fastener sleeve was caused by failure of the sleeve material directly above the anvil of the fastener sleeve. Failure of the sleeves was by buckling and the folding under of the sleeve shaft occurring between the anvil and the back of the specimen.

As in the instance of fastener hole #1 and specimen #2, subsequent splitting and extrusion of the fastener sleeve occurred twice before an acceptable coldwork was obtained. The fastener sleeves which failed during coldworking are shown in Figure 5.5. This type of sleeve slippage, which is marked by subsequent splitting and extrusion of the sleeve from beneath the anvil, was noted in a prior study by Cloud (4). As a result of sleeve failure, Cloud was forced to discard two of his specimens after they each exhibited three sleeve failures. Cloud completed testing on a third specimen that had its fastener sleeve extended 1/64 inch below the surface and concluded that the residual surface strains were consistent with his other experimental data. Since sleeve

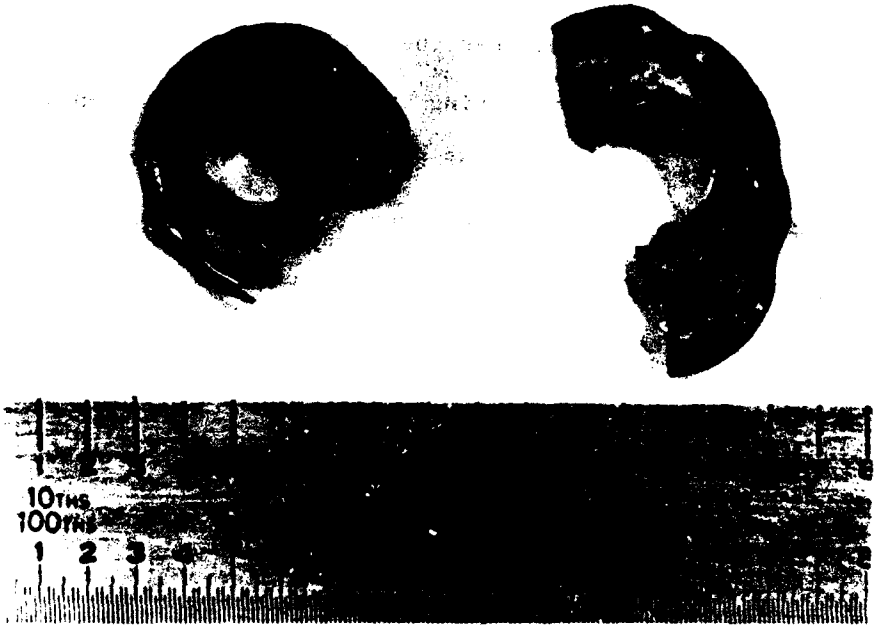

Figure 5.5 Photograph of Fastener Sleeves that Failed During the Coldworking Procedure.

failure has proven to be a common problem in the coldworking process, it was decided to complete the analysis on specimens #2 and #7 to check compatability with the experimental results of Cloud.

For each fastener hole, the diameter of the hole is greater than the diameter of the mandrel used in the coldworking procedure. It is apparent that there could be no direct coldworking of the surface layer at the immediate upper edge of each fastener hole and this is reflected in the experimental results. It can be concluded that the residual surface strains that exist between the coldworked fasteners are the result of coldworking the material lying .02 inches and more beneath the surface of the specimen. Examination of the strain distribution for these two specimens reveal that the maximum residual compressive strains occur at a radial point .04 to .05 inches away from the edge of the coldworked fastener hole. These maximum strains seem to occur at a 2:1 ratio between the radial distance away from the edge of the coldworked hole and the recession of the fastener sleeve from the surface of the specimen. Reference to Figure 5.6 illustrates this idea. These strain distributions are similar in concept to the stress distributions associated with the Boussinesq problem in linear elasticity (10).

Close examination of the strain distributions for specimen #7 leads to an assumption of the physical process by which Figure 5.7 is constructed from Figures 5.2 and 5.3. Figures 5.7 illustrates the idea that the linear superposition of strain fields may be valid for the interaction problem. It should be noted that the curves contained in Figure 5.7 are not numerically exact but are tracings obtained from the original strain plots. In Figure 5.7, curve (A) is the resultant strain distribution existing between the two fastener holes after both

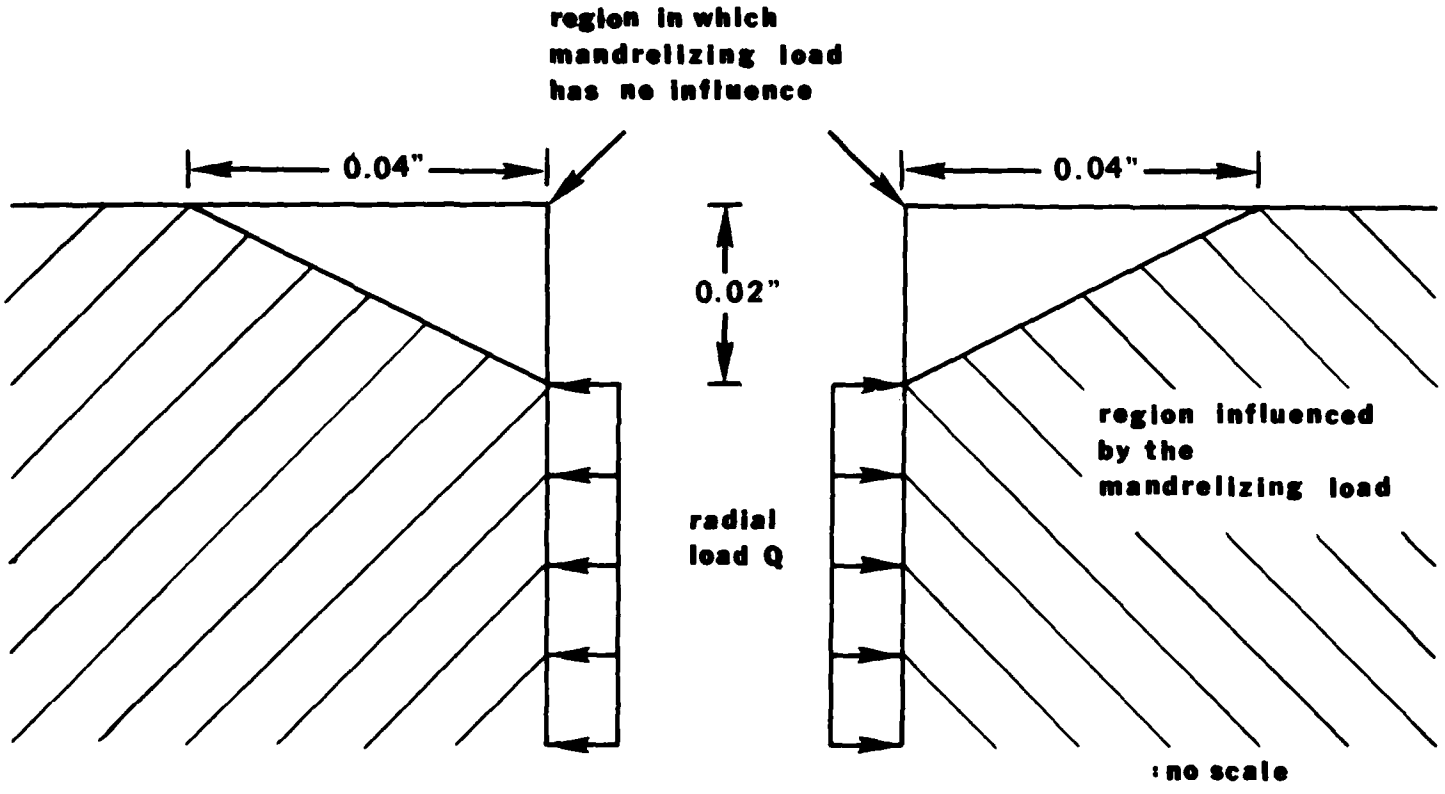

Figure 5.6 Illustration of the Possible Stress Distribution that may Occur when a Fastener Sleeve Slips Below the Specimen Surface During the Coldworking Procedure.

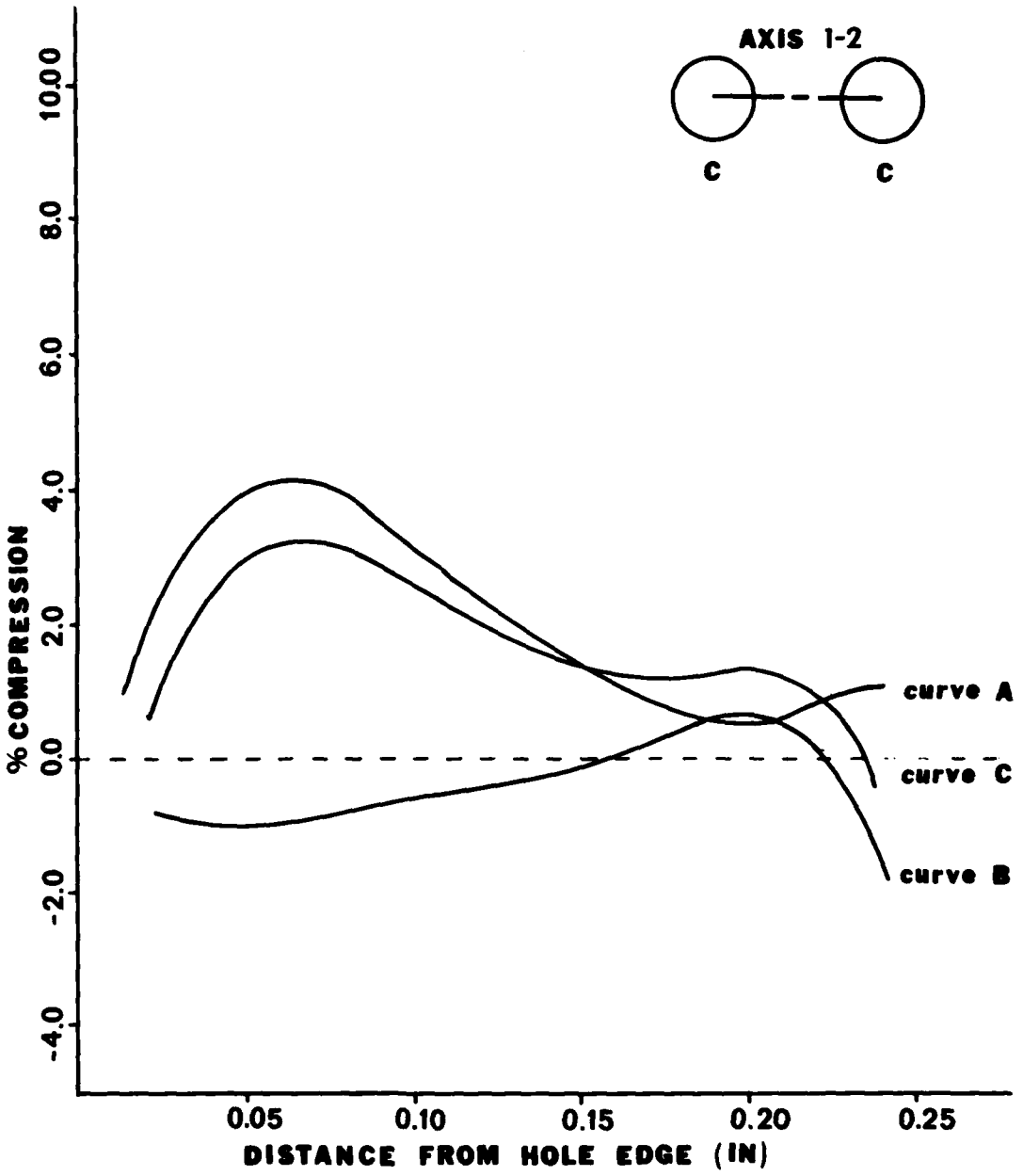

Figure 5.7 Illustration of the Superposition Principle as Related to the Interaction Problem.

have been coldworked. Curve (B) represents the strain distribution after hole #1 has been coldworked. Superposition requires that if curve (B) is subtracted from curve (A), then curve (C) represents the strain distribution caused by coldworking fastener hole #2. Examination of curve (C) enforces the idea that linear superposition of strain fields may serve as a valid model in the interaction problem. Along curve (C) the magnitude of the strains and their distributions resemble those that would be expected from the coldworking process. The concept of superposition suggested here gains further support in later sections by close examination of the intermediate and final strain plots for each hole pair.

Hole edge motion undergone by specimens #2 and #7 are listed in Tables 5.2 and 5.3. The initial and final fastener hole geometries are illustrated in Figure 5.8 and Figure 5.9.

In these illustrations and those that follow, the initial hole boundaries are noted as enclosing the cross hatched regions. Post-coldwork specimen hole boundaries are noncircular and are easily recognized. The illustrations are ten times actual specimen dimensions. Post-coldwork hole edge motions are scaled such that they are five times the actual scaled deformations. This procedure enables the visualization of the deformations and motions incurred by the fastener holes during the coldworking process. These hole edge motions were obtained from the mapping technique previously described. Edge motions were considered positive if the location of the post-coldworked hole edge was outside the boundary of the uncoldworked hole edge. Hole edge motions were negative when the coldworked hole edge location was located inside the original uncoldworked hole perimeter. Fastener hole #1 of specimen #2

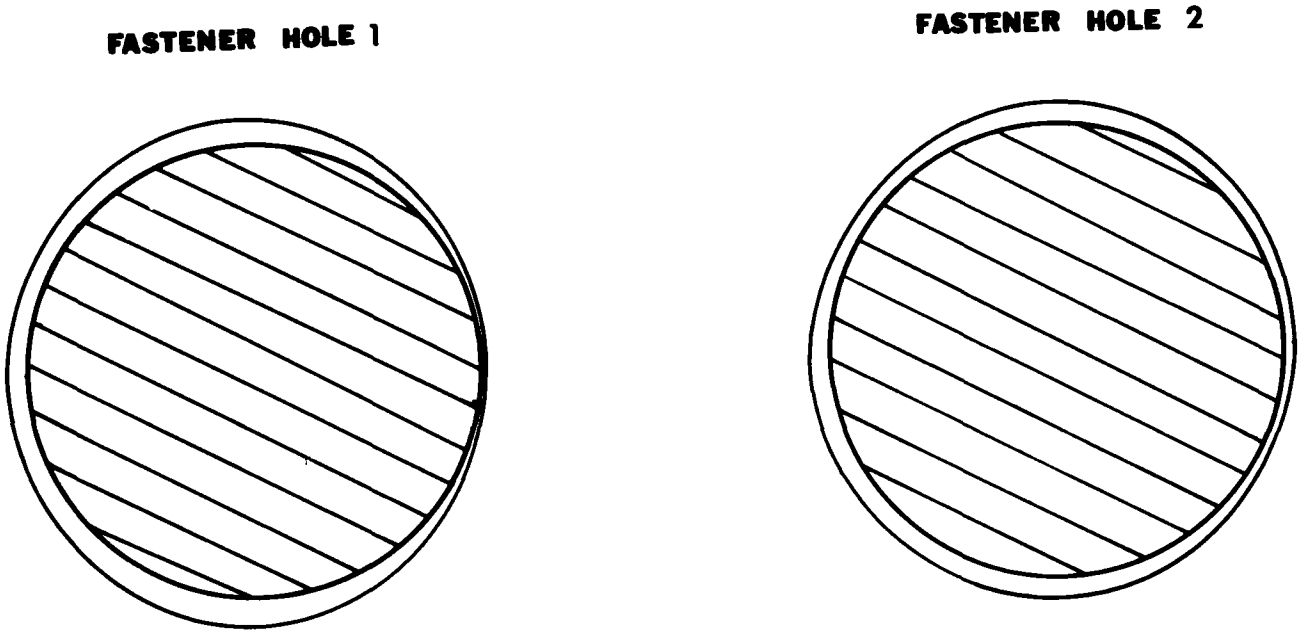

Figure 5.8 Initial and Post-Coldwork Hole Edge Boundries for Fastener Holes #1 and #2 (Specimen #2).

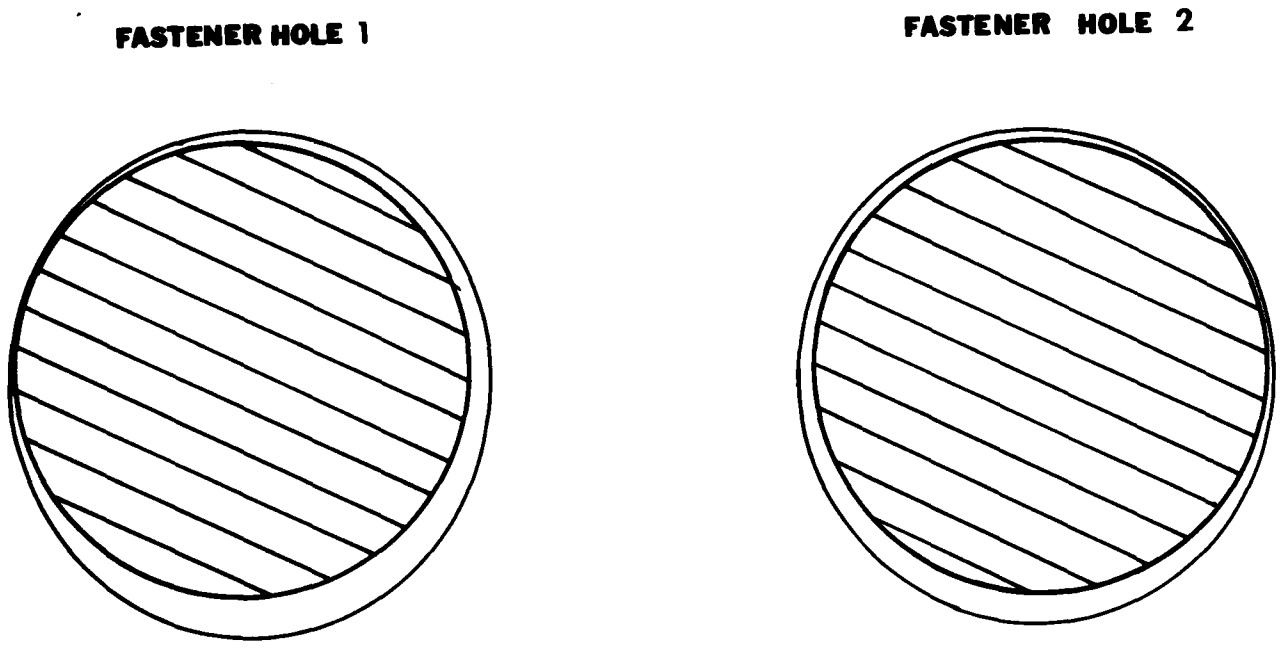

Figure 5.9 Initial and Post-Coldwork Hole Edge Boundries for Fastener Holes #1 and #2 (Specimen #7).

is the only fastener hole that exhibited small motion toward the adjacent uncoldworked fastener hole. Along axis (1-2) almost 90% of the residual diametral expansion of fastener hole #1 occurred in a direction opposite to that of fastener hole #2. The edge motion of fastener hole #2 is very typical for the study. When bounded on one side by solid plate material, about 60% of the residual diametral expansion occurs in the direction of the adjacent coldworked fastener hole. Residual diametral expansions along the minor axis were almost symmetrical. For specimen #7, about 90% of the residual diametral expansion undergone by fastener hole #1 occurred in the direction of fastener hole #2. For fastener hole #2, about 60% of the residual diametral expansion occurs in the direction of fastener hole #1.

5.1.3 Conclusion

Experimental results indicate that, when the center-to-center separation between two fastener holes is 2.0 diameters, coldworking of one of the fastener holes can induce small residual tensile strains at the edge of an adjacent uncoldworked fastener hole.

It has been shown that the center-to-center separation between fastener holes has a definite influence on the degree of interaction of the strain fields after the fastener holes have been coldworked. Coldworked fastener holes initially separated by 2.0 diameters show significantly less interaction than do fastener holes initially separated by 1.75 diameters.

When the fastener sleeves slips .02 inches or more below the surface of the specimen, coldworking of the subsurface material might alter the surface strain distribution that emanates from the edge of the coldworked

fastener hole. The magnitude of the residual strain quickly increases from zero at the edge of the coldworked hole to a magnitude comparable to the strains near a normal single coldworked fastener hole with similar radial interference.

Superposition of strain fields seems to serve as a possible model for the interaction process. Superposition may provide a relation between the relative motion undergone between the edges of two adjacent fastener holes and the order in which they were coldworked.

5.2 Nonconsecutive Coldworking of In-Line Fasteners

5.2.1 Introduction

This section presents the residual surface strains and hole edge displacements that occur between multiple in-line fastener holes that have been coldworked in a nonconsecutive order. The test pattern is intended to model a rework situation in which a set of three fasteners are removed and the fastener holes then coldworked. To lend physical meaning to the problem under study, pertinent data for specimen #4 are furnished in Figure 5.10 and Tables 5.4, 5.5, and 5.6. For the three-hole pattern under study, coldworking of the fastener holes was accomplished in the order indicated in Table 2.1. After coldworking the fastener sleeves remained flush to the surface of the specimen.

5.2.2 Experimental Results

Figures 5.11 and 5.12 are plots of the residual surface strains resulting from the coldworking of fastener holes #1 and #3. Reference to Figure 5.10 illustrates that these strain distributions correspond to an identical physical situation. Each coldworked fastener hole is

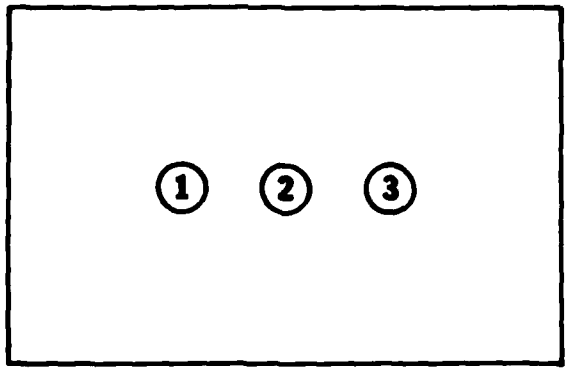

Figure 5.10 Three-Hole In-Line Fastener Pattern Used for Specimen #4.

TABLE 5.4 SPECIMEN DATA

SPECIMEN	HOLE NO.	INITIAL DIAMETER	RESIDUAL DIA. EXPANSION	RADIAL INTERFERENCE	MAX LOAD COLDWORK (LBS)
4	1	0.2618	0.0039	0.0072	1584
	2	0.2618	0.0024	0.0072	1273
	3	0.2630	0.0043	0.0072	1584

TABLE 5.5 HOLE EDGE MOTION - MAJOR AXIS

SPECIMEN	HOLE	EDGE	MOTION	EDGE	MOTION	SEPARATION
4	1	1-P	+0.0004	1-2	+0.0035	
						0.0055
	2	2-1	+0.0020	2-3	+0.0004	
						0.0039
	3	3-2	+0.0035	3-P	+0.0008	

TABLE 5.6 HOLE EDGE MOTION - MINOR AXIS

SPECIMEN	HOLE	EDGE	MOTION	EDGE	MOTION
4	1	1-N	+0.0039	1-S	+0.0051
	2	2-N	+0.0039	2-S	+0.0039
	3	3-N	+0.0020	3-S	+0.0043

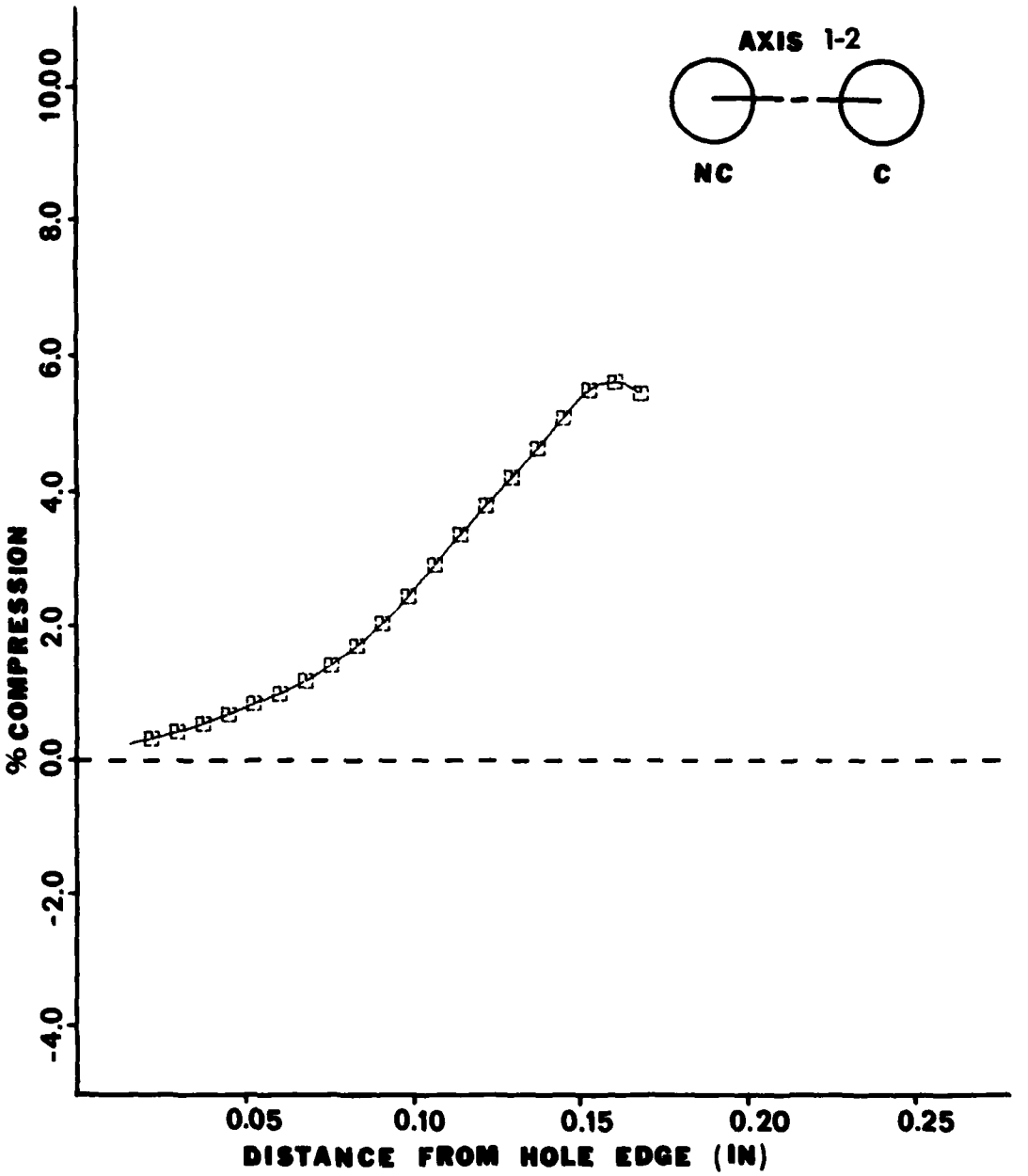

Figure 5.11 Strain Distribution Along Axis (1-2) After Fastener Hole #1 has been Coldworked (Specimen #4).

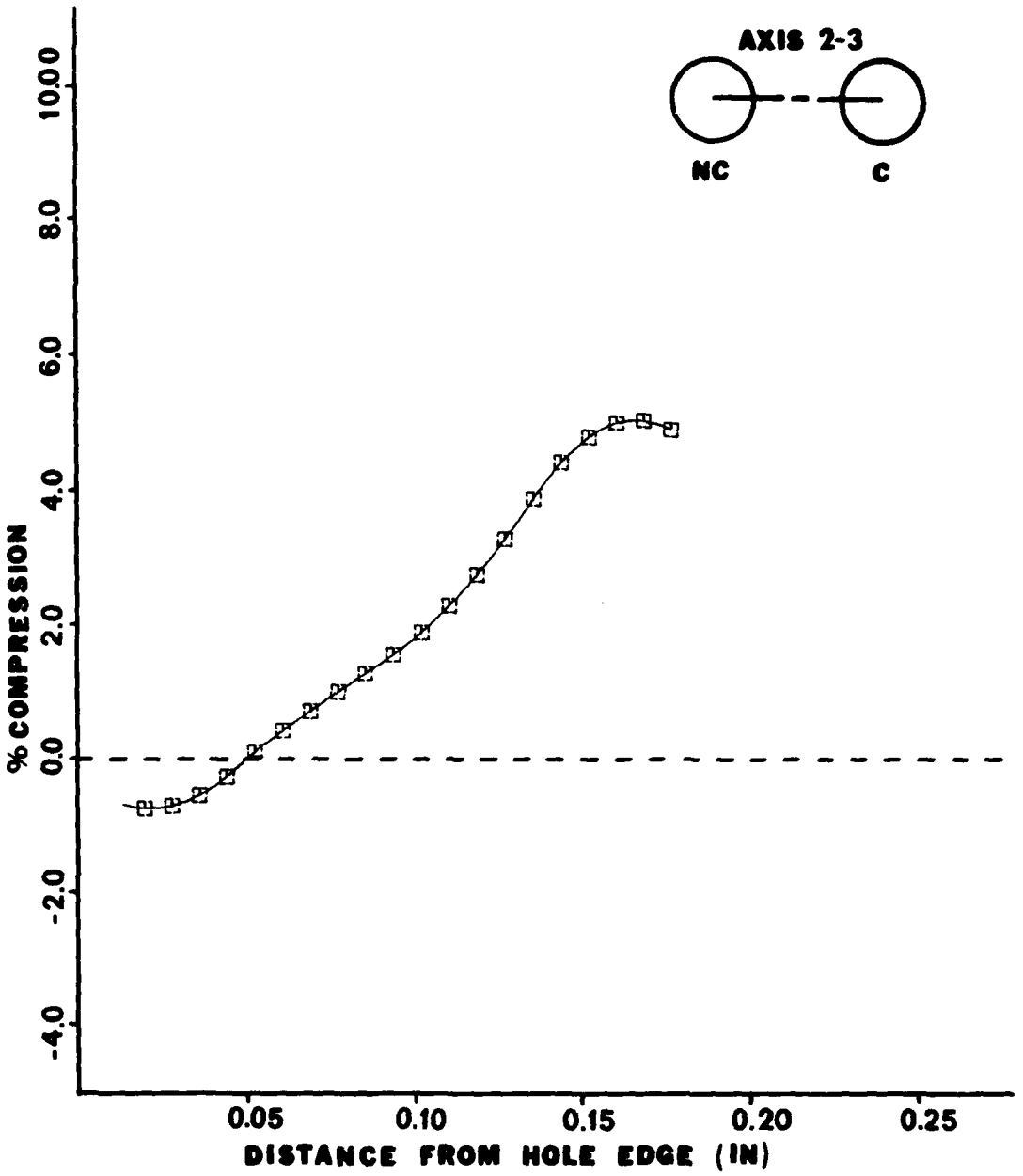

Figure 5.12 Strain Distribution Along Axis (2-3) After Fastener Hole #3 has been Coldworked (Specimen #4).

surrounded by undisturbed plate material and is adjacent to one uncoldworked fastener hole. The strain plots indicate high compressive strains near the edge of each coldworked hole and that these strains decrease as the edge of the adjacent uncoldworked fastener hole is approached.

The magnitudes of the residual compressive strains at the edge of the two coldworked fastener holes are quite similar. The maximum computed strains are 5.6% compression for edge (1-2) of hole #1 and 5.1% compression for edge (2-3) of hole #3. Agreement between the residual strains at each hole is surprisingly close considering the large plastic deformations that occur during the coldworking process. The magnitudes of the residual compressive strains are seen to decrease at an almost constant rate away from the coldworked fastener hole. A gradual decrease in the slope of the strain curves begins about midway between the coldworked and the uncoldworked fastener holes. The strains remain compressive along axis (1-2) as the edge of the uncoldworked fastener hole is approached. The strain along axis (2-3) goes slightly tensile. End conditions which are common to all the strain plots tend to add a slight curvature to each plot as it approaches either the coldworked or the uncoldworked hole edge.

An interesting comparison can be made with results obtained in the coldworking of single fastener hole specimens. In a study by Cloud (4), strain distributions were obtained for single-hole specimens at various levels of radial interference. For purposes of comparison, a composite strain plot from Clouds data is reproduced in Figure 5.13. Despite the aforementioned end conditions that arise at the hole edges of specimen #4, the three strain plots prove to be of about the same slope and the same general shape. For a level of radial interference of .0072

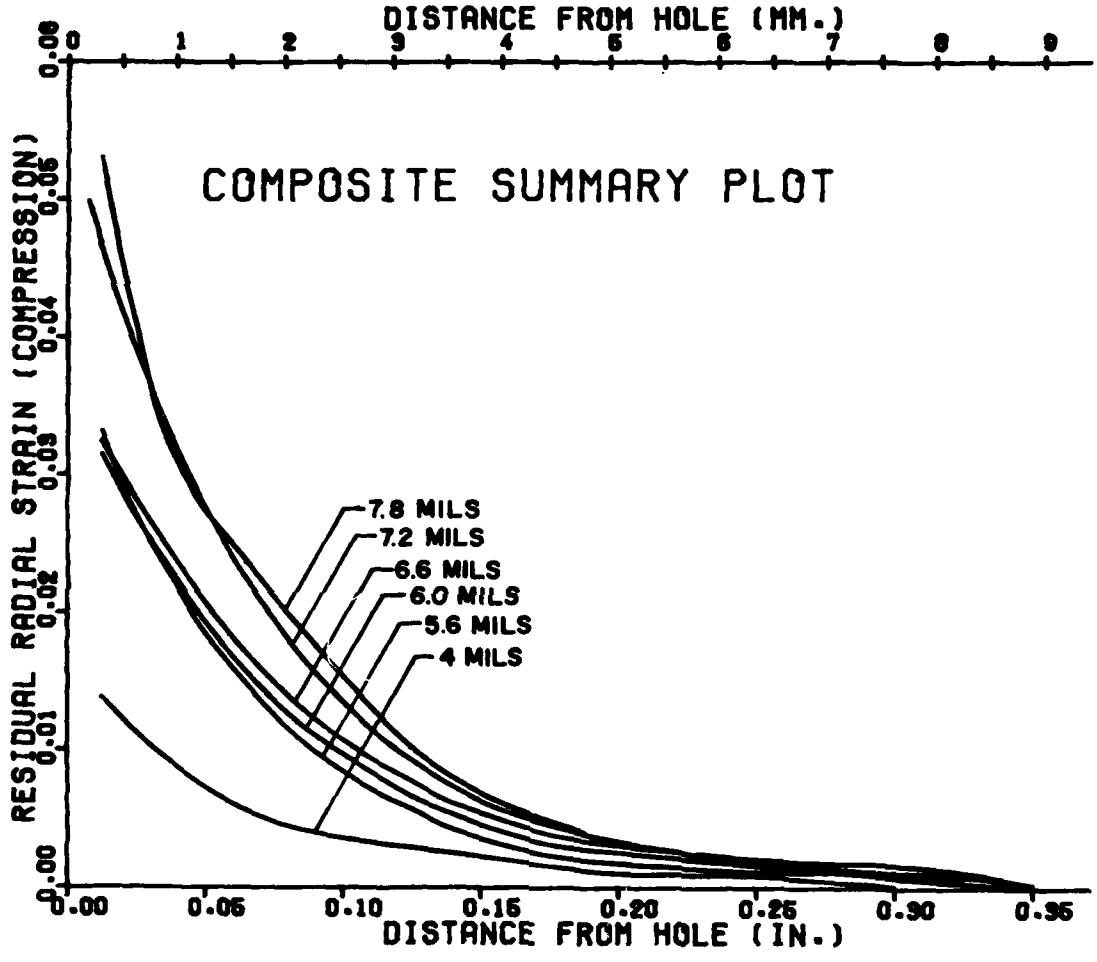

Figure 5.13 Composite Summary of Average Strains Measured for Several Coldworking Levels (Cloud (4)).

inches, Cloud's data indicate residual compressive strains near the edge of the coldworked hole of about 5%. Extrapolation to the hole edge gives about 5.5% strain. These values agree very well with the 5.1% and 5.6% residual compressive strains obtained for specimen #4 which had comparable levels of radial interference.

Figures 5.14 and 5.15 are the strain plots obtained for axes (1-2) and (2-3) after coldworking of fastener hole #2. By comparison of the strain plots, it can be seen that they are quite similar in their general forms. Maximum compressive strains are seen to occur about .03 to .05 inches away from either edge of hole #2. Discrepancies between the two plots arise when the actual magnitudes of the strains are compared. Axes (1-2) and (2-3) are geometrically symmetrical and represented a problem which was also thought to be symmetrical. The results indicate that the strains at edge (2-1) of hole #2 are substantially higher than those that exist at edge (2-3) of hole #2.

The apparent existence of non-symmetric strain fields for this system of three holes may be explained when the relative motions of the hole edges are computed from the mapping procedure. From this procedure, the coldworking process can be seen to be "dynamic" in that each edge of a coldworked fastener hole undergoes a small displacement. Residual diametral expansion caused the relative separation between adjacent fastener holes to decrease. Tables 5.5 and 5.6 lists the edge motions undergone by each of the coldworked fastener holes. From the table, it is noted that the relative separation between holes #1 and #2 has decreased by .0065 inches and that the relative separation between holes #2 and #3 has decreased by .0039 inches. Consideration of the change in relative edge separation lends insight as to why the strain

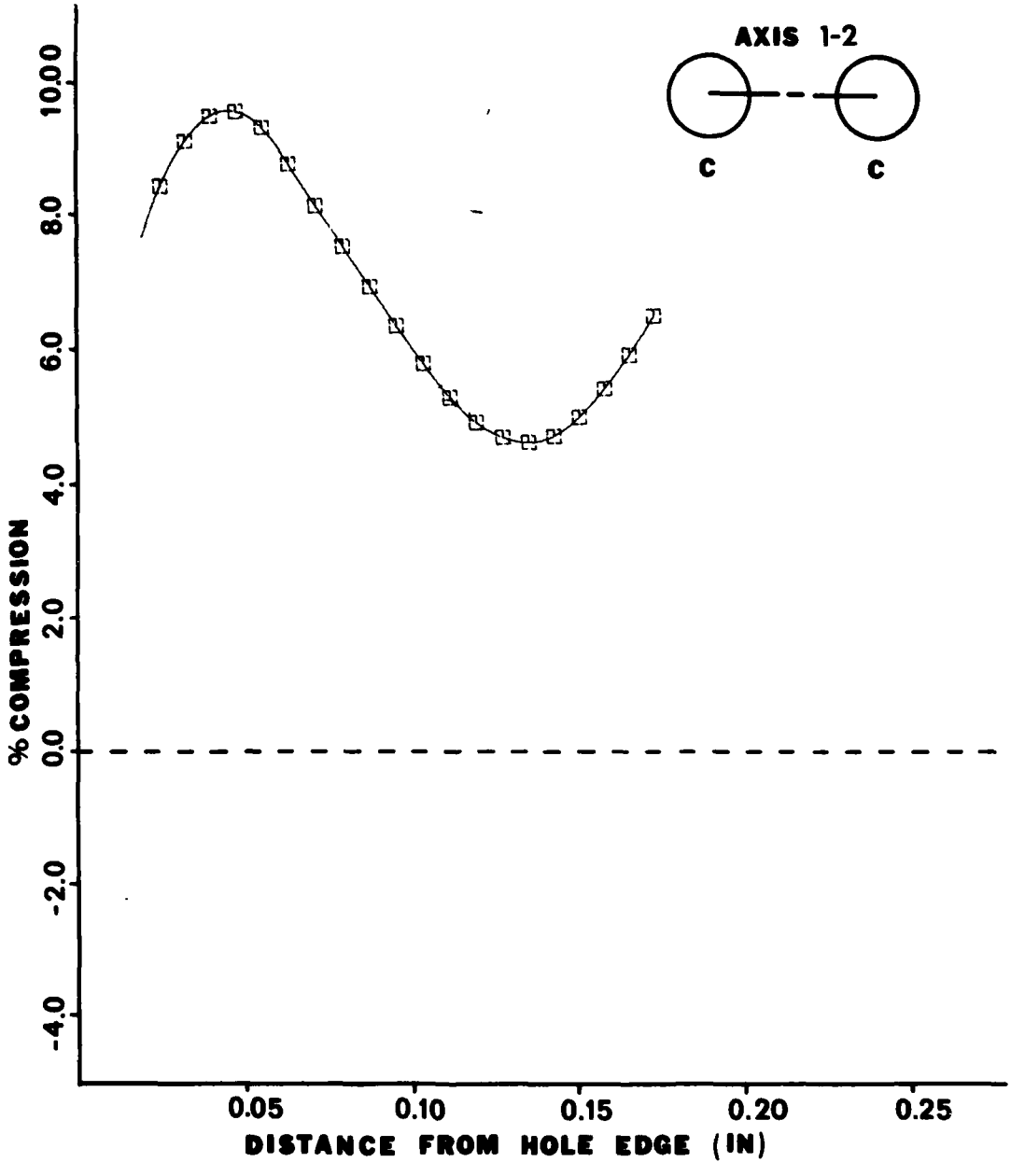

Figure 5.14 Strain Distribution Along Axis (1-2) After Fastener Holes #1 and #2 have been Coldworked (Specimen #4).

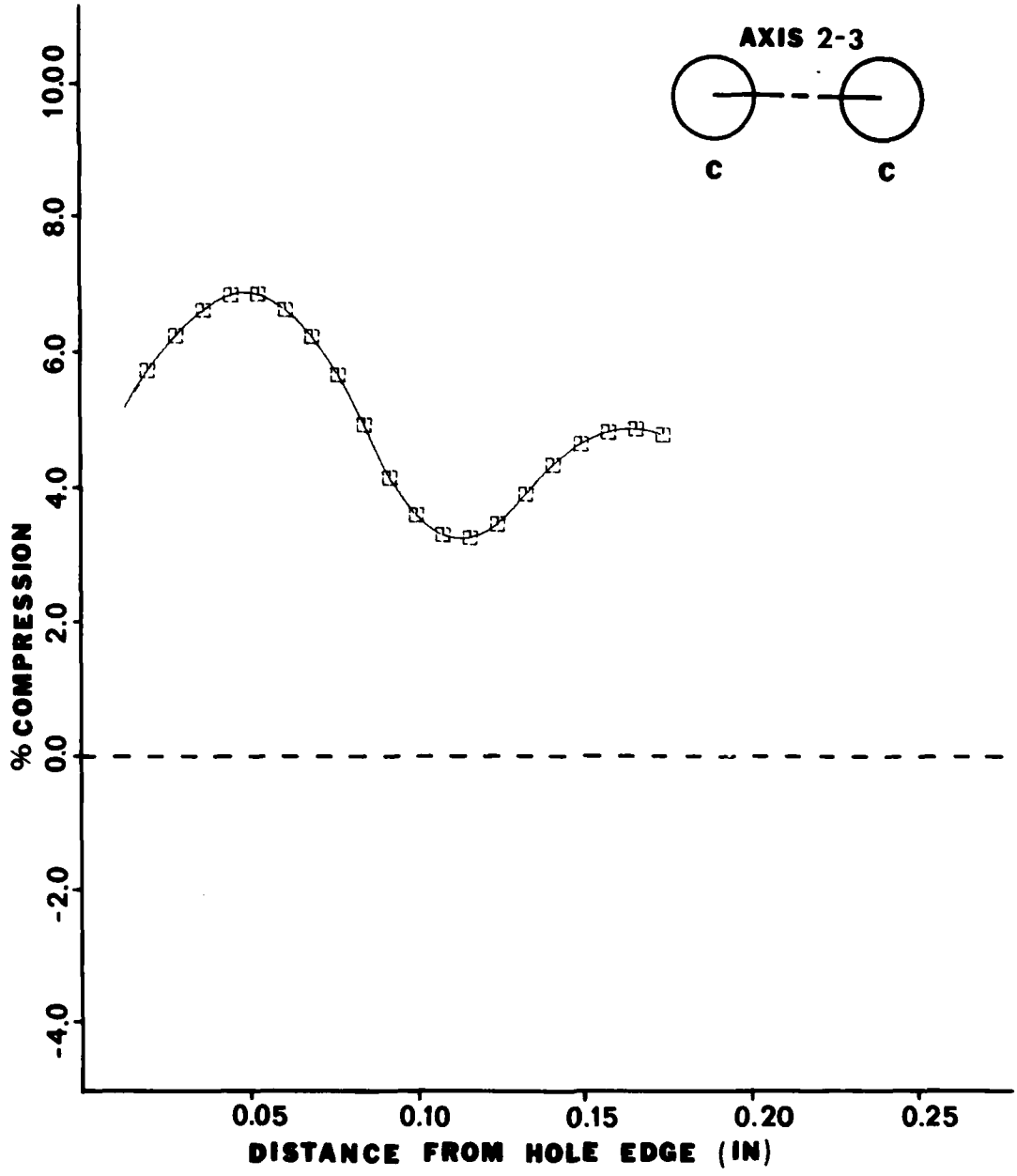

Figure 5.15 Strain Distribution Along Axis (2-3) After Fastener Holes #2 and #3 have been Coldworked (Specimen #4).

AD-A099 695 MICHIGAN STATE UNIV EAST LANSING DEPT OF METALLURGY --ETC F/G 11/6
AN EXPERIMENTAL STUDY OF THE INTERACTION OF STRAIN FIELDS BETWE--ETC(U)
MAR 81 G CLOUD, M TIPTON F33615-78-C-5123

UNCLASSIFIED AFWAL-TR-80-4205 NL

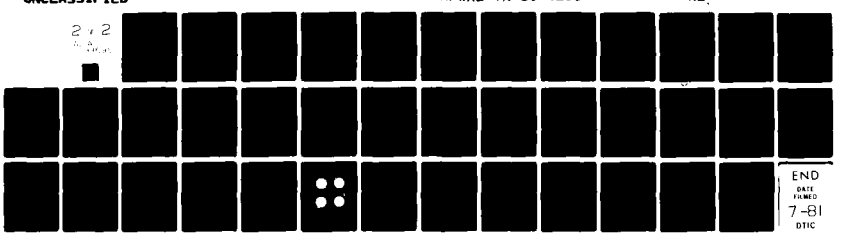

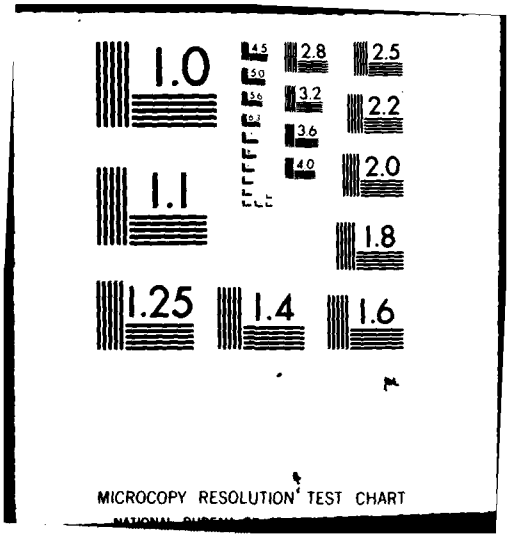
1.0
1.1
1.25
1.4
1.6
1.8
2.0
2.2
2.5
2.8
3.2
3.6
4.0
4.5
5.0
5.6
6.3
MICROCOPY RESOLUTION TEST CHART

distribution is significantly higher along axis (1-2) Figures 5.16 and 5.17 illustrates the relative position of the hole edges for specimen #4 after all fastener holes in the pattern have been coldworked.

A pattern developed earlier in the study and continued here is the occurrence of a preferred direction in which the residual diametral expansion tends to progress. Data indicate that 91% of the residual diametral expansion of hole #1 along axis (1-2) occurs in the direction of hole #2 and that 80% of the residual diametral expansion of hole #3 along axis (2-3) occurs in the direction of hole #2. Along the same axes, 83% of the residual diametral expansion of fastener hole #2 (the center hole) occurs in the direction of fastener hole #1. The nonsymmetry of the strain distribution is supported in the analysis by consideration of the final hole edge positions.

When the mapping procedure is applied to the minor axes, another preferred direction for hole edge motion is obtained. The center fastener hole shows a symmetric distribution of the residual diametric expansion. The two outside fastener holes, #1 and #3, possess unsymmetric distributions with 60% of the residual diametral expansion occuring in the same direction.

5.2.3 Conclusion

Experimental results indicate that when the center-to-center separation between two fastener holes is 1.75 diameters, the coldworking of one fastener hole can induce small tensile strains at the edge of the adjacent uncoldworked fastener hole. The magnitudes of the strains that emanate from the coldworked hole are comparable to those that would be expected if the adjacent uncoldworked fastener hole was not present. In

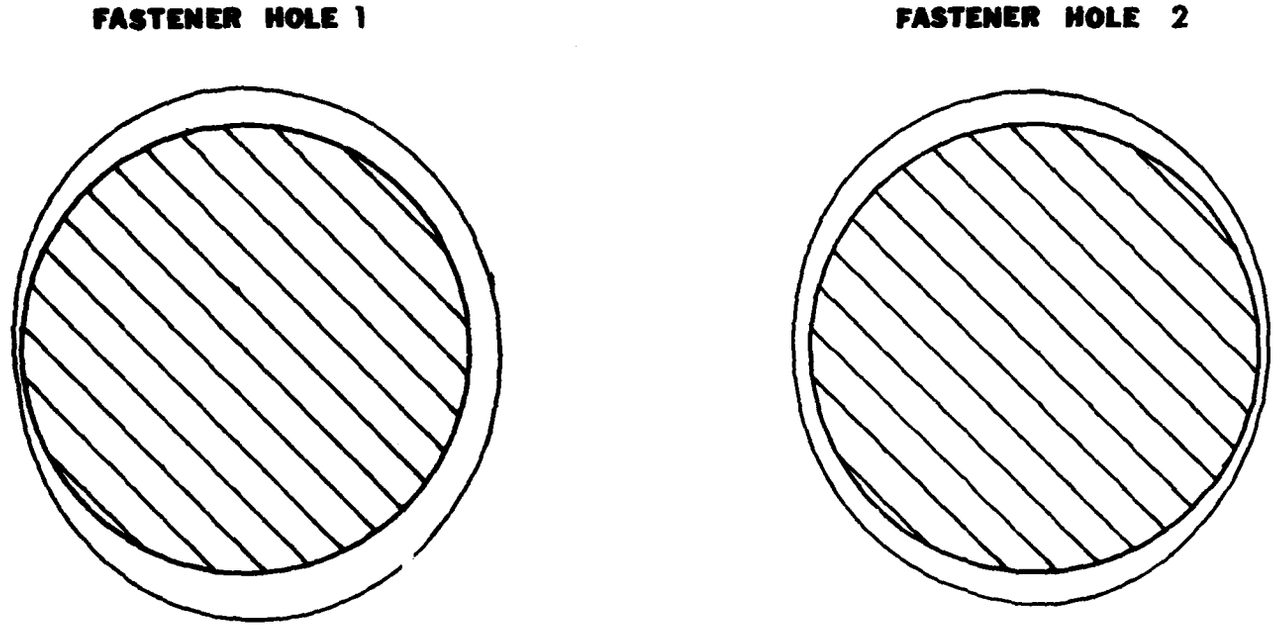

Figure 5.16 Initial and Post-Coldwork Hole Edge Boundries for Fastener Holes #1 and #2 (Specimen #4).

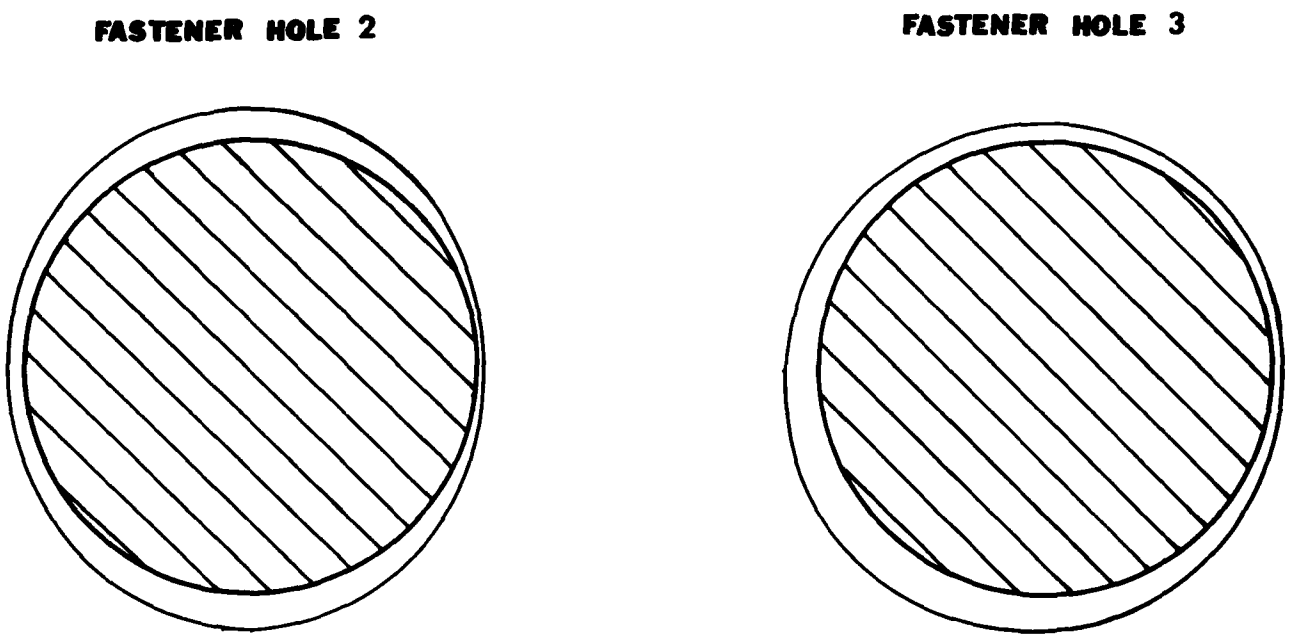

Figure 5.17 Initial and Post-Coldwork Hole Edge Boundries for Fastener Holes #2 and #3 (Specimen #4).

the test pattern, coldworking of the intermediate fastener hole induced high residual compressive strains near its edge. The magnitudes of these strains are significantly higher than those that exist at the edges of the adjacent coldworked holes. Similar, but nonsymmetric strain fields are shown to arise from a geometrically symmetrical problem. The largest strains near the center hole are on the edge toward the hole that was coldworked second. Measurements of the specimen geometry after coldworking suggest that there exists a relationship between the magnitude of the residual strains, the relative motion undergone between the edges of two adjacent fastener holes, and the order in which they were coldworked.

5.3 Consecutive Coldworking of In-line Fasteners

5.3.1 Introduction

This section presents the residual surface strains and hole edge displacements that occur between in-line fastener holes that have been coldworked in consecutive order. Relevant to this section is specimen #3. Specimen data and other pertinent information are furnished in Figure 5.18 and Tables 5.7, 5.8, and 5.9. Used for the specimen was one level of radial interference and a center-to-center separation of 1.75 diameters. The test pattern is intended to model a rework situation in which a set of five fasteners are removed and the fastener holes then coldworked.

5.3.2 Experimental Results

Results for Axis (1-2)

Figure 5.19 is the strain distribution along axis (1-2) after fastener hole #1 has been coldworked. At edge (1-2) of fastener hole

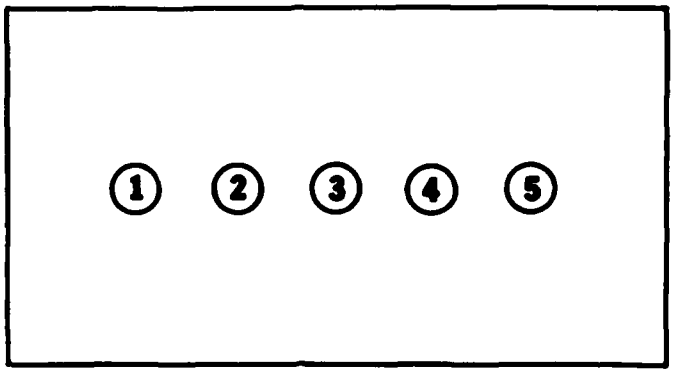

Figure 5.18 Five-Hole In-Line Fastener Pattern Used for Specimen #3.

TABLE 5.7 SPECIMEN DATA

SPECIMEN	HOLE NO.	INITIAL DIAMETER	RESIDUAL DIA. EXPANSION	RADIAL INTERFERENCE	MAX LOAD COLDWORK (LBS)
3	1	0.2618	0.0063	0.0072	1584
	2	0.2614	0.0055	0.0074	1528
	3	0.2618	0.0036	0.0072	1556
	4	0.2614	0.0016	0.0074	1584
	5	0.2618	0.0075	0.0072	1556

TABLE 5.8 HOLE EDGE MOTION - MAJOR AXIS

SPECIMEN	HOLE	EDGE	MOTION	EDGE	MOTION	SEPARATION
3	1	1-P	+0.0012	1-2	+0.0051	
						0.0047
	2	2-1	-0.0004	2-3	+0.0059	
						0.0043
	3	3-2	-0.0016	3-4	+0.0051	
						0.0043
	4	4-3	-0.0008	4-5	+0.0024	
						0.0063
	5	5-4	+0.0039	5-P	+0.0035	

TABLE 5.9 HOLE EDGE MOTION - MINOR AXIS

SPECIMEN	HOLE	EDGE	MOTION	EDGE	MOTION
3	1	1-N	+0.0024	1-S	+0.0043
	2	2-N	+0.0016	2-S	+0.0075
	3	3-N	+0.0012	3-S	+0.0083
	4	4-N	+0.0008	4-S	+0.0083
	5	5-N	+0.0008	5-S	+0.0071

#1, the residual surface strains are about 4.5% compression. As illustrated in Figure 5.13, Cloud obtained residual compressive strains at the hole edge of about 5% for a similar coldwork level. The magnitudes of the residual strains are comparable, but the general shape of the strain distributions are very different.

A large transition region is noted towards the midpoint of axis (1-2). This transition region is where the residual surface strains change from compression to tension. The general shape of the strain distribution in this region suggests the lack of sufficient data points to enable the analysis program to construct the proper curve fitting functions. A region of constant or near constant strain seems most probable in the transition region. After passing through this transition region, the residual tensile strains increase in magnitude and attain a maximum of 5% tension at edge (2-1) of fastener hole #2.

Figure 5.20 is the strain distribution along axis (1-2) after fastener hole #2 has been coldworked. Comparison between Figure 5.20 and 5.19 illustrates that a complete strain reversal has occurred at edge (2-1) of fastener hole #2. The large compressive strains are twice the magnitude of the tensile strains that were present at edge (2-1) prior to coldworking fastener hole #2.

Tables 5.8 and 5.9 lists the edge motions undergone by each of the coldworked fastener holes. Illustrated in Figure 5.27 is the deformation undergone by fastener holes #1 and #2. Post-coldwork measurements along axis (1-2) indicate that the separation between the edges of fastener holes #1 and #2 has decreased by 0.0046 inches. Along axis (1-2), eighty percent of the residual diametral expansion of fastener hole #1 occurs in the direction of fastener hole #2. This means that edge (1-2) of

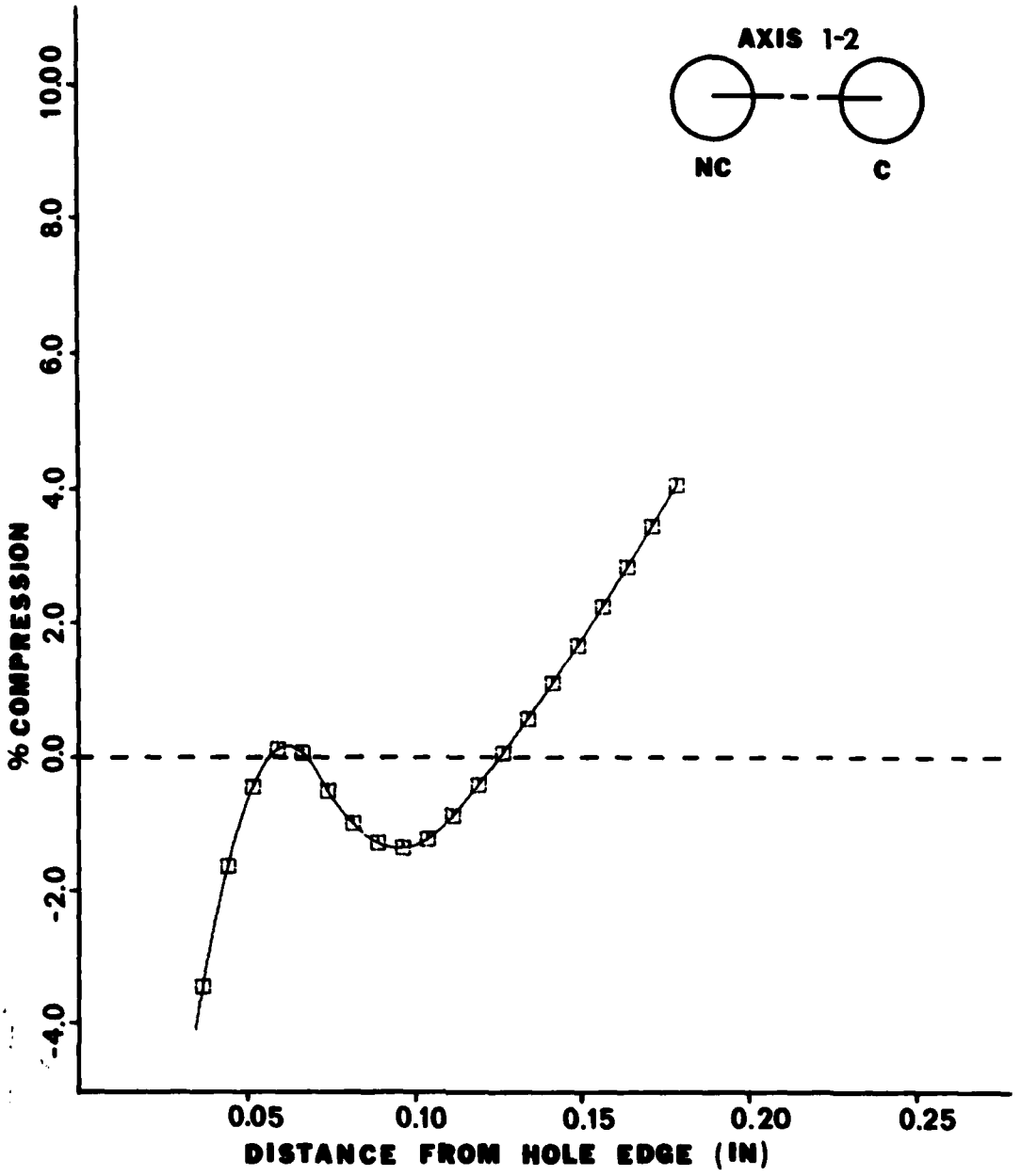

Figure 5.19 Strain Distribution Along Axis (1-2) After Fastener Hole #1 has been Coldworked (Specimen #3).

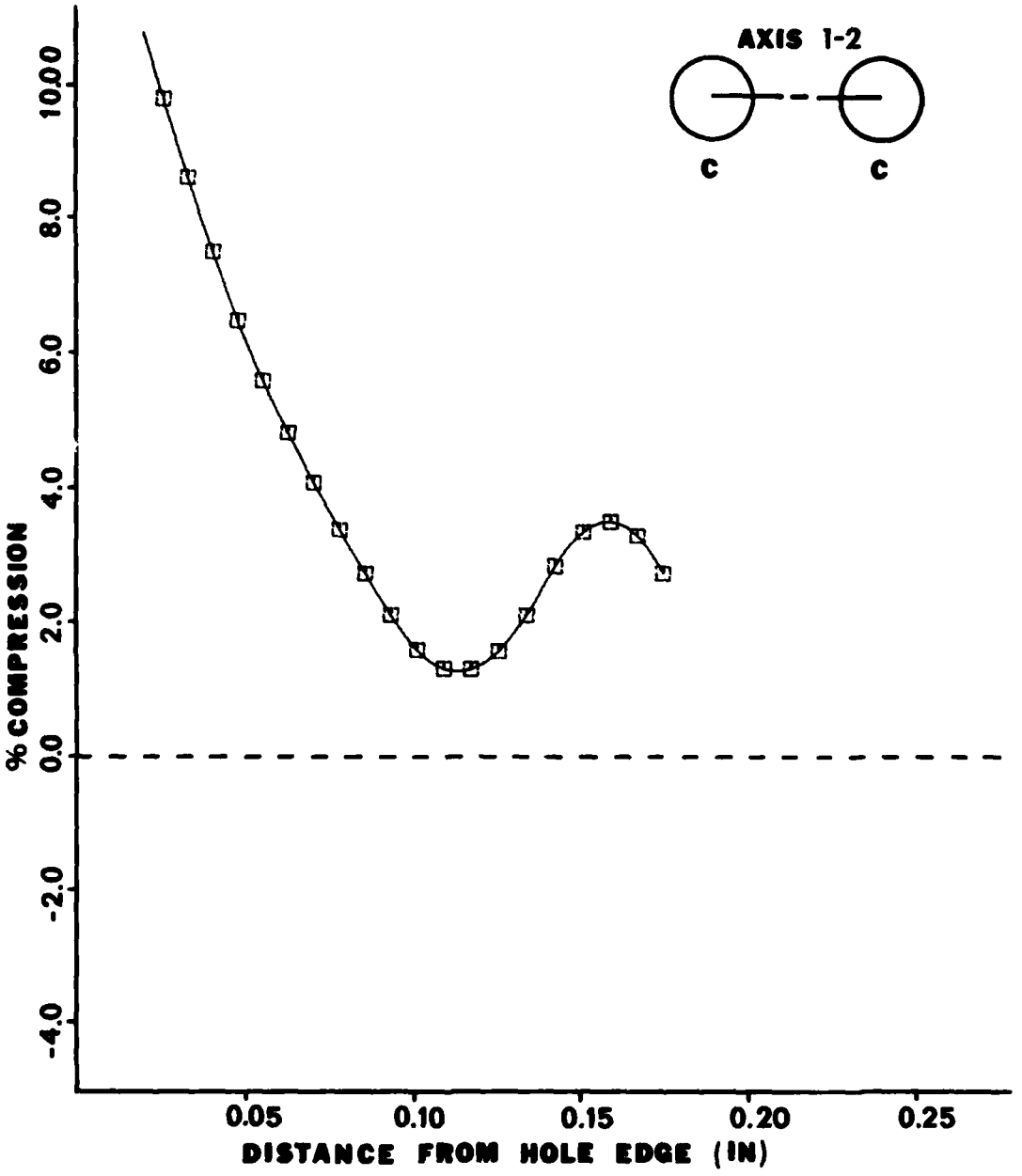

Figure 5.20 Strain Distribution Along Axis (1-2) After Fastener Holes #1 and #2 have been Coldworked (Specimen #3).

fastener hole #1 has moved 0.0050 inches outward from the original position of its uncoldworked hole edge. The data implies that the material along axis (1-2) has undergone both a deformation and a rigid body motion. The coldworking process has functioned to shift the fastener pattern towards the adjacent and previously uncoldworked fastener hole, which in this instance was fastener hole #2.

Results for Axis (2-3)

Figure 5.21 is the strain distribution along axis (2-3) after fastener hole #2 has been coldworked. Large compressive strains of eight percent are noted at edge (2-3) of fastener hole #2. These residual strains are much larger than those obtained for a single coldworked fastener hole. This result suggests that there was a higher level of radial interference for the fastener hole due to deformation that previously occurred along axis (1-2).

There is again a large transition region towards the midpoint of axis (2-3). This transition region occurs where the residual surface strains change from compression to tension. The observation that this transition region is an area of constant or near-constant strain in enforced. After passing through the transition region, the residual tensile strains increase in magnitude and attain the maximum at edge (3-2) of fastener hole #3.

Figure 5.22 is the strain distribution along axis (2-3) after fastener hole #3 has been coldworked. Comparison between Figures 5.22 and 5.21 illustrates that a complete strain reversal has occurred for edge (3-2) of fastener hole #3. The large compressive strain at edge (3-2) is about twice the magnitude of the tensile strains that were present at the hole edge prior to coldworking fastener hole #3.

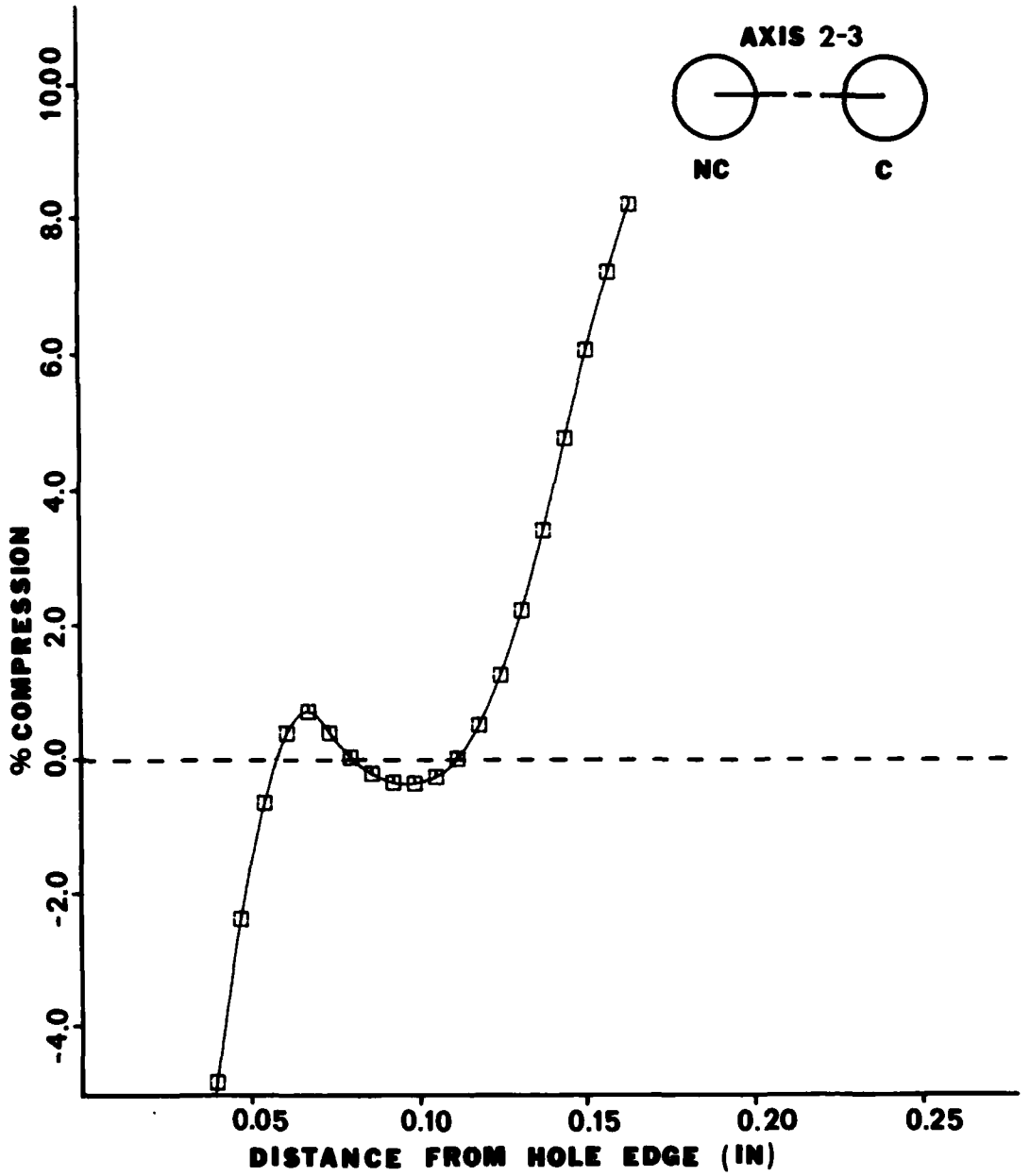

Figure 5.21 Strain Distribution Along Axis (2-3) After Fastener Hole #2 has been Coldworked (Specimen #3).

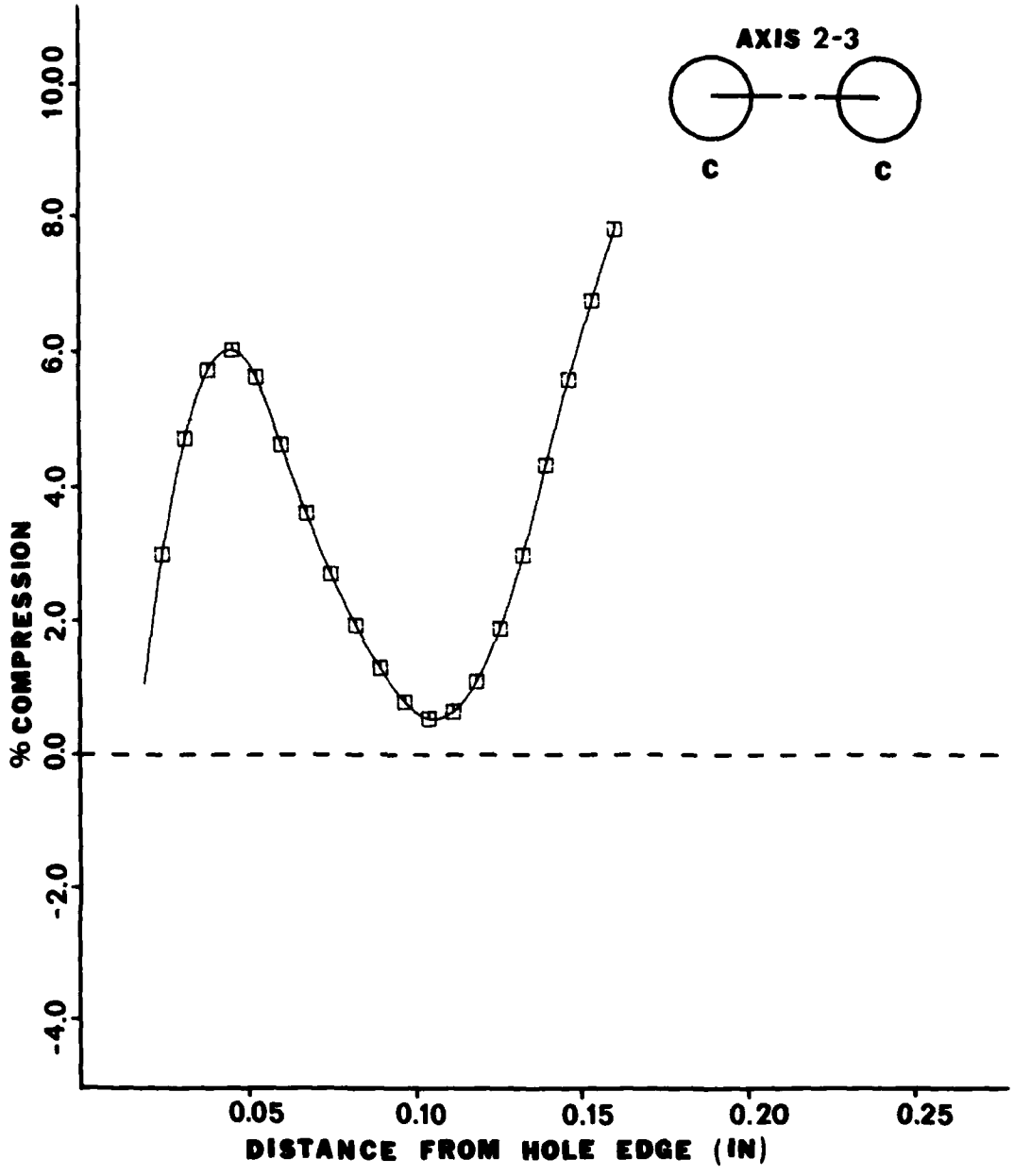

Figure 5.22 Strain Distribution Along Axis (2-3) After Fastener Holes #2 and #3 have been Coldworked (Specimen #3).

The edge motions undergone by each of the coldworked fastener holes are listed in Tables 5.8 and 5.9. Post-coldworked measurements along axis (2-3) indicate that the relative separation between the edges of fastener holes #2 and #3 has decreased by 0.0042 inches. Edge (2-3) of fastener hole #2 has moved 0.0059 inches outward from the original position of its uncoldworked hole edge. Edge (3-2) of fastener hole #3 has moved inward by 0.0016 inches from the original position of its uncoldworked hole edge. The material along axis (2-3) has undergone both a deformation and a rigid body motion. The coldworking process has functioned to shift the fastener pattern towards the next adjacent and previously uncoldworked fastener hole which in this instance was fastener hole #3. The deformation undergone by fastener holes #2 and #3 is illustrated in Figure 5.28.

Results for Axis (3-4)

Figure 5.23 is the strain distribution along axis (3-4) after fastener hole #3 has been coldworked. Large residual compressive strains are at edge (3-4) of fastener hole #3. The magnitude of the residual strains at this point are slightly higher than the strains about a single coldworked fastener hole with a similar level of radial interference. Reference to Figure 5.13 reinforces this observation. The magnitude of the residual strains decrease at an almost constant rate away from the edge of the coldworked fastener hole. A small transition region is noted near the midpoint of axis (3-4). This transition region is very smooth and seems to be very representative. After passing through the transition region, the residual tensile strains increase in magnitude and attain a maximum of 5% at edge (4-3) of fastener hole #4.

Figure 5.24 is the strain distribution for axis (3-4) after fastener hole #4 has been coldworked. The small residual surface strains at edge (4-3) of fastener hole #4 are shown to be tensile. This result seems contrary to the results that would be expected from the coldworking process. A data check was made to insure that no mistakes were made in the digitizing process. No errors were discovered so the strain distribution is assumed to be representative and correct. Close examination of the specimen revealed that within fastener hole #4, the fastener sleeve was recessed from the surface of the specimen by .02 inches. As noted for specimens #2 and #7, recession of the fastener sleeve was caused by failure of the sleeve material directly above the anvil of the fastener sleeve. Failure of the sleeve was by buckling and folding under of the sleeve shaft occurring between the anvil and the back of the specimen. Due to the recession of the fastener sleeve there could be little or no coldworking of the materials at the upper .02 inches of the fastener hole. The results obtained through this accident are in total agreement with those obtained for specimens #2 and #7.

Tables 5.8 and 5.9 lists the edge motions undergone by each of the coldworked fastener holes. Post-coldwork measurements along axis (3-4) indicate that the relative separation between the edges of fastener holes #3 and #4 has decreased by 0.0042 inches. Edge (3-4) of fastener hole #3 has moved 0.0051 inches outward from the original position of its uncoldworked hole edge. Edge (4-3) of fastener hole #4 has moved inward 0.0008 inches from the original position of its uncoldworked hole edge. The data implies that the material along axis (3-4) has undergone both a deformation and a rigid body motion. This again illustrates that the coldworking process has functioned to shift the fastener pattern towards

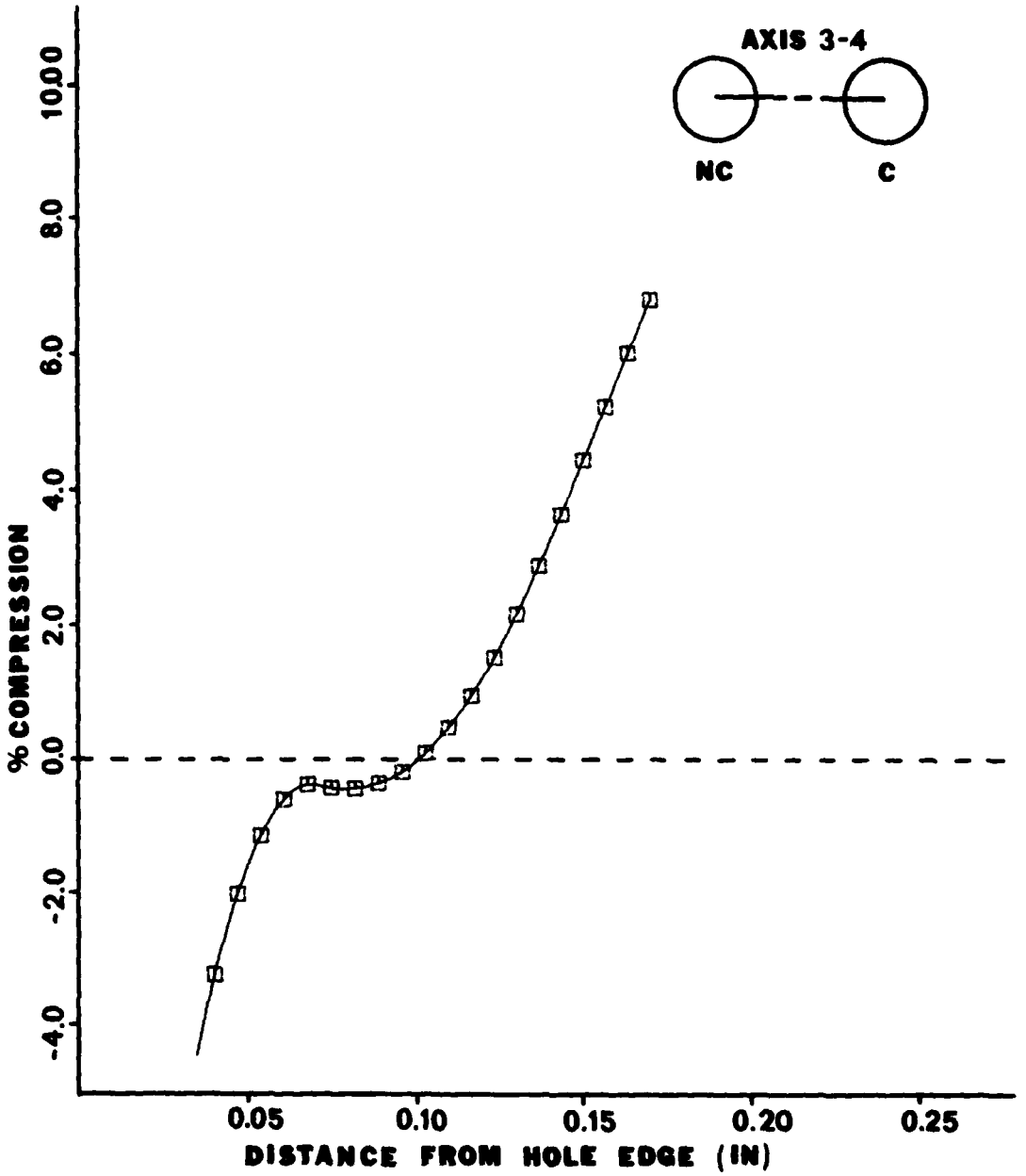

Figure 5.23 Strain Distribution Along Axis (3-4) After Fastener Hole #3 has been Coldworked (Specimen #3).

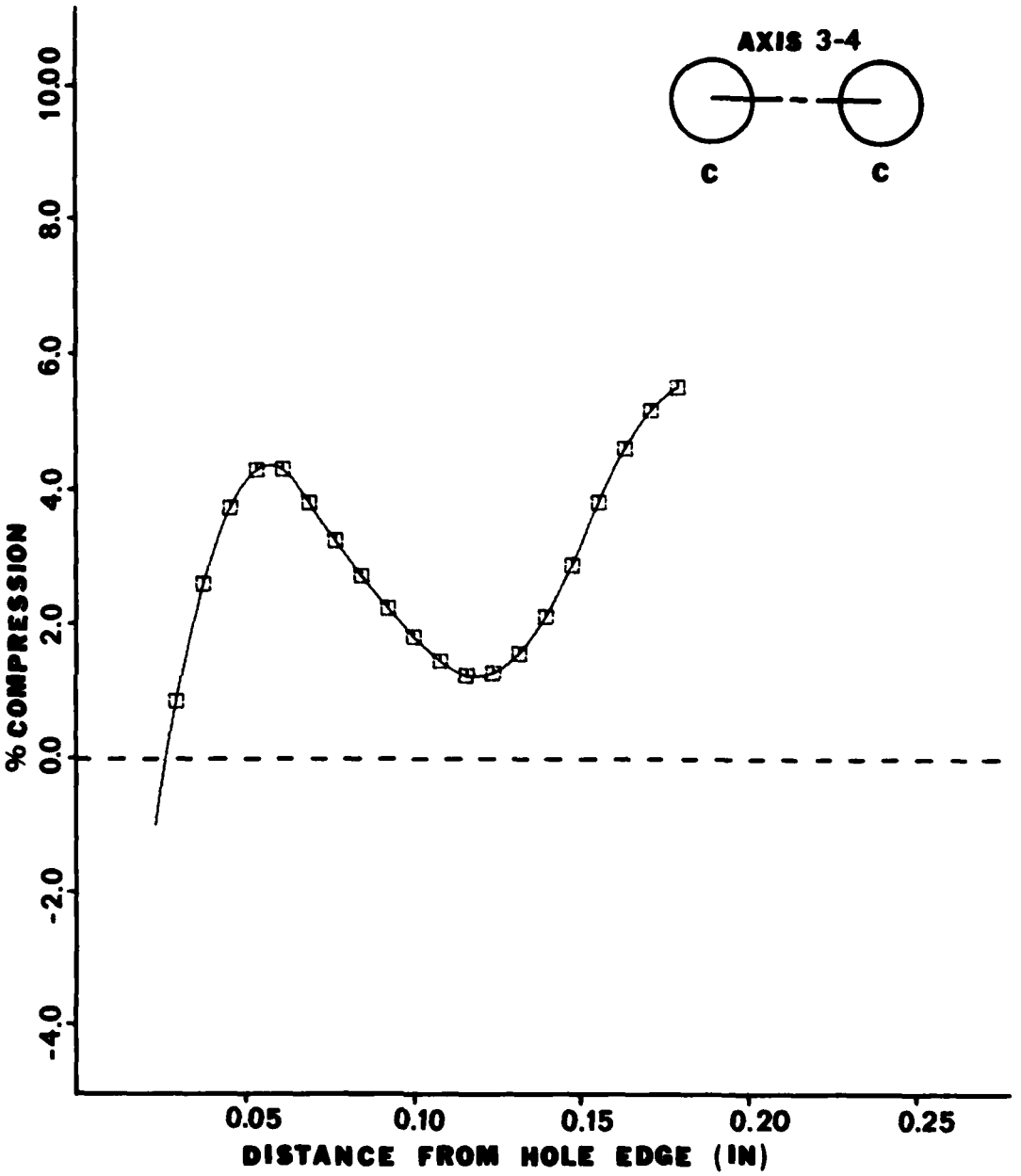

Figure 5.24 Strain Distribution Along Axis (3-4) After Fastener Holes #3 and #4 have been Coldworked (Specimen #3).

the next adjacent and previously uncoldworked fastener hole #4. The deformation undergone by fastener holes #3 and #4 is illustrated in Figure 5.29.

Results for Axis (4-5)

Figure 5.25 is the strain distribution along axis (4-5) after fastener hole #4 has been coldworked. The strain distribution is noticeably different from the strain plots obtained for the other interhole axes. Very small compressive strains are noted only near edge (4-5) of fastener hole #4 are explained by the fastener sleeve recession noted in the above analysis of axis (3-4).

Figure 5.26 is the strain distribution along axis (4-5) after fastener hole #5 has been coldworked. Large compressive strains are present at edge (4-5) of fastener hole #5 and are seen to decrease at a fairly constant rate as edge (4-5) of fastener hole #4 is approached. Significant tensile strains are noted at edge (4-5) of fastener hole #4. The coldworking of fastener hole #5 has caused tensile strains at the edge of an adjacent and previously coldworked fastener hole. It is recognized that coldworking of the material near fastener hole #4 was not complete due to the recession of the fastener sleeve beneath the surface of the specimen. Some degree of coldwork did exist at fastener hole #4, but it was effectively nullified by the coldworking of the adjacent fastener hole #5.

Tables 5.8 and 5.9 list the edge motions undergone by each of the coldworked fastener holes. Post-coldwork measurements along axis (4-5) indicate that the relative separation between fastener holes #4 and #5 has decreased by 0.0063 inches. Edge (4-5) of fastener hole #4 has

moved 0.0024 inches outward from the original position of its uncold-worked hole edge. Edge (5-4) of fastener hole #5 had moved 0.0039 inches outward from the original position of its uncoldworked hole edge. Fastener hole #5 has the largest residual diametral expansion of any fastener hole in the pattern and this is reflected in the high residual compressive strains at its edge (5-4). Fifty-five percent of the residual diametral expansion undergone by fastener hole #5 along axis (4-5) occurs in the direction of fastener hole #4. The residual diametral expansion of fastener hole #5 is similar to the deformation incurred by fastener hole #2 of specimens #2 and #7; which are similar in their geometric configuration. This implies that the material in the direction of the adjacent coldworked hole, fastener hole #4, offers less resistance to hole edge motion after coldworking than does undisturbed plate material. The coldworking process has functioned to shift the fastener pattern towards the adjacent and previously coldworked fastener hole. The deformation undergone in the coldworking process is illustrated in Figure 5.30.

5.3.3 Conclusions

Experimental results indicate that the sequential coldworking of in-line fastener holes can lead to large hole edge deformations. Progression of the coldworking process across the specimen further defined the previously noted nonsymmetry of the coldworking process.

It was shown that the material that separates two adjacent fastener holes undergoes a deformation and a rigid body motion. As a direct result of the deformation and rigid body motion, the post coldwork boundaries of the fastener holes will shift in the direction in which the pattern is being coldworked.

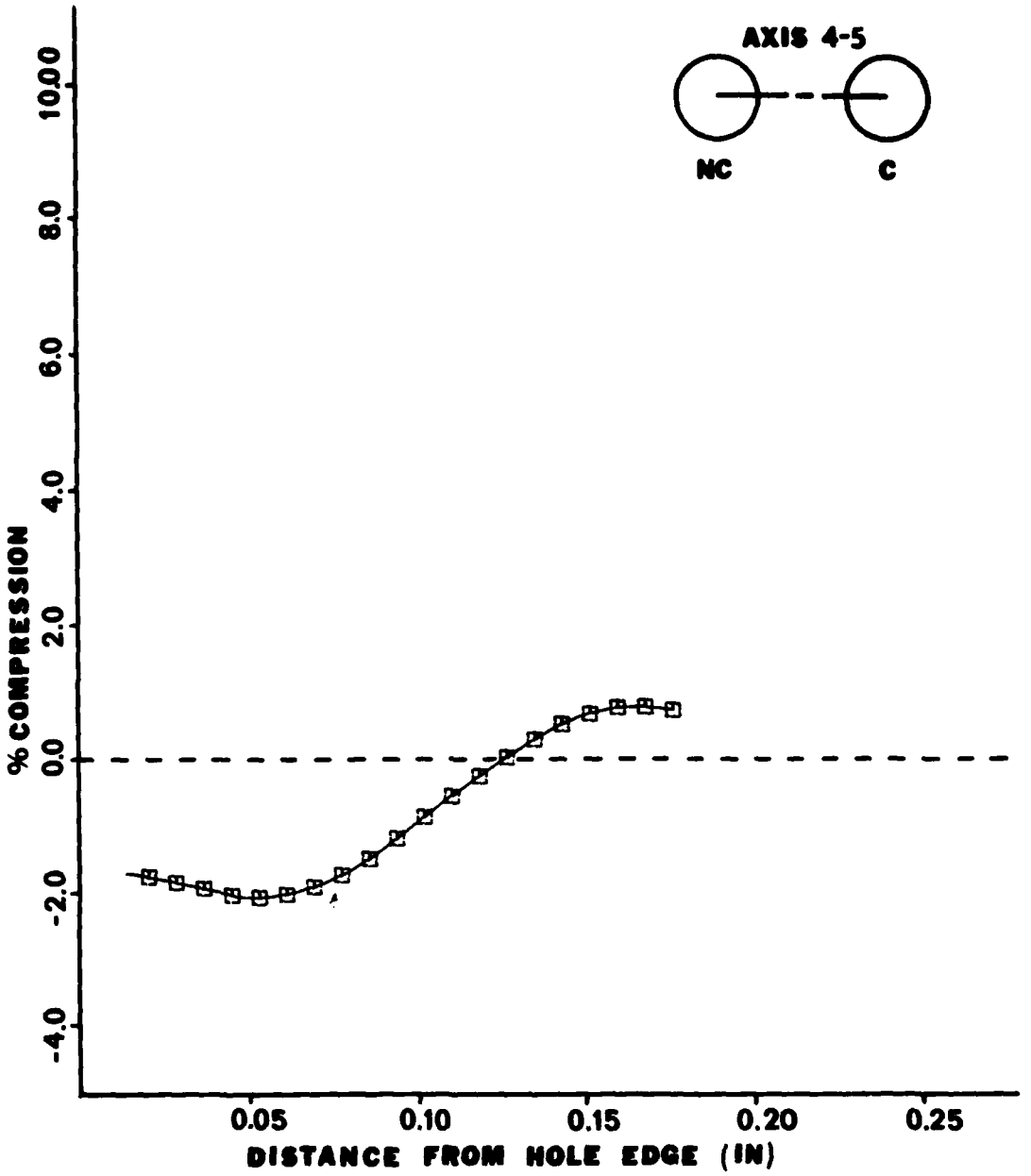

Figure 5.25 Strain Distribution Along Axis (4-5) After Fastener Hole #4 has been Coldworked (Specimen #3).

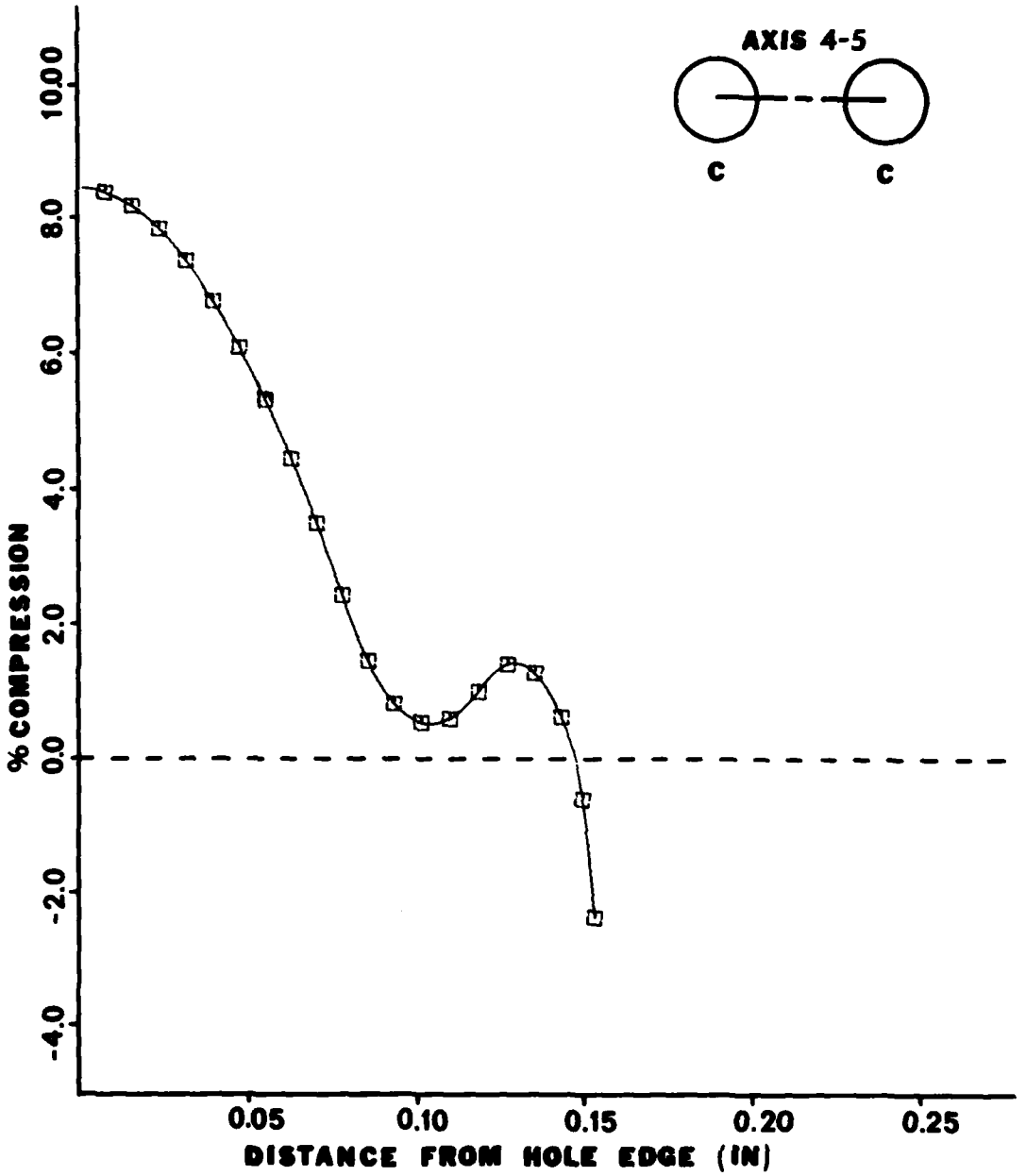

Figure 5.26 Strain Distribution Along Axis (4-5) After Fastener Holes #4 and #5 have been Coldworked (Specimen #3).

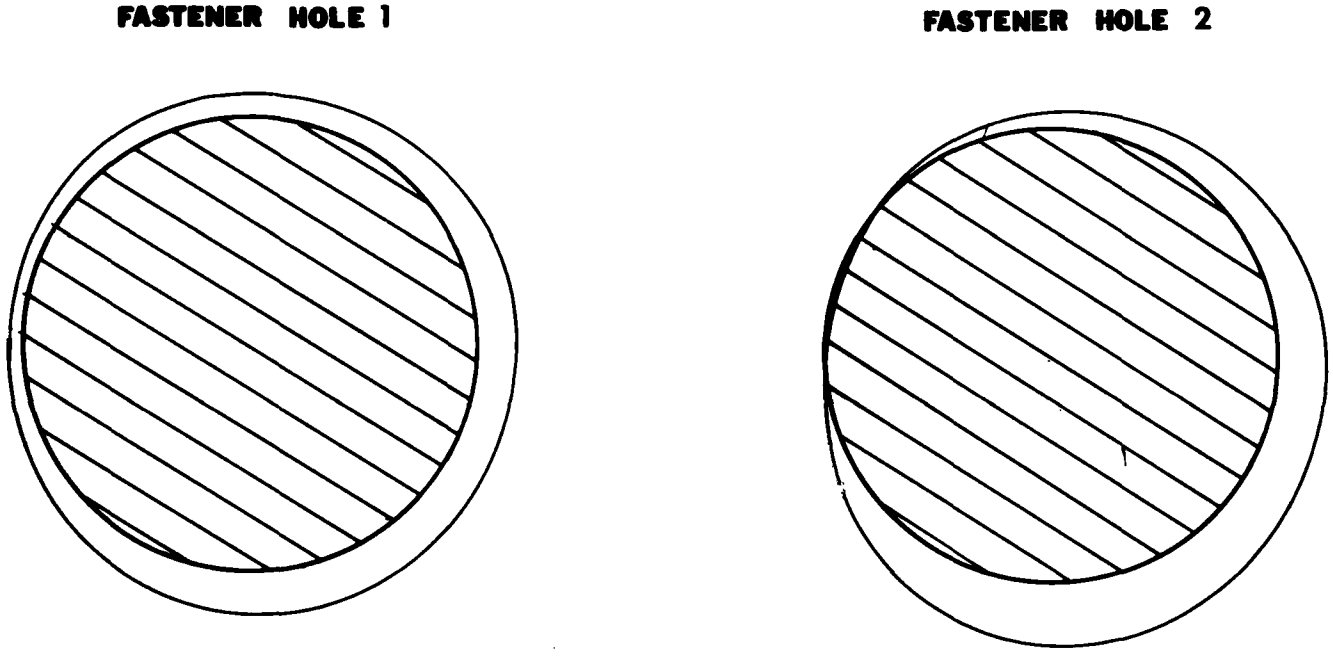

Figure 5.27 Initial and Post-Coldwork Hole Edge Boundries for Fastener Holes #1 and #2 (Specimen #3).

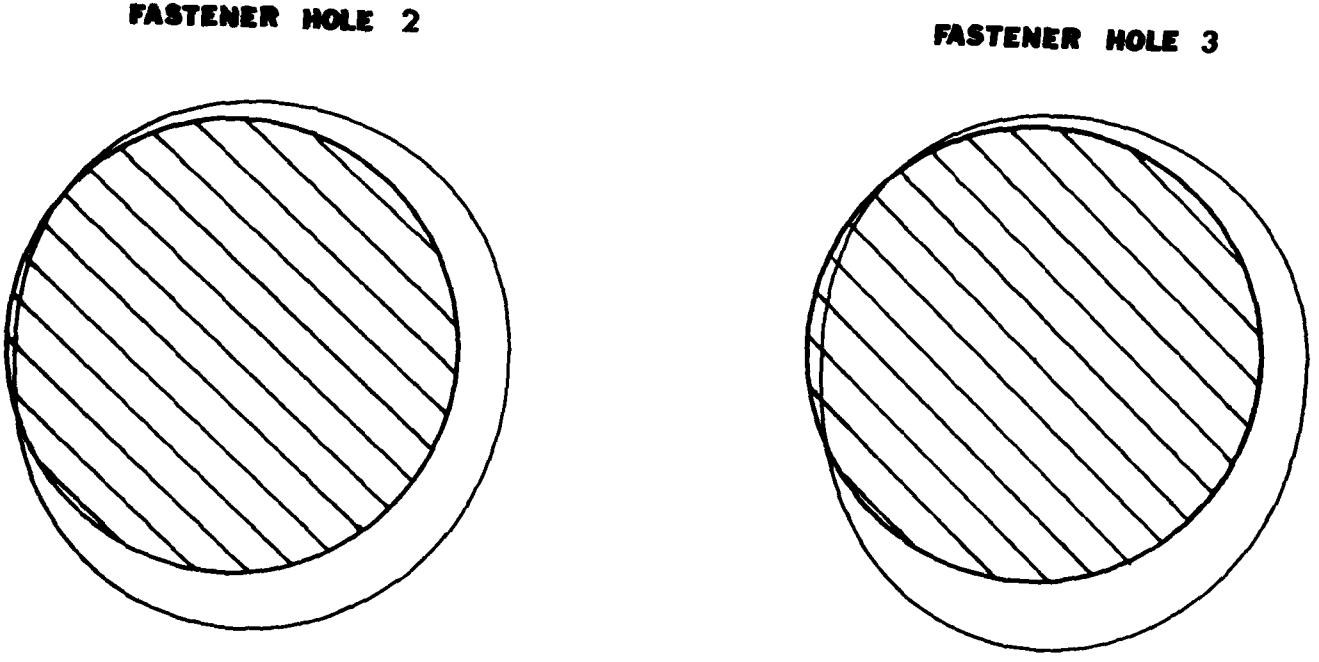

Figure 5.28 Initial and Post-Coldwork Hole Edge Boundries for Fastener Holes #2 and #3 (Specimen #3).

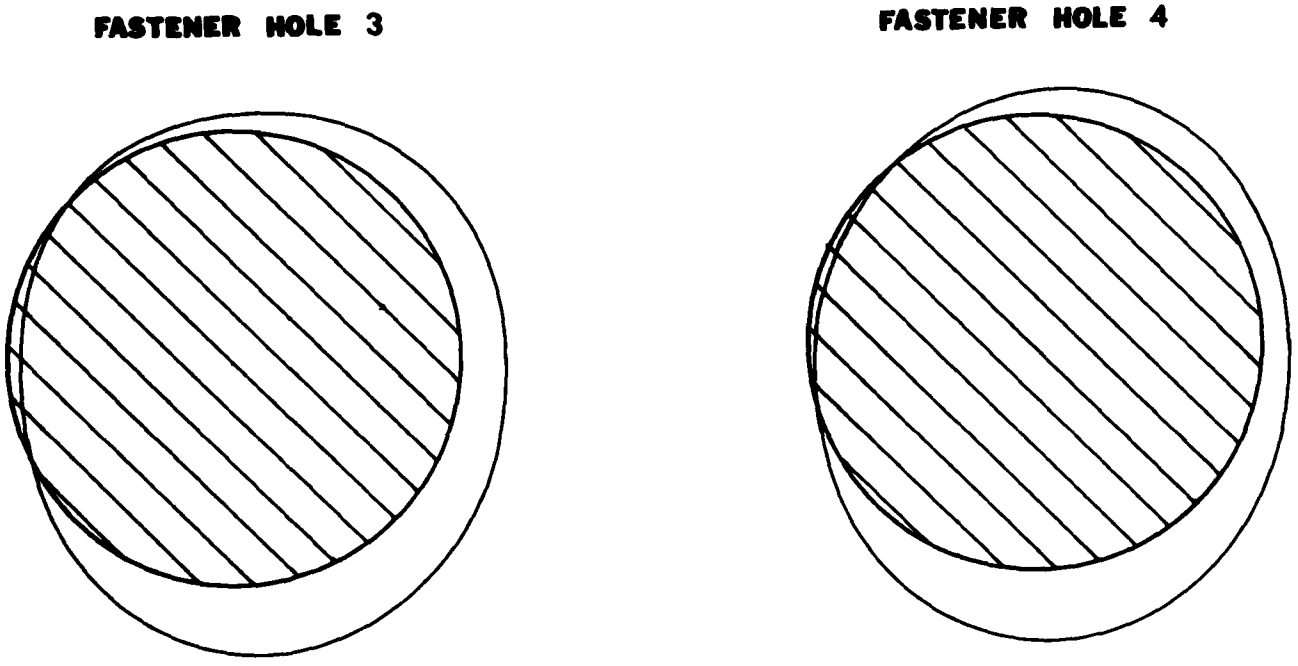

Figure 5.29 Initial and Post-Coldwork Hole Edge Boundries for Fastener Holes #3 and #4 (Specimen #3).

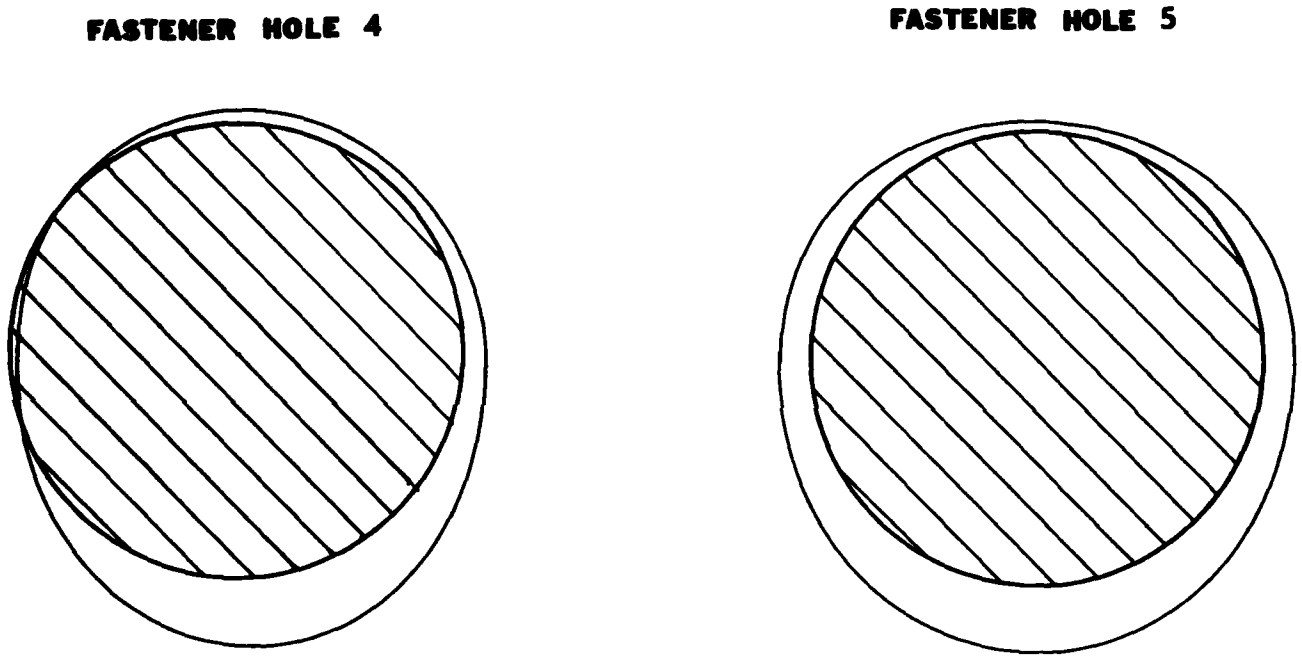

Figure 5.30 Initial and Post-Coldwork Hole Edge Boundries for Fastener Holes #4 and #5 (Specimen #3).

It was determined that if coldworking of the in-line pattern was not complete then large residual tensile strains could arise at the edge of an adjacent uncoldworked fastener hole. When coldworked, this hole edge will undergo a complete strain reversal. A noticeable transition region appears near the midportion of each strain distribution between a coldworked and a noncoldworked hole. This transition region becomes more complex as coldworking progresses through the pattern. When coldworking of the pattern is complete, the resultant strain distributions are shown to be highly nonsymmetric. For any inter-hole axis, the larger residual compressive strains will always appear at the edge of the fastener hole that was coldworked last. This will not be true for instances of sleeve failure.

The buckling and folding type failure of the fastener sleeve was shown to result in little or no coldworking of the material at the surface of the fastener hole. After coldworking an adjacent hole, significant tensile strains may be left near the hole where the sleeve became slightly recessed. Such failure of the fastener sleeve has proven to be a reoccurring problem and should be investigated further.

5.4 Inter-row Influence of Coldworking

5.4.1 Introduction

Residual influence strains are the residual surface strains that exist between two fastener holes caused by coldworking that has occurred in an adjacent fastener row. It is the purpose of this section to determine the extent of these residual influence strains.

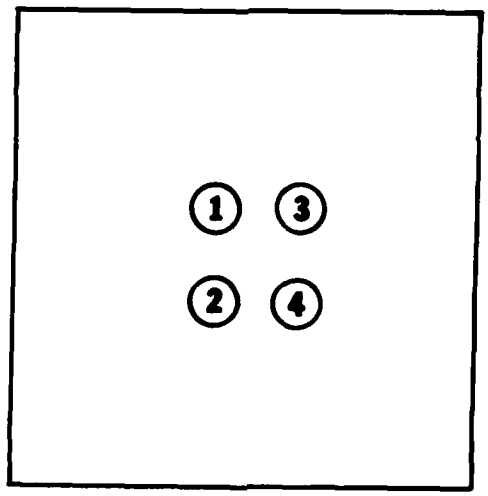

Figure 5.31 Double-Row Fastener Pattern Used for Specimens #5 and #6.

TABLE 5.10 SPECIMEN DATA

SPECIMEN	HOLE NO.	INITIAL DIAMETER	RESIDUAL DIA. EXPANSION	RADIAL INTERFERENCE	MAX LOAD COLDWORK (LBS)
5	1*	0.2616	0.0038	0.0063	1358
	2*	0.2614	0.0032	0.0064	1414
	3*	0.2614	0.0036	0.0064	1188
	4*	0.2616	0.0038	0.0063	1527
6	1	0.2614	0.0067	0.0074	1670
	2	0.2610	0.0059	0.0076	1641
	3	0.2610	0.0071	0.0076	1810
	4	0.2610	0.0059	0.0076	1840

* Serrations in coldwork record.

TABLE 5.11 HOLE EDGE MOTION - MAJOR AXIS

SPECIMEN	HOLE	EDGE	MOTION	EDGE	MOTION	SEPARATION
5	1	1-P	+0.0008	1-3	+0.0028	0.0020
	3	3-1	-0.0008	3-P	+0.0043	
	2	2-P	+0.0016	2-4	+0.0012	0.0016
	4	4-2	+0.0004	4-P	+0.0031	

TABLE 5.12 HOLE EDGE MOTION - MINOR AXIS

SPECIMEN	HOLE	EDGE	MOTION	EDGE	MOTION	SEPARATION
5	1	1-N	+0.0004	1-2	+0.0031	0.0012
	2	2-1	-0.0020	2-S	+0.0051	
	3	3-N	+0.0012	3-4	+0.0024	0.0020
	4	4-3	-0.0004	4-S	+0.0039	

TABLE 5.13 HOLE EDGE MOTION - MAJOR AXIS

SPECIMEN	HOLE	EDGE	MOTION	EDGE	MOTION	SEPARATION
6	1	1-P	+0.0063	1-3	+0.0004	0.0051
	3	3-1	-0.0047	3-P	+0.0024	
	2	2-P	+0.0067	2-4	-0.0008	0.0028
	4	4-2	+0.0035	4-P	+0.0024	

TABLE 5.14 HOLE EDGE MOTION - MINOR AXIS

SPECIMEN	HOLE	EDGE	MOTION	EDGE	MOTION	SEPARATION
6	1	1-N	+0.0016	1-2	+0.0047	0.0039
	2	2-1	-0.0008	2-S	+0.0071	
	3	3-N	+0.0008	3-4	+0.0043	0.0043
	4	4-3	-0.0012	4-S	+0.0067	

The test pattern chosen for the study was intended to model the double-row fasterner patterns noted in the TCTO drawings furnished by AFWAL/ML (see Figure 2.1). Two specimens with identical hole spacing but different levels of radial interference were used to study the interrow strain influence problem. The double-row fastener pattern for specimens #5 and #6 is illustrated in Figure 5.31 and relevant specimen data is included in Tables 5.10, 5.11, 5.12, 5.13 and 5.14.

The test pattern is composed of two parallel rows with two fastener holes in each row. The center-to-center separations between adjacent fasteners and adjacent rows is 1.75 diameters. The fastener holes are not staggered, and they form a symmetric 2 x 2 matrix. If it is required to study the progression of the strain influence problem, then each specimen has its own defined sequence of coldwork. For the four-hole symmetric patterns under study, there exists only two unique coldworking sequences. Other coldworking sequences exist but are redundant in that they are mirror images of the two unique coldworking sequences.

5.4.2 Experimental Results

For the double-row test specimens #5 and #6, initial residual influence strains were measured along axis (2-4) after fastener hole #1 had been coldworked. The distribution of these influence strains is illustrated in Figures 5.32 and 5.33. The residual influence strains never attain a magnitude greater than +/- .5%. These residual influence strains are almost insignificant in comparison with the magnitudes of the residual surface strains caused by coldworking two adjacent in-line fastener holes.

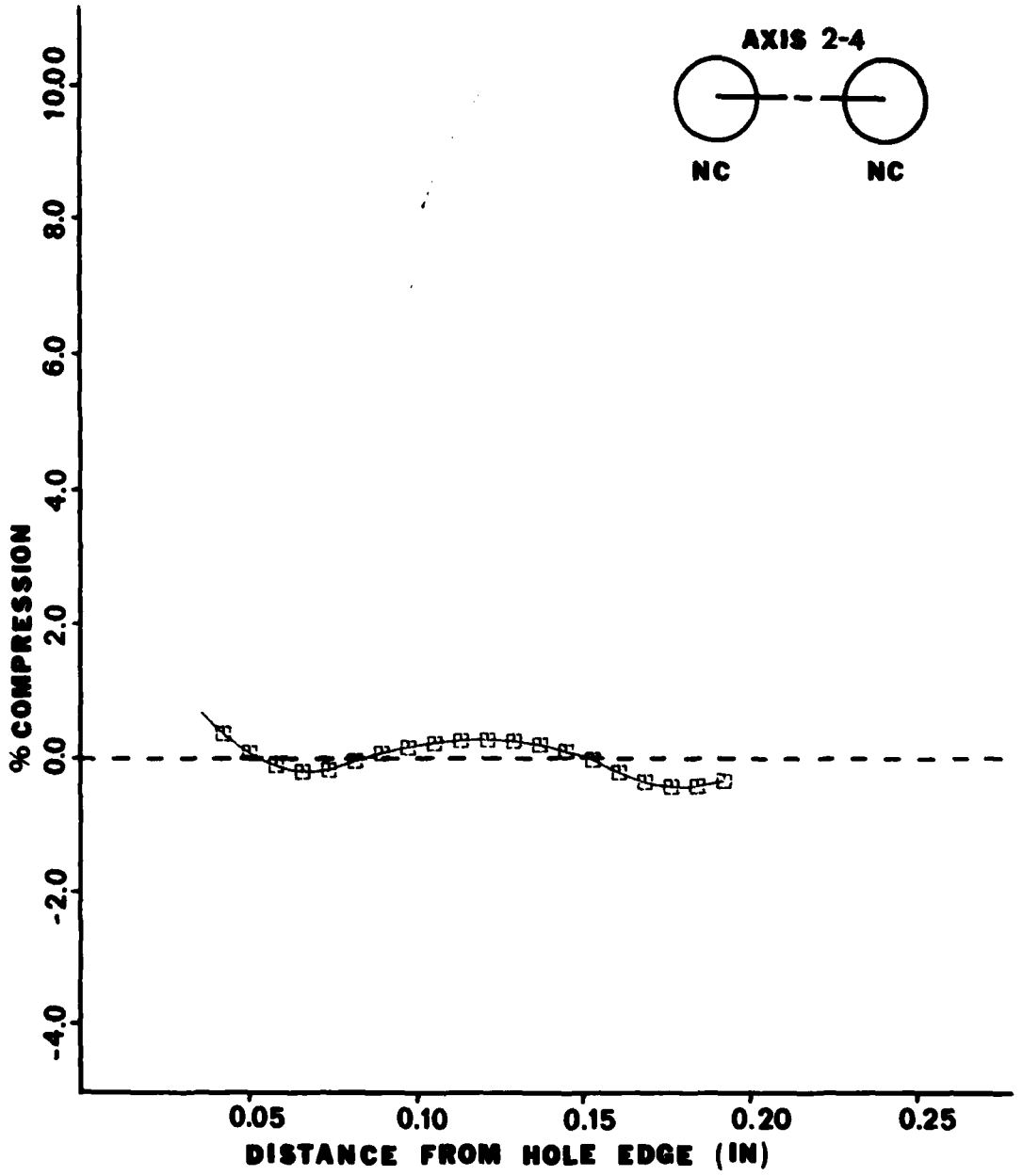

Figure 5.32 Strain Distribution Along Axis (2-4) After Fastener Hole #1 has been Coldworked (Specimen #5).

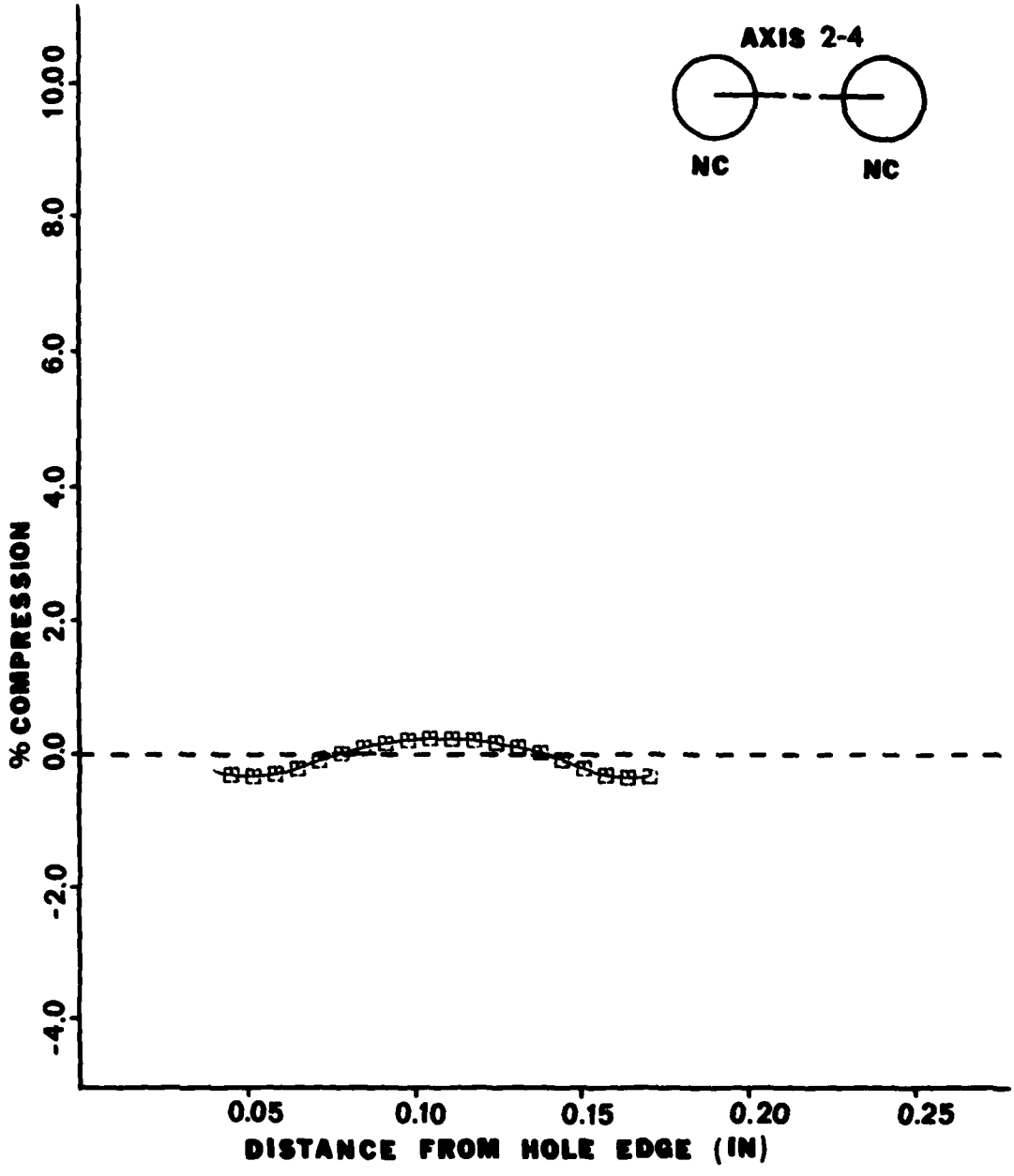

Figure 5.33 Strain Distribution Along Axis (2-4) After Fastener Hole #1 has been Coldworked (Specimen #6).

Figure 5.34 Typical Fringe Pattern for Axis (2-4), as Caused by the "Influence Strains" Occuring After Fastener Hole #1 has been Coldworked.

It should be noted that, for the two different levels of radial interference, the magnitude and the general shape of the influence strain distributions are almost identical. Both specimens indicate small tensile strains at edge (2-4) of fastener hole #2 and at edge (4-2) of fastener hole #4. These tensile strains could most probably be attributed to the complex strain fields that exist near the edges of fastener holes #2 and #4. Reference to the fringe pattern in Figure 5.34 illustrates this idea.

5.4.3 Conclusion

The influence of the residual surface strains caused by coldworking adjacent rows of fasteners can be considered negligible as compared with the magnitude of the residual surface strains caused by coldworking adjacent in-line fastener holes. When the adjacent rows of fasteners are separated by 1.75 diameters, the maximum influence strains to be expected are +/- .5%. These strains are significantly less than the 5%-9% compressive strains associated with the coldworking of adjacent in-line fastener holes separated by 1.75 diameters.

5.5 General Conclusions

The interaction of the residual strain fields between coldworked fastener holes in the near vicinity of one another has proven to be a very complex problem. Results from the study indicate that the interaction of the residual surface strains are dependent upon, at least, the following experimental parameters:

1. The geometric configuration of the fastener pattern.
2. The center-to-center hole spacing.

3. Inter-row influence caused by coldworking adjacent rows of fastener holes.
4. The sequence in which the fastener holes are coldworked.
5. The level of radial interference for each coldworked fastener hole.
6. The post-coldwork position of the fastener sleeve inside the fastener hole (sleeve failure).
7. The material.

In any coldwork situation, consideration must be given to the geometric configuration of the fastener pattern under study. In the case of multiple-hole in-line fastener pattern, the behavior of two-hole patterns are different from the behavior exhibited by the five-hole patterns. Behavior is denoted by the residual surface strains at the edge of the fastener holes and the resultant motion undergone by the hole edges as caused by the coldworking technique.

Almost without exception, for any fastener pattern, eighty percent or more of the residual diametral expansion of any fastener hole will occur toward the adjacent uncoldworked fastener hole. Additionally, in the case of multiple in-line fasteners, the material that separates the adjacent fastener holes will undergo both rigid body motion and deformation. It is in this situation that the fastener pattern can shift, no longer retain its symmetry, and the magnitude of the residual compressive strains at the edge of a given fastener hole can become exceptionally large.

When two adjacent fastener holes are coldworked, the resultant interaction of the residual surface strain fields is directly related to the initial separation between the centers of the fastener holes.

Experimental results indicate that significantly less interaction between the strain fields occurs for fastener holes separated by 2.0 diameters than for fastener holes separated by 1.75 diameters. The physical distribution of the residual strain fields are very similar, but the resultant strain magnitude will be different. To generalize, as adjacent fastener holes are separated by increasingly greater distances, the interaction of their strain fields will decrease and the resultant strain distribution will become two individual strain distributions.

The double-row fastener patterns were used to study the influence of coldworking adjacent rows of fastener holes. Residual radial influence strains were measured along a line that connects the centers of two adjacent fastener holes that are in a row separate from that of the fastener hole being coldworked. A standard separation of 1.75 diameters was used as the spacing between adjacent fastener holes as well as the spacing between the adjacent rows of fasteners. The influence of the residual surface strains caused by coldworking adjacent rows of fasteners could be considered negligible as compared with the magnitude of the residual surface strains caused by coldworking adjacent in-line fastener holes. Residual influence strains of +/- .5% were the maximum influence strains recorded for the test specimens. These strains are significantly less than the 5%-9% compressive strains caused by coldworking adjacent in-line fastener holes separated by 1.75 diameters.

It has been indicated that the order or sequence in which the fastener pattern is coldworked is very important in the determination of the resulting inter-hole strain distributions. Attention was focused on the coldworking sequences of the three-and five-hole in-line fastener patterns. It was learned that the nonconsecutive order of coldwork functions to

counteract the rigid body motions exhibited by the inter-hole material of the five-hole fastener pattern. The test data for the three-hole nonconsecutively coldworked specimen illustrated the nonsymmetry of the coldworking process. In this instance, the geometrically symmetrical fastener pattern prior to coldworking proved to be unsymmetrical in its geometry and in its resultant strain distributions after being coldworked. Extreme nonsymmetry of the strain distributions and the hole edge motions were exhibited by the five-hole in-line fastener pattern that was coldworked in a consecutive order. The "dynamic" aspects now associated with the coldworking procedure could prove extremely detrimental in a tight-tolerance fastener situation.

The level of radial interference is an important parameter in determining the magnitude of the residual surface strains that will exist at the edge of a coldworked fastener hole. In any fastener pattern and when the adjacent fastener hole is still uncoldworked, the magnitude and distribution of the residual surface strains are comparable to those expected from the coldworking of a single fastener hole in a plate. These comparisons were made in reference to a prior study by Cloud (4), and the agreement between the experimental results was very good.

A very important result from this study was the revelation of possible tensile strains at the edge of the adjacent uncoldworked fastener hole. This was evident in every fastener pattern and in every coldworking sequence. The magnitude of these residual tensile strains was usually less than 1% but proved to be substantial in the case of the multiple hole in-line fastener pattern. The presence of these tensile strains could enhance stress corrosion or provide for a possible starting point for fatigue cracks. Under such circumstances, the entire

coldworking process could be detrimental. Results are opposite to the original intentions of structural life extension.

It has become apparent that the post-coldwork position of the fastener sleeve is significant as an indicator of the state of strain that exists near the edge of the coldworked fastener hole. Recession of the fastener sleeve from the surface of the specimen by .02 inches can lead to zero or possibly small residual tensile surface strains at the edge of the coldworked hole. It was determined that sleeve recession was caused by a folding type failure of the sleeve material directly above the anvil of the fastener sleeve. Sleeve failure and slippage has proven to be detrimental to the coldworking process.

5.6 Future Research

The research conducted in this study has revealed many new and interesting aspects about coldworking fastener holes in the near vicinity of one another. This study was structured on specific fastener patterns functioning as intermediate steps in determining the characteristics of the coldworking process for an interaction type situation. Further research on any or all of the fastener patterns and the ideas behind their conception would prove especially rewarding in that it would lead eventually to the optimization of fastener and fastener pattern design.

Initial or primary research should be directed toward the determination of the total state of strain that exists between two adjacent coldworked fastener holes. Current research utilizing two-way gratings near a single coldworked hole has proven its feasibility. Its subsequent adaption to the interaction problem would yield the desired results. Cartesian strains would be most applicable, most easily obtained, and

simple coordinate transformations would serve to yield the strains in polar coordinates.

Further experimental study should be directed toward the "dynamic" aspects exhibited in the coldworking process. A whole field mapping technique should be utilized through all intermediate coldworking steps and correlated to yield empirical relations for various fastener geometries, coldworking sequences, and levels of radial interference.

The existence of small residual tensile strains at the edges of both coldworked and uncoldworked fastener holes necessitates that some future research be conducted in the areas of fatigue and crack propagation. Testing of simple fastener geometries and nominal levels of radial interference would easily serve to provide for the required experimental information. It has been indicated that by design or by methodology, improvements are required in the coldworking process in order to reduce the incidence of occasional sleeve failure and slippage, which leads to subsequent creation of adverse residual strain states.

LIST OF REFERENCES

1. Adler, W. F., and Dupree, D. M., "Stress Analysis of Coldworked Fastener Holes," Technical Report AFML-TR-74-44, Wright Patterson AFB, Ohio, July 1974.

2. Cesarz, W. J., Jr., "An Experimental Study of Fatigue Crack Growth from Fastener Holes Repaired by Coldworking," A Masters Thesis, Michigan State University, Department of Metallurgy, Mechanics and Materials Science, 1977.

3. Chandawanich, N., "An Experimental Study of Crack Initation and Growth from Coldworked Holes," A Doctoral Dissertation, Michigan State University, Department of Metallurgy, Mechanics and Materials Science, 1978.

4. Cloud, G. L., "Residual Surface Strain Distribution Near Holes Which are Coldworked to Various Degrees," Air Force Materials Laboratory, Technical Report AFML-TR-78-153, Wright Patterson AFB, Ohio.

5. Cloud, G. L., "Measurements of Strain Fields near Coldworked Holes," Experimental Mechanics, p. 9-16, (January 1980).

6. Cloud, G. L., "Simple Optical Processing of Moiré Grating Photographs," August 1980 Experimental Mechanics, to be published, Vol. 20, No. 8.

7. Cloud G., R. Radke, and J. Pieffer, "Moiré Gratings for High Temperatures and Long Times," Experimental Mechanics, Vol. 19, No. 10, October 1979, pp. 1-4.

8. Duffy, D., "Measurement of Surface Displacement Normal to the Line of Sight," Experimental Mechanics, Vol. 14, No. 9, September 1974, pp. 378-384.

9. Durelli, A. J. and V. J. Parks, "Moiré Analysis of Strain," Englewood Cliffs, N.J., Prentice-Hall Inc., 1970.

10. Perloff, W. H., and W. Baron, "Soil Mechanics-Principles and Applications," Ronald Press, 1976.

11. Sharpe, W. N., Jr., "Measurement of Residual Strains Around Coldworked Fastener Holes," Scientific Report, AFOSR Grant 75-2817, Bolling AFB, Washington D.C., April 1976.

*U.S.Government Printing Office: 1981 — 757-002/545